

Aus der Klinik für Allgemein-, Viszeral-und Transplantationschirurgie
Klinikum der Ludwig-Maximilians-Universität München



**The SPOCK2 expression is downregulated in pancreatic
ductal adenocarcinoma due to hypermethylation of its gene**

Dissertation

zum Erwerb des Doktorgrades der Medizin

an der Medizinischen Fakultät der

Ludwig-Maximilians-Universität München

vorgelegt von

Kaifeng Su

aus

Shandong, Volksrepublik China

2023

Mit Genehmigung der Medizinischen Fakultät der
Ludwig-Maximilians-Universität zu München

Erster Gutachter: Prof. Dr. med. Jan G. D'Haese

Zweiter Gutachter: apl. Prof. Dr. Alexandr Bazhin

Dritter Gutachter: Priv. Doz. Dr. Michael Haas

Mitbetreuung durch den
promovierten Mitarbeiter:

Dekan: Prof. Dr. med. Thomas Gudermann

Tag der mündlichen Prüfung: 11.01.2023

Table of content

Table of content	1
Zusammenfassung (Deutsch):	4
Abstract (English):	6
List of figures	8
List of tables	10
List of abbreviations	11
1. Introduction	14
1.1 Pancreatic ductal adenocarcinoma (PDAC)	14
1.2 The Protein Family of SPARC	21
1.2.1 SPARC	22
1.2.2 Hevin/SPARC-like 1.....	23
1.2.3 SPOCK1	24
1.2.4 SPOCK2	24
1.2.5 SPOCK3	25
1.2.6 SMOC1	25
1.2.7 SMOC2	26
1.2.8 FSTL1	27
1.3 DNA methylation.....	27
1.4 Epithelial-mesenchymal transition	29
1.5 Aim of this study	30
2. Material and Methods	31
2.1 Materials	31
2.1.1 Consumables	31
2.1.2 Chemicals	32
2.1.3 Antibodies	35
2.1.4 Primers	35
2.1.5 Commercial Assays kits.....	36
2.1.6 Apparatus	37
2.1.7 Software.....	39

2.1.8	Buffer and Solutions	39
2.2	Methods	42
2.2.1	Cell culture	42
2.2.2	Quantitative real-time polymerase chain reaction (qRT-PCR).....	43
2.2.3	Western blot analysis.....	45
2.2.4	Treatment with 5-aza-2'-deoxycytidine (5-aza-dC).....	48
2.2.5	Small interfering RNA (siRNA) transfection	48
2.2.6	MTT	49
2.2.7	Flow Cytometric Analysis of Cells.....	49
2.2.8	Transwell assay	50
2.2.9	Bioinformatic analysis	51
2.2.10	Statistical analysis	52
3.	Results.....	53
3.1	Expression of the SPOCK2 is lower in the pancreatic cancer cell lines and pancreatic stellate cells than in the normal pancreatic cell line	53
3.2	The low level of SPOCK2 is associated with poor prognosis of patients with pancreatic cancer in a bioinformatic analysis	56
3.3	Decreased SPOCK2 expression in PDAC due to hypermethylation	59
3.4	Hypermethylation of SPOCK2 correlates with poor survival in PDAC.....	62
3.5	Knockdown of SPOCK2 induces certain phenotypic effects in PDAC.....	64
3.5.1	Knockdown of SPOCK2 increases the cell growth rate in PDAC cells.....	65
3.5.2	Knockdown of SPOCK2 causes the cell cycle change in PDAC cells.....	66
3.5.3	Knockdown of SPOCK2 can stimulate migration in PDAC.....	68
3.5.4	Knockdown of SPOCK2 resulted in the downregulation of ZO-1	69
4.	Discussion.....	71
4.1	SPOCK2 as a potential prognostic marker.	72
4.2	SPOCK2 is methylated in PDAC and correlates with poor prognosis.	74
4.3	SPOCK2 might inhibit the growth of PDAC cells.	76
4.4	SPOCK2 might participate in cell migration and EMT in PDAC.	78
4.5	The limitations of this research.	80
5.	Conclusion	82
	References.....	83

Supplemental materials.....	98
Acknowledgements	108
Affidavit.....	109

Zusammenfassung (Deutsch):

Bauchspeicheldrüsenkrebs ist eine sehr schwere Erkrankung mit einer 5 Jahres Überlebensrate zwischen 2-9%. Die operative Entfernung ist die einzige kurative Behandlung, die allerdings nicht für alle Patienten geeignet ist, da zu dem Zeitpunkt der Diagnose die Krankheit häufig bereits fortgeschritten ist. Die Standardtherapien wie Chemotherapie, Radiotherapie und Immunotherapie verbessern die Situation der Patienten mit Pankreaskarzinom nicht maßgeblich. Daher ist die Suche nach Biomarkern für Bauchspeicheldrüsenkrebs zwecks der Prävention, Früherkennung und Heilung von größter Bedeutung. Die Proteinfamilie SPARC umfasst SPARC, Hevin, FSTL1, SPOCK1,2,3 und SMOC1,2, welche sich jeweils in drei Domänen ähneln und bei multiplen Krebsarten eine wichtige Rolle spielen. Mehrere Studien belegen, dass SPARC, Hevin, SPOCK1 und FSTL1 eine relevante Funktion bei der Progression des Bauchspeicheldrüsenkrebses haben. Die Bedeutung der anderen Familienmitglieder für den Krebs ist jedoch bisher ungeklärt.

Mittels qRT-PCR haben wir den Level von mRNA in folgenden unterschiedlichen Bauchspeicheldrüsenzellen verglichen: gesunde Zelllinien (HPDE), Bauchspeicheldrüsenkrebszelllinien (PCC) und primären Stellatumzellen (PSCs). Hier haben wir feststellen können, dass die Expression von SPOCK2 in allen PCC und PSC deutlich und stabil verringert war im Vergleich zur Kontrolle HPDE. Die anschließende Analyse des Zusammenhangs zwischen der Expression der vier Gene und der Lebenserwartung der Patienten hat gezeigt, dass ausschließlich SPOCK2 ausschlaggebend war für eine gute Prognose. Daher haben wir uns bei den weiteren Untersuchung auf SPOCK2 fokussiert.

Mithilfe der Bioinformatik haben wir initial den Mechanismus der geringen Expression in Bauchspeicheldrüsenkrebszellen analysiert und haben einen negativen Zusammenhang zwischen einer Methylierung und mRNA Expression von SPOCK2 festgestellt. Nach der Behandlung mit dem Demethylierungskomponent 5-aza-dC zeigte sich ein Anstieg der mRNA und Proteinexpression. Unterdessen trägt die Hypermethylierung von SPOCK2 zur schlechten Prognose von Patienten mit Bauchspeicheldrüsenkrebs bei und stellt einen Hochrisikofaktor dar. Darüber hinaus zeigte sich, dass durch ein Ausschalten von SPOCK2 mithilfe von si-RNA die Proliferation und Migration in Pankreaskarzinomzellen der Capan-2 Zelllinie gesteigert werden kann. Das Verhältnis der Zellen in der G0/G1 Phase und der mRNA und Proteingehalt von ZO-1 zeigten sich nach dem SPOCK2 knockdown verringert.

Zusammenfassend konnte ich mit dieser Arbeit zeigen, dass die Expression von SPOCK2 im Pankreaskarzinom signifikant verringert ist, was durch eine erhöhte Methylierung verursacht wird. Dies scheint ein Hochrisikofaktor bei der Prognose der Patienten zu sein. Darüber hinaus reguliert SPOCK2 die Proliferation und Migration in Bauchspeicheldrüsenkrebszellen. Aus diesem Grund könnte SPOCK2 ein potenzieller Prognose- und Zielmarker bei Bauchspeicheldrüsenkrebs sein.

Abstract (English):

Pancreatic cancer is a very dismal disease, and the five-year survival rate is low as 2-9%. Surgery is the only curative treatment, but most patients miss the best opportunity when diagnosed because of the tumor's spread out. The standard therapies, including chemotherapy, radiotherapy and immunotherapy, fail to significantly improve the prognosis of patients with pancreatic cancer. Hence, it is critical to look for accurate tumor biomarkers for the prevention, early detection, and treatment of pancreatic cancer. The SPARC protein families include SPARC, Hevin, FSTL1, SPOCK1,2,3 and SMOC1,2, which share three main domains, and function in several cancers. Meanwhile, previous studies reported that SPARC, Hevin, SPOCK1 and FSTL1 performed biological processes in pancreatic cancer. However, the role of the rest family members is unclear until now in the pancreatic cancer.

First, we compared the mRNA level of the rest family members among normal pancreatic cell line (HPDE), pancreatic cancer cell lines (PCCs), and pancreatic stellate cells (PSCs) using qRT-PCR. We found only SPOCK2 decreased significantly and stably in all PCCs and PSCs compared to HPDE. Next, we analyzed the relationship between these four genes' expression and the prognosis of pancreatic cancer, indicating only SPOCK2 influences the patients' survival and a high level of it contribute to prognosis. Therefore, we finally selected the SPOCK2 gene to continue to research deeply.

We initially explored the mechanism of lower expression in pancreatic cancer and observed a negative relationship between the degree of methylation and mRNA expression of SPOCK2 through bioinformatics. Furthermore, its mRNA and protein expression increased after the demethylating agent 5-aza-dC treatment. Meanwhile, hypermethylation of SPOCK2 contributes to the poor prognosis of patients with pancreatic cancer

and is a high-risk factor. In addition, the knockdown of SPOCK2 by si-RNA significantly increased the proliferation and migration of Capan2 cells. Moreover, the proportion of Capan-2 cells in the G0/G1 phase was remarkably shortened, and both the mRNA and protein levels of the tight junction protein ZO-1 were decreased after SPOCK2 knockdown.

Overall, our data show that SPOCK2 decreased in pancreatic cancer due to hypermethylation, which is also a high-risk factor for survival. Meanwhile, SPOCK2 regulates proliferation and migration in pancreatic cancer cells. Therefore, SPOCK2 might be a potential prognostic and target marker in pancreatic cancer.

List of figures

Figure 1: Map shows the estimated age-standardized incidence and mortality rate for pancreatic cancer worldwide in 2020, including both sexes and all ages.

Figure 2. The domain structure of SPARC families.

Figure 3. The expression of SPOCK2, SPOCK3, SMOC1, and SMOC2 in the normal pancreatic cell line, seven pancreatic cancer cell lines, and three pancreatic stellate cells in mRNA level.

Figure 4. The mRNA level of SPOCK2, SPOCK3, SMOC1, and SMOC2 in HPDE, PCCs, and PSCs.

Figure 5. KM survival analysis of SPOCK2, SPOCK3, SMOC1, and SMOC2 in PDAC patients via KM Plotter.

Figure 6. Kaplan–Meier curves show survival patterns for high and low expression (red and blue) in SPOCK2 gene (a), SPOCK3 gene (b), SMOC1 gene (c), and SMOC2 gene (d) in PDAC patients.

Figure 7. The correlation between expression and methylation of SPOCK2.

Figure 8. The mRNA expression of SPOCK2 in Panc1, Dang, and Capan2 cell lines after treatment with 5-aza-dC.

Figure 9. The protein expression of SPOCK2 in Panc1 and Capan2 cell lines after treatment with 5-aza-dC.

Figure 10. Kaplan–Meier curves show survival patterns for hypermethylation and non-hypermethylation (red and blue) of SPOCK2 in PDAC patients.

Figure 11. Time-dependent ROC curves were drawn to predict the survival for one year (A) and two year (B) in PDAC.

Figure 12. The expression of SPOCK2 after transfection of siRNA in Capan2.

Figure 13. Effects of SPOCK2 knockdown on cell proliferation.

Figure 14. Cell cycle analysis of SPOCK2 knockdown in Capan2 cells.

Figure 15. Effects of SPOCK2 knockdown on migration in PDAC cells.

Figure 16. The changes of EMT markers (E-cadherin, N-cadherin, ZO-1, Vimentin) after SPOCK2 knockdown in Capan2 cells.

Figure 17. The ZO-1 protein decreased after SPOCK2 knockdown in Capan2 cells.

Figure 18. Graphic summary of SPOCK2.

List of tables

Table 1: The reverse-transcribed reaction settings

Table 2: Reaction setup of QuantiNova™ SYBR Green PCR Kit

Table 3. Correlation of SPOCK2, SPOCK3, SMOC1, and SMOC2 expression with survival in PDAC patients.

Table 4. Correlation of SPOCK2 methylation with survival in PDAC patients.

Table 5. Some potential prognostic/therapeutic markers for PDAC.

Supplementary Table 1. ICGC original data.

Supplementary Table 2. mRNA expression and methylation level of SPOCK2 from TCGA.

Supplementary Table 3. The prognosis of patients and methylation of SPOCK2 from TCGA.

List of abbreviations

°C	Degree Celcius
%	Percentage
h	Hour
PDAC	Pancreatic ductal adenocarcinoma
PanINs	Pancreatic intraepithelial neoplasms
MCNs	Mucinous cystic neoplasms
HCC	Hepatocellular carcinoma
CRC	Colorectal cancer
ASIR	Age-standardized incidence rates
IPMN	Intraductal papillary mucinous neoplasm
SPOCK1	Osteonecton, cwcvc, and kazal-like domain proteoglycan 1
ASDR	Age-standardized death rates
H. pylori	Helicobacter pylori
CP	Chronic pancreatitis
SPARC	Secreted protein acidic and rich in cysteine
PALB2	Partner And Localizer Of BRCA2
SPOCK2	Osteonecton, cwcvc, and kazal-like domain proteoglycan 2
SPOCK3	Osteonecton, cwcvc, and kazal-like domain proteoglycan 3
SMOC1	Secreted Modular Calcium Binding-1
SMOC-2	Secreted Modular Calcium Binding-2
FSTL1	Follistatin-like protein 1
nm	Nanometer
BRCA1	Breast cancer type 1
ECM	Extracellular matrix
Hevin	SPARC-like 1
APC	Adenomatous Polyposis Coli
EMT	Epithelial-mesenchymal transition

MMP	Matrix metalloproteinase
CDKN2A	Cyclin Dependent Kinase Inhibitor 2A
FBS	Fetal bovine serum
BRCA2	Breast cancer type 2
ATM	Ataxia telangiectasia mutated
TLR4	Toll Like Receptor 4
RAS	Rat sarcoma virus
CSC	Cancer stem cell
AKT	Protein kinase B
DMEM	Dulbecco's Modified Eagle Medium
HPDE	Human Pancreatic Duct Epithelial cell
µm	Micrometer
SFM	Serum-Free Medium
qRT-PCR	Quantitative real-time polymerase chain reaction
EGF	Epidermal growth factor
SDS-PAGE	Sodium dodecyl sulfate–polyacrylamide gel electrophoresis
PSCs	Pancreatic stellate cells
PCCs	Pancreatic carcinoma cells
µL	Microliter
ml	Milliliter
ATCC	American Type Culture Collection
BPE	Bovine pituitary extract
RPMI 1640	Gibco Roswell Park Memorial Institute 1640 Medium
BCA	Bicinchoninic Acid Assay
5-aza-dC	5-aza-2'-deoxycytidine
PVDF	Polyvinylidene fluoride
TBS	Tris-buffered saline
PBS	Phosphate-buffered saline
SPSS	Statistical Package for the Social Sciences

MTT	3-(4,5-Dimethylthiazol-2-yl)-2,5-diphenyltetrazolium bromide
siRNA	Small interfering RNA
AUC	Area Under the ROC Curve
s	Second
DMSO	Dimethyl sulfoxide
mM	Millimolar
μ M	Micromolar
FACS	Fluorescence-activated cell sorting
BrdU	5-bromo-2'-deoxyuridine
CV	Crystal Violet
HM450	Illumina HumanMethylation450
ICGC	International Cancer Genome Consortium
GAPDH	Glyceraldehyde 3-phosphate dehydrogenase
r	Correlation coefficient
FPKM	Fragment per kilobase million
B2M	Beta-2 microglobulin
ROC	Receiver Operating Characteristic
FPR	False positive rate
MS-PCR	Methylation-specific PCR
TCGA	The Cancer Genome Atlas
μ g	Microgram
mg	Milligram
SEM	Standard Error of Mean
TPR	True positive rate
SEM	Standard error of mean
18S	18S ribosomal RNA
H. pylori	Helicobacter pylori

1. Introduction

1.1 Pancreatic ductal adenocarcinoma (PDAC)

The pancreas is a digestive organ and an endocrine gland in the human body, and it has both a digestive exocrine and an endocrine function [1]. As a digestive organ, it functions as an exocrine gland, secreting pancreatic juice, including bicarbonate and digestive enzymes, into the duodenum by the pancreatic duct, which can neutralize the acid from the stomach and break down carbohydrates, protein, and fat from food [2]. The endocrine section is composed of discrete islets of Langerhans, which contains several cell types secreting various hormones, for example, the most common α - and β - cells produce glucagon and insulin, which regulate blood glucose [3]. Besides, around them, stroma includes blood vessels, fibroblasts, pancreatic stellate cells, extracellular matrix, and soluble proteins to support the architecture of the pancreas [4].

Pancreatic cancer is a global burden due to poor prognosis and is very difficult to treat in most cases [5]. The five-year survival can be as low as 2-9% [6]. PDAC represents the majority (90%) of pancreatic neoplasms; other types include acinar carcinoma, pancreatic blastoma, and neuroendocrine tumors [7].

PDAC is generally a solitary lesion; approximately 60%-70% are placed in the head of the pancreas, and the others are primarily located in the body and tail [8]. The pathogenesis of PDAC usually follows a series of mutations, from normal tissue, forming a precursor lesion and finally mutating to an invasion malignancy [9]. The pancreatic intraepithelial neoplasms (PanINs) are the most common neoplastic precursor of PDAC, microscopic tumors that diameters less than 5mm [10]. The other kinds, such as mucinous cystic

neoplasms (MCNs) and intraductal papillary mucinous neoplasm (IPMN), also can develop into PDAC, even if not frequently [11].

1.1.1. Epidemiology and risk factors of PDAC

The morbidity rate of PDAC increases year by year [12]. From 1990 to 2019, it showed an increasing trend, the age-standardized incidence rates (ASIR) from 5.22 to 6.57 (per 100,000 population); at the same time, it also maintains an upward trend in death rate, the age-standardized death rates (ASDR) [5.34 to 6.62], increasing about 24% [13]. In global cancer statistics 2020, PDAC was the 7th common reason for cancer-related death; meanwhile, because of its dismal prognosis, PDAC causes nearly as many deaths (466,003) as cases (495,773) [14]. In terms of geographic area, the incidence and mortality rate is higher in Europe and North America, as shown in Figure 1. Given the stable upward prevalence and fatality rate, it is anticipated that PDAC will overtake breast cancer as Europe's third greatest cause of cancer-related mortality by 2025 [15].

The etiology has been studied, and several risk factors are usually classified into two main categories: non-modifiable and modifiable [16].

Non-modifiable risk factors:

Age

With age, the chance of having a PDAC rises; the peak usually occurs between 60 and 80 [17]. According to statistics from 2015 to 2019, PDAC predominantly occurred in the older population in the USA; new incidents were diagnosed most frequently among adults over 55 [18]. Worldwide, PDAC is rarely diagnosed among individuals under 30 years [19].

Gender

The new estimated cases are 32,970 among males and 29,240 among females, and the cancer-related deaths are 25,970 and 23,860, respectively, in the United States in 2022 [20]. In Europe, the incidence and mortality are 67,200 and 65,400 among males and 65,000 and 63,000 among females in 2018 [21]. Globally, the incidence and mortality of PDAC are also higher in males than females [14].

Ethnicity

Several studies revealed that race is a risk factor with a significant incidence disparity [16]. The incidence rate for African-Americans in the USA is higher than for Caucasians, while Asian-Americans and Pacific Islanders seem to have the lowest rate [17]. Indeed, PDAC is more common in black people than in other races [22, 23]. The difference in incidence may be attributed to socioeconomic factors, lifestyle, diet, etc. [17, 24]. Therefore, understanding the reasons for the ethnic difference in incidence may help us study and prevent this disease.

Diabetes

Diabetes, including type I and type II, is linked with pancreatic tumors and can increase nearly 7-fold risk compared to patients without it [25, 26]. Long-standing diabetes has been a high-risk factor, and studies showed that patients with type II diabetes for more than ten years could significantly increase developing risk [27].

Family history

It is reported that approximately 5-10% of PDAC patients have a family history of the illness [28-30]. Most studies defined familial pancreatic cancer as families in which a pair of first-degree kinfolks, including parents, siblings, or children, had the disease [17]. A prospective analysis showed that the

pancreatic cancer risk was nine times greater in first-degree relatives of those with the disease than in the general population [31].

Genetic mutation

Genetic mutation (or variation) significantly impacts pancreatic cancer risk [32]. About 10% of pancreatic cancer cases exist genetic predisposition, including gene variation or alteration leading to developing PDAC [33]. Some genes have been linked to elevated pancreatic cancer risk, such as PALB2, CDKN2A, BRCA1/2, ATM, APC, and mismatch repair genes [32]. For example, PALB2 has been identified as a susceptible gene for pancreatic cancer, and about 3% of germ-line mutations were recorded in familial pancreatic cancer [34-36].

Modifiable risk factors:

Smoking

One of the modifiable pancreatic risk factors is tobacco smoking, which can increase a PDAC risk two-fold. [37]. Tobacco products contain some carcinogens, which are associated directly with PDAC. On the other hand, smoking is an indirect common reason for PDAC through diabetes and pancreatitis [38]. A prospective investigation from Europe in 2012 researched that five cigarettes daily can raise the risk of pancreatic cancer and noticed passive smoking was also a high-risk factor [39, 40].

Alcohol

It is known that excessive consumption of alcoholic beverages has been identified as a high-risk factor in PDAC [17]. Alcohol plays a crucial role in developing PDAC associated with fibrosis created by stellate cells; meanwhile can boost the creation of PanIN lesions and induce M2 macrophages under chronic pancreatitis [41]. Furthermore, alcohol can

cause oxidative stress and lipid peroxidation to promote cancer development, and alcohol abuse also exacerbates tumor progression by accelerating pancreatic inflammation [42].

Obesity

Obesity has been identified as a risk for PDAC incidence and death [43]. A paper published in 2022 reported that almost 34.7% of pancreatic cancer patients were obese from 2002 to 2017 in Korea [44]. Besides, obesity may be connected with physical inactivity, an unhealthy lifestyle, and uncovered genetic factors that may raise pancreatic cancer risk.

Infection

Some research showed that hepatitis B and C viruses had a link with pancreatic cancer, and hepatitis B virus had a stronger relationship [45-51]. *Helicobacter pylori* (*H. pylori*) is a common pancreatic cancer reason and is estimated to account for a 4-25% [52]. A meta-analysis including seven papers showed patients with *H. pylori* infection increased their risk of pancreatic cancer by 65% [53].

Pancreatitis

Pancreatitis is an inflammatory disease, including acute and chronic inflammation, which can damage the pancreas because digestive enzymes have been active before they release into the small intestine [17]. Recurrent bouts of acute pancreatitis can induce a progressive, destructive inflammation process, resulted in chronic pancreatitis (CP) [54]. CP can support an atypical cell production and carcinogenesis [55]. The underlying mechanisms of this malignant transformation are still unclear. However, it is believed that excessive cytokine expression and upregulation of certain

transcription factors during chronic pancreatic inflammation can promote carcinogenesis [56].

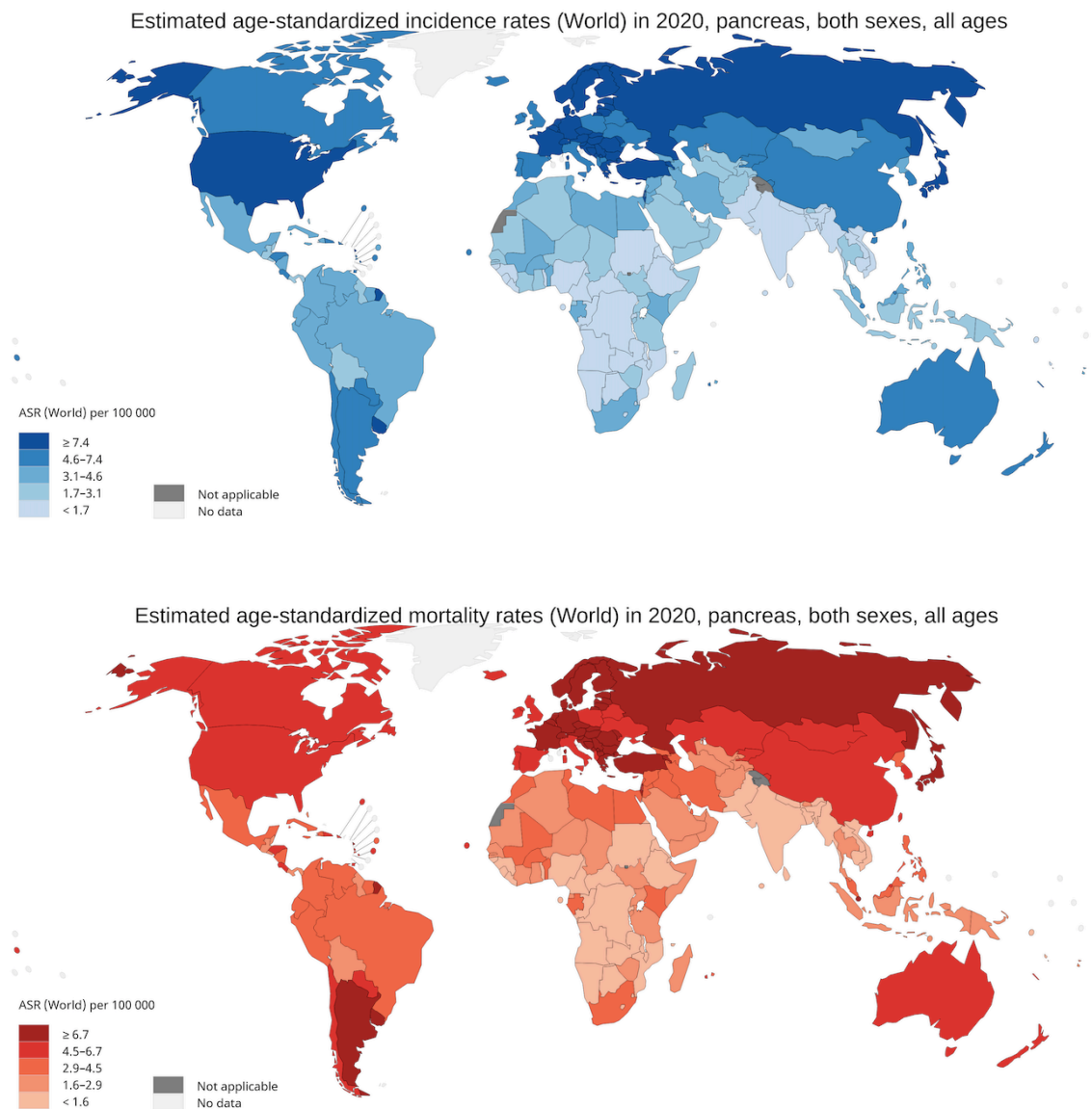


Figure 1: Map shows the estimated age-standardized incidence and mortality rate for pancreatic cancer worldwide in 2020, including both sexes and all ages. Data source: Global Cancer Observatory: Cancer Today. Lyon, France: International Agency for Research on Cancer (IARC). Available data from: <http://gco.iarc.fr/today>.

1.1.2. Current therapy options

Surgery

The only possibly curative therapy for PDAC is surgery. At the time of diagnosis, however, only 30% of patients are suitable for resection (resectable or borderline resectable). The remaining patients present locally advanced tumors and metastasis; for these patients, chemotherapy and radiation remain the main option [57]. One of the chemotherapeutic agents is Gemcitabine, which has been accepted since 1997 as a first-line anti-cancer drug for patients with PDAC [58].

Chemotherapy

Gemcitabine, a pyrimidine nucleoside antimetabolite, is a new cytotoxic agent [59]. A Multi-centre Randomised Controlled Trial studied that adjuvant systemic chemotherapy with gemcitabine can increase the cure rate by up to 20%, doubling long-term survival [60, 61]. However, patients usually developed gemcitabine resistance; evidence showed combining chemotherapy can improve survival more than mono-chemotherapy [62]. A clinical trial researched that gemcitabine combined with Nab-Paclitaxel could increase 2-year- survival from 4 to 9% [63]. A large random control trial showed patients with resected PDAC received mFOLFIRINOX (modified FOLFIRINOX (5-fluorouracil, oxaliplatin, irinotecan, and leucovorin)) can significantly increase survival time compared to gemcitabine [64]. A meta-analysis found that patients who underwent mFOLFIRINOX had a better survival than gemcitabine plus capecitabine and gemcitabine plus nab/paclitaxel, suggesting mFOLFIRINOX is feasible and manageable and could as a first option for fit individuals with resected pancreatic cancer [65]. Currently, mFOLFIRINOX is recommended for patients who have performed well after resection of PDAC of any stage [66].

Radiotherapy

The impact of radiotherapy is always controversial. Chemoradiotherapy appears to have no sustainable survival advantage for individuals with locally advanced pancreatic cancer compared to chemotherapy alone [57]. Some randomized trials found that patients benefit from survival with adjuvant chemotherapy after pancreatectomy, but adjuvant chemoradiotherapy is adverse [67, 68].

1.2 The Protein Family of SPARC

SPARC is a type of prototypic-binding matricellular protein that has various biological functions such as healing wounds, cellular differentiation, proliferation and migration of cells, and angiogenesis [69]. The SPARC family composed of eight members including SPARC, Hevin/SPARC-like 1, SPOCK-1, 2 and 3, SMOC-1 and 2, FSTL-1; these proteins share three main domains: I, II, and III [70], shown in Figure 2. Domain II is a follistatin-like domain made up of kazal-like domains that bind growth factors; domain III, commonly known as the EC domain, is a calcium-binding domain with a high affinity involved in collagen response. The follistatin and EC domains are remarkably conserved in the SPARC family. On the contrary, domain I is highly variable, except holding an overall acidic nature, thus regarded as the difference in each member of the SPARC family [70]. In addition to these main domains, each member holds particular domains respectively; for example, SPOCK members have a glycosaminoglycan-binding domain, thyroglobulin domains present in SMOC and SPOCK members; meanwhile, FST-1 comprises a von Willebrand factor type-C domain [70].

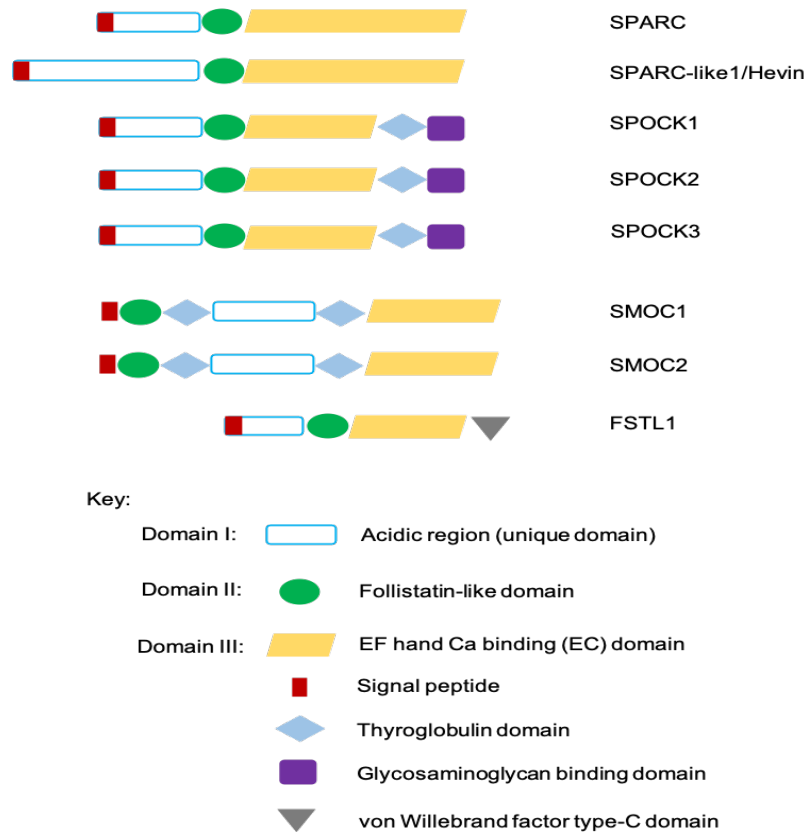


Figure 2. The domain structure of SPARC families.

1.2.1 SPARC

SPARC, also called osteonectin or basement membrane-40 protein (BM-40), was first found in bone and endothelial cells; it plays a role in wound healing, interacts with some ECM components, and regulates matrix metalloproteinase (MMP) activity [71-73]. The role of SPARC has been studied in various malignancies, including the biliary tract [74], breast [75], gastric [76], colorectal [77], and ovarian [78].

In PDAC, SPARC is overexpressed in tumor tissue compared to normal tissue [71]. Miyoshi et al. investigated that high SPARC mRNA level was linked to a worse prognosis than low SPARC, indicating the SPARC expression can act as a prognostic marker for PDAC [79]. Interestingly, SPARC is commonly expressed in the normal pancreatic cell line while

remarkably less in most pancreatic cancer cell lines due to promoter CpG islands hypermethylation [80, 81]. *In vitro*, the treatment with exogenous SPARC can suppress the proliferation of pancreatic cell lines [82]; furthermore, down-regulated endogenous SPARC could increase its proliferation [83]. On the contrary, overexpression of SPARC in stromal fibroblasts/PSCs was related to a poor outcome in PDAC [82, 84]. Furthermore, SPARC expression near the tumor margin promoted the invasion of PDAC cells, which might partly via inducing MMP-2 activation [82, 85]. Sato, N. et al. [80] found that SPARC expression could be increased in fibroblasts/PSCs after co-culture with PDAC cells, indicating its expression in fibroblasts/PSCs nearby cancer cells may be modulated by tumor-stroma paracrine loops. The role of SPARC remains controversial today; in the summary of the above mention, high SPARC expression is prevalent in stromal fibroblasts/PSCs, as opposed to PDAC cells, and is related to poor outcomes.

1.2.2 Hevin/SPARC-like 1

Hevin or SPARC-like 1 is the structurally closest family member to SPARC [69]. It is first cloned from the mouse brain and widely expressed in neurons and glia during development [86]. In prostate and gastric cancer, Hevin was found to suppress tumor cell migration and invasion; increasing Hevin could benefit patients' survival [87-90]. On the contrary, Hevin was overexpressed in colorectal cancer, contributing to a poor prognosis [91]. In PDAC, Esposito et al. [92] studied that Hevin expression is less in tumor cells, and their growth and invasion could be inhibited by recombinant Hevin protein *in vitro*, suggesting a tumor-suppressor function.

1.2.3 SPOCK1

SPOCK1 was found in human testis initially and belonged to the SPARC family [93]. SPOCK1 is regarded as an oncogene commonly and plays an important role in DNA repair, metastasis, and apoptosis [94]. In liver cancer, SPOCK1 was extensively abundant in tumor tissues, especially metastatic sites, and associated with poor prognosis [95]. Similarly, a high level of SPOCK1 could promote tumor development and metastasis in prostate cancer; besides, its increased expression was associated with shorter overall survival [96, 97]. Furthermore, Miao, L. et al. found that SPOCK1 was a novel downstream target of TGF- β and could induce EMT in lung cancer [98].

In PDAC, Li, J. et al. discovered that SPOCK1 expression was greater in tumor tissues, and high levels of SPOCK1 in patients exhibited a lower overall and disease-free survival [94]. Moreover, *in vitro*, it can promote PDAC cell proliferation and metastasis, besides inhibiting apoptosis [94]. In addition, V.L. et al. [99] studied that SPOCK1 was expressed abundantly in the stroma area of PDAC and strongly contributed to tumor growth and invasiveness, indicating depletion of stromal SPOCK1 might suppress the growth and invasion of cancer cells.

1.2.4 SPOCK2

Also known as testinca-2, belongs to the SPARC family, and it encodes a protein binding to glycosaminoglycans to form part of ECM [100]. In endometrial cancer, Ren, F. et al. found SPOCK2 protein expression is substantially greater in healthy tissue than in cancer tissue, and the absence of it contributed to distant metastases and myometrial invasion; meanwhile, *in vitro*, increasing SPOCK2 could inhibit the endometrial cancer cell lines

proliferation and promote apoptosis [100]. Similarly, Liu, G. et al. [101] showed that mRNA expression of SPOCK2 is significantly lower in prostate cancer tissue than benign prostate hyperplasia tissue; the upregulated SPOCK2 could inhibit invasion and migration of prostate cancer cell lines *in vitro*, indicating partial due to decreasing MMP-2. Until now, there has been no research about the SPOCK2 function in PDAC.

1.2.5 SPOCK3

The human SPOCK3 gene was found on chromosome 4q32.3 and encoded for a poorly characterized, putative calcium-binding extracellular heparin /chondroitin sulfate proteoglycan [102]. A study found SPOCK3 was downregulated and could induce stroke in the mouse brain experiment [103]. Kamioka, M. et al. [104] found that SPOCK3 was highly expressed in adult T-cell leukemia and can reduce MMP-2 activity in human T-lymphotropic virus type I (HTL V-I) related cell lines. Contrary, Nakada, M. et al. [105] studied that SPOCK3 mRNA level is downregulated in glioma tissue compared to normal brain and can inhibit tumor invasion by suppressing the activity of pro-MMP2. There are significantly fewer studies about SPOCK3, even no research in the digestive system, but some think it is similar to SPOCK1 [102], which may support an idea in the future.

1.2.6 SMOC1

SMOC1 is an extracellular glycoprotein of the SPARC-related modular calcium-binding protein family and was first found to localize predominantly with the basement membrane [69, 106]. SMOC1 is found in many body parts, including the brain, thymus, heart, skeletal muscle, lung, and liver; furthermore, its EC domain in the basement membrane can also bind to

collagen IV [107]. There is also little research about it currently. In glioma, the SMOC1 expression was positively related to five years of overall survival, and higher-level showed a better prognosis [108]. Aoki et al. [109] found that the increasing SMOC1 could suppress colorectal cancer cells' proliferation and colony formation, and its methylation correlated with the progression of CRC. Hence, whether it performs biological functions in PDAC needs further investigation.

1.2.7 SMOC2

SMOC-2 was found to be expressed in embryogenesis and wound healing [110]. There have been some studies about SMOC2 participation in the advancement of tumors. For example, high SMOC-2 expression in endometrial cancer was positively correlated with high grade and a large volume of tumors, lymph nodes, and distant metastasis; meanwhile, positive expression patients had worse five-year overall and disease-free survival [110]. On the contrary, another study reported that SMOC-2 was negatively related to tumor size and stage in human hepatocellular carcinoma (HCC); besides, its expression contributed to the prognosis [111]. Furthermore, *in vitro* overexpressing SMOC-2 could inhibit the cells' proliferation, colony formation, migration, and invasion, besides suppressing HCC tumorigenesis and metastasis *in vivo* [111]. Jang et al. [112] suggested SMOC-2 as a tumor suppressor candidate in colorectal cancer (CRC). In summary, SMOC-2 may play a different role in various organs, and there is no research about its function in pancreatic cancer; it is worth continuing to study in the future.

1.2.8 FSTL1

Follistatin-like protein 1 (FSTL1) is isolated initially in mouse osteoblastic MC3T3E cells as a cDNA and can upregulate by transforming growth factor-beta1 (TGF- β 1) stimulating [113]. Some studies showed that FSTL1 notably played an essential role in the inflammatory response to various pathogens; it activated the immune cells, increased the related gene expression, and released proinflammatory cytokines [113]. To some extent, inflammation is a crucial inducement in the progression of tumors. Hence, more and more researchers are interested in the function of FSTL1 in tumor progression due to its particular role in inflammation. GU et al. [113] studied that FSTL1 expression was upregulated in colorectal cancer (CRC) and positively related to infiltrating depth, lymph node metastasis, and poor prognosis; enhancing its expression could promote liver metastasis *in vivo*. In gastric malignancy, FSTL1 was found to enhance cancer cells' invasion by activating AKT via regulating TLR4/CD14 partially [114].

On the contrary, FSTL1 could inhibit tumor cells' growth, migration, invasion, and induced apoptosis in lung cancer [115]. In pancreatic cancer, FSTL1 was found to produce by stroma cells to suppress tumor cell growth, suggesting it is a novel tumor suppressor [70]. The function of FSTL1 is different in various organs, and the particular mechanism requires to be researched in the future.

1.3 DNA methylation

DNA methylation is one of the epigenetic modifications of genes present in all higher organisms. Generally, hypermethylation status implies inactivation/silencing of gene expression, and the hypomethylation state indicates activation/activation of gene expression [116]. Early studies found

that the DNA methylation status of tumor cells was extensively hypomethylation at the genome-wide level, resulting in the activation of proto-oncogenes and increased genomic instability. Later studies found that the methylation status of tumor cells was elevated in the promoter regions of antioncogenes and repair genes, i.e., hypermethylation, which resulted in the suppression of the expression of the corresponding antioncogenes [117, 118]; meanwhile, the hypermethylated genes in tumor cells were found to occur in the CpG islands in the promoter region, while the CpG islands in the promoter region of normal cells were mainly in the non-methylated state.

The relationship between aberrant methylation changes in genomic DNA of cancer cells, especially the silencing of antioncogene expression due to DNA hypermethylation, and pancreatic cancer has been extensively studied. For example, RAS association domain family 1 (RASSF1) has been discovered to be a candidate tumor suppressor gene. It has been suggested that the RASSF1A gene mainly functions as a promoter of apoptosis and senescence, which may be achieved by repressing the RAS pathway [119]. In a study researched among 45 pancreatic cancer tissues, 29 (64%) had detected RASSF1A promoter methylation [120]. Secreted apoptosis-related protein 2 (SARP2) is currently considered one of the target genes for abnormal methylation in PDAC, and it regulates apoptosis by acting on the Wnt-coiled protein signaling pathway; aberrant hypermethylation in its promoter region leads to inactivation of the gene, inhibits apoptosis, and promotes the development and progression of pancreatic malignancies [121, 122].

Like hypermethylation, abnormal hypomethylation of specific proto-oncogenes also performs an essential role in the formation and progression of PDAC. Mucins (MUCs) are a group of highly glycosylated macromolecular proteins intimately linked to the development and progression of various malignancies [123]. Studies [124-128] have

demonstrated that MUC4 performs an important role in tumor formation, progression, and distant metastasis in PDAC and can evade the body's immune surveillance; its expression was abnormal in PDAC and PanINs, but not in normal pancreatic cells, therefore, the abnormal expression of MUC4 is considered one of the indicators for early diagnosis, intervention, and prognosis of pancreatic cancer. Zhu Y et al. [129] showed that abnormal hypomethylation of MUC4 is intimately linked to the progression of PDAC and suggested that early diagnosis and assessment of the occurrence and progression of pancreatic cancer can be achieved by quantitative detection.

Through continuous exploration of the pathogenesis of PDAC, it is generally accepted that abnormal DNA methylation is significantly associated with the development of PDAC. Both abnormal DNA hypermethylation and hypomethylation lead to abnormal gene expression and encourage the transition of healthy cells into malignant tumors. At the same time, DNA methylation alteration also provides a new idea for diagnosing and treating pancreatic malignancies. By detecting the methylation status of target DNA, we can analyze the presence of pancreatic cancer early and then correct the abnormal DNA methylation to prevent further or even reverse cell carcinogenesis. Further elucidation of the mechanism of tumor cell-specific DNA methylation alteration and its relationship with tumor development will finally provide a new way of thinking to overcome the therapeutic challenges of pancreatic cancer.

1.4 Epithelial-mesenchymal transition

EMT is the process of epithelial cells changing into mesenchymal cells under particular physiological and pathological situations. It is described as the conversion of epithelial cells with polar, tightly connected properties into independent, migratory, and invasive mesenchymal cells with the ability to

invade the extracellular matrix [130]. In this progression, EMT is generally detected in the loss of epithelial markers, such as E-cadherin and ZO-1, and the acquisition of mesenchymal markers, such as vimentin and N-cadherin, at the molecular level [131]. Omar E et al. [132] emphasized EMT participated in the resistance of gemcitabine in pancreatic cancer. Moreover, it seems that cells undergoing EMT acquire stem-like characteristics, suggesting that EMT plays a significant role in CSC formation in PDAC [133]. Therefore, the genesis and progression of pancreatic cancer are remarkably linked to EMT. The study of signaling pathways and associated genes regulating the EMT process in tumor cells has recently gained a growing interest and has become a hot spot in tumor research [130].

1.5 Aim of this study

This research aims to initially compare the expression of remaining SPARC family genes, which have not been studied in pancreatic cancer, between the normal pancreatic cell line, pancreatic cancer cell lines, and pancreatic stellate cells. Choose the meaningful gene in pancreatic cancer using bioinformatics, and continue to investigate the cell function of this gene.

2. Material and Methods

2.1 Materials

2.1.1 Consumables

Consumables	Company or source
6-well plates	Thermo Fisher Scientific, Roskilde,Denmark
12-well plates	Thermo Fisher Scientific, Roskilde,Denmark
96-well plates	Thermo Fisher Scientific, Roskilde,Denmark
5ml pipette	Costar, Maine, USA
10ml pipette	Costar, Maine, USA
25ml pipette	Costar, Maine, USA
50ml pipette	Costar, Maine, USA
1.5ml tips	Eppendorf, Hamburg, Germany
2.0ml tips	Eppendorf, Hamburg, Germany
15ml tube	Falcon, Reynosa, Mexico
50ml tube	Falcon, Reynosa, Mexico
Blot paper	Bio-Rad, California, USA
Cell culture flask T25	Thermo Fisher Scientific, Roskilde,Denmark
Cell culture flask T75	Thermo Fisher Scientific, Roskilde,Denmark

Cell culture flask T125	Thermo Fisher Scientific, Roskilde, Denmark
Cell scraper	TPP, Trasadingen, Switzerland
FACS tubes	Falcon, New York, USA
Filter paper	Whatman, Maidstone, UK
Polyvinylidene difluoride membranes	Merck Group, Darmstadt, Germany
Low-attachment 96-well plates	Corning, Krailling, Germany
Transwell plates	Corning, New York, USA

2.1.2 Chemicals

Chemicals	Company or source	Identifier
β -Mercaptoethanol	Sigma-Aldrich, Steinheim, Germany	M6250
Agarose	Life science, leuven, Belgium	18J034129
Ammonium persulfate (APS)	Serva, Heidelberg, Germany	13376.01
BSA	Biomol, Plymouth Meeting, USA	9048-46-8
Crystal violet	Sigma-Aldrich, Steinheim, Germany	C0775
6X DNA Sample Loading Buffer	Thermo Fisher Scientific, Schwerte, Germany	R0611

30% PolyAcrylamid	Carl Roth, Karlsruhe, Germany	Art.-Nr 3029.1
DMSO	Sigma-Aldrich, Karlsruhe, Germany	D2650
DMEM/F12 Medium	Gibco, New York, USA	11330-032
DNA-Ladder standard	Invitrogen, California, USA	10787-018
ECL™ Western Blotting Detection System	Bio-Rad Laboratories, California, USA	102031594 102031597
80% Ethanol	Apotheke GH, Munich, Germany	603-002-00-5
>99% Ethanol	PanReac AppliChem, Germany	0v013438
FBS	Sigma-Aldrich, Steinheim, Germany	35079017
Loading buffer 4x	Bio-Rad, California, USA	161-0747
Methanol	Merck, Darmstadt, Germany	1.06009.1000
MTT powder	Thermo Fisher Scientific, Massachusetts, USA	2216966
Methyl cellulose	Sigma-Aldrich, Steinheim, Germany	Lot BCCB8250
Opti-MEM™	Thermo Fisher Scientific, Massachusetts, USA	31985070

PBS	PAN-Biotech, Munich, Germany	P04-36500
Protein standards	Bio-Rad, California, USA	RB227155
10X Tris/Glycine/ SDS buffer (Running buffer)	Bio-Rad Laboratories, California, USA	Cat#1610772
RNase-free water	Qiagen, Hilden, Germany	129112
RPMI 1640 Medium	Gibco, New York, USA	21875-034
Dulbecco's modified Eagle medium (DMEM)	Gibco, New York, USA	11995-065
Keratinocyte-SFM (1X)	Gibco, New York, USA	10724-011
EGF	Gibco, New York, USA	10450-013
Bovine Pituitary Extract (BPE)	Gibco, New York, USA	13028-014
RIPA lysis buffer 10X	Millipore, Darmstadt, Germany	20-188
SDS	Carl Roth, Karlsruhe, Germany	2326.2
TEMED	Thermo Fisher Scientific, Massachusetts, USA	17919
Transfer Buffer (20X)	Novex, Van Allen Way Carlsbad, CA	BT00061
Tris Base	Carl Roth, Karlsruhe, Germany	9090.3
Trypsin/EDTA	Lonza, St. Louis, USA	BE17-161E
Trypsin Inhibitor	Gibco, USA	17075-029

Tween 20	Sigma-Aldrich, Heidelberg, Germany	P1379
----------	---------------------------------------	-------

2.1.3 Antibodies

Primers	Company or source	Identifier
SPOCK2	Abcam, Cambridge, UK	Ab217044
ZO-1	Cell Signaling Technology, Frankfurt am Main, Germany	Cat#5406S
GAPDH	Cell Signaling Technology, Frankfurt am Main, Germany	Cat#2118
anti-rabbit IgG HRP	Cell Signaling Technology, Frankfurt am Main, Germany	Cat#7074
Precision Plus Protein Dual Color Standards	Bio-Rad, California, USA	Cat#1610374

2.1.4 Primers

Primers	Company or source	Identifier
SPOCK1	Qiagen, Hilden, Germany	Cat#RT ² 004598
SPOCK2	Qiagen, Hilden, Germany	Cat# RT ² 014767
SPOCK3	Qiagen, Hilden, Germany	Cat# RT ² 016950

SMOC1	Qiagen, Hilden, Germany	Cat# RT ² 022137
SMOC2	Qiagen, Hilden, Germany	Cat# RT ² 022138
CDH1	Qiagen, Hilden, Germany	Cat# RT ² 004360
CDH2	Qiagen, Hilden, Germany	Cat# RT ² 001792
ZO-1	Qiagen, Hilden, Germany	Cat# RT ² 175610
VIM	Qiagen, Hilden, Germany	Cat# RT ² 003380
B2M	Qiagen, Hilden, Germany	Cat# RT ² 004048
GAPDH	Qiagen, Hilden, Germany	Cat# RT ² 002046
RPS18	Qiagen, Hilden, Germany	Cat# RT ² 022551

2.1.5 Commercial Assays kits

Product	Company or source	Identifier
BCA protein Assay kit	Thermo Fisher Scientific, Schwerte, Germany	Cat# 23227
BEGM BulletKit™	Lonza, Basel, Switzerland	Cat#: CC-3170
BrdU cell cycle kit	BD Pharmingen, San Diego, CA	Cat# 559619

FlexiTube siRNA - SPOCK2	Qiagen, Hilden, Germany	Cat# 014767
Control (non-sil.) siRNA	Qiagen, Hilden, Germany	Cat#1022076
Lipofectamine RNAiMAX	Invitrogen, California, USA	Cat#13778-100
QuantiNova™ SYBR Green PCR Kit	Qiagen, Hilden, Germany	Cat#208154
Reverse-transcribed kit	Thermo Fisher Scientific, Schwerte, Germany	Cat#11756050
RNA isolate kit	Qiagen, Hilden, Germany	Cat#74904

2.1.6 Apparatus

Apparatus	Company or source
Autoclave	Unisteri, Oberschleißheim, Germany
Bio-Rad CFX96 Real-Time PCR system	Bio-Rad Laboratories, California, USA
Centrifuge	Hettich, Ebersberg, Germany
Cool Centrifuge	Eppendorf, Hamburg, Germany
Microcentrifuge	Labtech, Ebersberg, Germany
CO ₂ Incubator	Binder, Tuttlingen, Germany
DNA workstation	Uni Equip, Martinsried, Germany
Drying cabinet	Thermo Fisher Scientific, Schwerte, Germany

Electronic pH meter	Knick Elektronische Messgeräte, Berlin, Germany
FACS Fortessa	BD Biosciences, Heidelberg, Germany
Fridge (4°C, -20°C, and -80°C)	Siemens, Munich, Germany
Ice machine	KBS, Mainz, Germany
Inverted light microscope	Nikon, Tokyo, Japan
Liquid Nitrogen tank	MVE Goch, Germany
Lamina flow	Thermo Fisher Scientific, Schwerte, Germany
Microscope	Olympus, Hamburg, Germany
Micro weigh	Micro Precision Calibration, California, USA
Thermocycler	Eppendorf, Hamburg, Germany
Pipette boy	Eppendorf, Hamburg, Germany
Trans-Blot Turbo	Bio-Rad Laboratories, California, USA
Thermomixer comfort	Eppendorf, Hamburg, Germany
ChemiDoc Imaging System	Bio-Rad Laboratories, California, USA
VersaMax ELISA Microplate Reader	Molecular Devices, California, USA
Shaker	Edmund Bühler, Bodelshausen, Germany
Seahorse XFp Analyzer	Agilent, California, USA
Vortex Mixer VF2 (Janke & Kunkel)	IKA, North Carolina, USA

Water bath	Memmert, Schwabach, Germany
------------	-----------------------------

2.1.7 Software

Software and version	Company
FlowJo Version 10.0	BD Biosciences
Graphpad Prism 7.04	GraphPad
ImageJ version 1.50i	National Institutes of Health
R software 4.1.2	Comprehensive R Archive Network (CRAN)
SPSS	Version 26, US

2.1.8 Buffer and Solutions

MTT solution

MTT powder	25mg
PBS	50ml

Western blot

Separating Gel (10% and 12%)

	10%	12%
H ₂ O	4.1ml	3.4ml
1.5M Tris pH8.8	2.5ml	2.5ml
30% PolyAcrylamid	3.3ml	4.0ml
10% SDS	0.1ml	0.1ml
10% APS	50ul	50ul

TEMED	5ul	5ul
-------	-----	-----

Stacking Gel

H ₂ O	2.4ml
1.5M Tris pH6.8	1ml
30% PolyAcrylamid	0.6ml
10% SDS	0.04ml
10% APS	20ul
TEMED	4ul

1x Running Buffer

10X Tris/Glycine/ SDS buffer	100ml
H ₂ O	900ml

1x Transfer Buffer

Transfer Buffer 20x	50ml
Ethanol	150ml
H ₂ O	800ml

10x TBS

Tris Base	24g
NaCl	80g
H ₂ O	1000ml
PH	7.6

1x TBS-T

10x TBS	100ml
H ₂ O	900ml

Tween	1ml
-------	-----

Blocking Buffer

BSA	2.5mg
H ₂ O	50ml

Protein lysis Buffer

10x RIPA buffer	1ml
H ₂ O	9ml
Phospho Stop	1 Table
Protease Inhibitor	1 Table

1M Tris-HCl

Tris-base	12.12g
H ₂ O	200ml
PH	6.8

1.5M Tris-HCl

Tris-base	36.34g
H ₂ O	200ml
PH	8.8

Loading buffer

4xloading buffer	3600ul
β-Mercaptoethanol	400ul

10% SDS

SDS	10g
H ₂ O	100ml

10%APS

APS	10g
H ₂ O	100ml

2.2 Methods

2.2.1 Cell culture

2.2.1.1 Pancreatic carcinoma cells (PCCs)

The seven PCC cell lines Panc1, Dang, Aspc1, Capan1, Capan2, Miapaca-2, and Bxpc3 were originally purchased from ATCC and stored in bio-liquid nitrogen tanks in the laboratory of our department. Following ATCC guidelines, Panc1 and Miapaca-2 cell lines were used and cultured in a DMEM medium containing 10% FBS. In addition, the cell lines Dang, Aspc1, Capan1, Capan2, and Bxpc3 were cultured in RPMI 1640 media with 10% FBS. They all were cultivated in a humidified incubator with 5% CO₂ at 37 degrees Celsius. Replace the culture media every two to three days.

2.2.1.2 Human pancreatic duct epithelial cells (HPDE)

HPDE cells were borrowed from the laboratory of The Technical University of Munich (TUM). It was cultured in Keratinocyte-SFM Medium, supplemented with 10% FBS, meanwhile added 2.5µg EGF and 25mg BPE. Similarly, set in a 5% CO₂ incubator at 37 °C and passaged when it got about 80% confluence.

2.2.1.3 Pancreatic stellate cells (PSCs)

The three PSC cells were obtained from Yang Wu's group, which worked in our lab. These three PSC cells were activated stellate cells from three patients with PDAC. They woke up from the liquid nitrogen tank, cultured with DMEM/F12 containing 10% FBS in the incubator (37 °C, 5% CO₂/air), and changed the fresh medium twice weekly. Cell passage on when they were 80% confluence, then used for the experiment after 2-3 passages stable.

All the cells mentioned above were regularly screened for mycoplasma following laboratory regulations every four months and annually authenticated by IDEX BioResearch (Ludwigsburg, Germany).

2.2.2 Quantitative real-time polymerase chain reaction (qRT-PCR)

2.2.2.1 RNA extraction

After removing the cell-culture medium and washing the cells three times with PBS, the RNA was extracted using the Qiagen RNeasy Micro Kit. Firstly, I lysed cells by 350µl RLT buffer for about 10 minutes. Then, I pipetted 350µl of 70% ethanol and mixed it well. Next, 700µl was put into the RNeasy spin column from the mixture. The flow-through was thrown away after 30-second, 8,000-g centrifugation. Added 700µl RW1 buffer and followed by centrifugation (30s, 8000g). Flow-through was abandoned, added 500µl RPE buffer and followed by centrifugation (30s, 8000g). Then, I removed the flow-through, added 500µl RPE buffer, and spun at 8000g for two minutes. After centrifugation, I transferred the RNeasy spin column to a fresh 2ml collection tube carefully and turned for 1 minute at maximum speed. Then I transferred the RNeasy spin column to a new 1.5 ml collection

tube, put 30-50 μ l RNase-free water into it, and centrifugation was performed (1min, 8000g). Nanodrop 2000 was used to quantify RNA, and the A260/A280 ratio determined the purity. Finally, RNA samples were kept in a refrigerator at -80°C.

2.2.2.2 Reverse transcription and cDNA amplification

Reverse-transcribed using the SuperScript™ IV VILO™ Master Mix kit (Thermo Fisher, Inc.) and the reverse-transcribed reaction settings are shown in Table 1 below. In a thermocycler, RNA samples were reverse-transcribed according to the following protocol: Priming, 25 °C for 10 minutes, reverse transcription, 42 °C for 60 minutes, inactivation, 85 °C for 5 minutes. Finally, cDNA was stored in a -20°C fridge.

Table 1: The reverse-transcribed reaction settings

ezDNase enzyme	2ul
10X ezDNase buffer	4ul
Template RNA (1pg to 2.5ug to total RNA)	varies
RNase-free water	to 20ul

2.2.2.3 qRT-PCR

For the RT-PCR tests, the QuantiNova™ SYBR Green PCR Kit (Qiagen, Inc.) was employed. The kit's response configuration is detailed in Table 2 below. On a BioRad CFX96 RealTime PCR equipment (BioRad Laboratories, Inc.), the manufacturer's specified procedures were performed in a 20 μ l PCR mixture. The following were the RT-PCR amplification procedures: After 10 minutes of holding at 95°C, 15 seconds at 95°C and 1 minute at 60°C were performed for 40 cycles. Every sample was run in

triplicate, and instead of template DNA, sterile RNase-free H₂O was utilized as a negative control. The housekeeping genes 18S, B2M, and GAPDH were employed to standardize cDNA variation. Three independent tests were administered to each group. $2^{-\Delta CT}$ ($\Delta CT = CT_{\text{target gene}} - CT_{\text{housekeeping gene}}$) was utilized to compute the relative gene expression level. Meanwhile, in comparative intervention trails, it was normalized to the relative expression detected in the respective control groups, which was set at 1.0.

Table 2: Reaction setup of QuantiNova™ SYBR Green PCR Kit

SYBR Green PCR Master Mix	10ul
QN ROX Reference Dye	2ul
Primer	1ul
RNase-free water	varies
cDNA (≤ 100 ng/reaction)	varies
Total reaction volume	20ul

2.2.3 Western blot analysis

2.2.3.1 Protein extraction

Removed the old cell culture medium and washed it with PBS three times. Added the RIPA solution and placed it on ice for 40 minutes. After that, scraped the cells with a cold plastic scraper, collected them into a new 1.5ml tube, then centrifuged the tube with 10000g for 10 min at 4 degrees Celcius. Finally, sucked the supernatant into a new tube and immediately put them in an icebox.

2.2.3.2 Quantification of protein

To quantify proteins, I used the BCA Protein Assay Kit. Depending on the kit's protocol, the 195 μ l mixture reagents (reagent A: reagent B = 50:1) were added into each well of the 96-well plate. The Equiproportional dilution of standard or target proteins (5 μ l) was placed into each well containing the mixture reagents. Then, put the plate into the incubator at 37 °C for 30 minutes. After that, a plate reader was used to detect absorbance (562nm), plotting average blank-adjusted readout versus concentration (μ g/ml) yielded the standard curve based on standard proteins. According to the analysis result, added the corresponding loading buffer and ddH₂O, set the samples in the heater at 95 °C for 10 minutes and finally stored them in a -20°C fridge.

2.2.3.3 Preparation of polyacrylamide gel

First, cleaning the glass and spacers. On a flat desktop, I assembled glass sheets with spacers. The adequate running gel was filled into between two glass sheets. The running gel was coated with isopropanol and left for 30 minutes at room temperature. Then the isopropanol overlaid over the running gel was removed, and I filled the stacking gel solution until it overflowed. After that, I inserted a comb quickly and make sure there was no bubble between gel and comb. Set the gel to solidification for 30 min at room temperature and use for experiment immediately or stored at 4°C.

2.2.3.4 Polyacrylamide gel electrophoresis

SDS-PAGE wells were properly pipetted with samples containing 20g proteins and a weighted marker in the first and last lanes. Electrophoresis

equipment and running buffer were added under the manufacturer's instructions. The gel was then run at 120V for approximately 1 hour, as directed by the manufacturer.

2.2.3.5 Membrane transfer

PVDF membranes were stimulated with methanol for a few seconds to get them stimulated. Put the activated PVDF membrane on the filter paper and sponge and poured the transfer buffer into the transfer container. Then carefully removed the gel from the glass plates and put it on the membrane, covered with another filter paper and sponge to build a “sandwich”. Poured out the excessive transfer buffer and put the container into the machine to transfer at 25V for 30 minutes.

2.2.3.6 Immunoblotting

After transfer, I blocked the membrane with 5 % BSA for 1 hour at room temperature. Then I covered the membranes with particular primary antibodies for overnight at 4°C. These antibodies were used in the experiment: SPOCK2 Antibody (dilution: 1:1000), GAPDH Antibody (dilution 1:5000), ZO-1 Antibody (dilution: 1:1000).

On the second day, after removed the primary antibodies, I washed the membranes three times about 5 minutes by tris buffered saline containing Tween20 (TBS-T). On a shaker, membranes were treated for one hour with secondary antibodies (anti-rabbit IgG HRP, dilution 1:5000) at room temperature. Similarly, washed the membranes with TBS-T three times for 5 min.

2.2.3.7 Detection

Placed the membranes in the film cassette and added an X-ray agent, the autoradiography film was used to evaluate immunoreactive bands in the darkroom. Image J was used to calculate the grey values of the bands, which were afterward employed for statistical analysis.

2.2.4 Treatment with 5-aza-2'-deoxycytidine (5-aza-dC)

A vial containing 5 mg of 5-aza-dC lyophilized powder was obtained (Sigma- Aldrich). To make a 1 mM solution, the vial was reconstituted with 20 ml sterile water and stored at 4°C [134]. On the first day, in a 6-well plate, 1×10^5 cells per well were planted and cultivated overnight at 37°C in a 5% CO₂ incubator. On the second day, washed cells with PBS twice and changed the medium containing a concentration of 1µM 5-aza-dC for 48 hours [135]. This period changed the fresh medium containing a concentration of 1µM 5-aza-dC every day. After treatment, the cells were subjected to RNA extraction right away.

2.2.5 Small interfering RNA (siRNA) transfection

In 6-well plates containing RPMI1640 medium only with 10% FBS, cells were sown to about 60% confluence. After an overnight incubation period, the previous media was discarded, and PBS was used to wash the cells twice. Then, I appended 1.5 mL of fresh medium devoid of serum into each dish. For each transfected well, prepared the siRNA and Lipofectamine RNAiMAX mix as follows: 100 pmol of siRNA was put into 250µl of serum-free medium and gently mixed; then 5µl of Lipofectamine RNAiMAX was put into 250µl of serum-free medium for dilution and 5 minutes of room

temperature incubation; the diluted siRNA and Lipofectamine RNAiMAX were then scrambled gently and left for 20 min. After that, I put the mixture into each plate in a final volume of 2 ML per well and shook gently to mix. The plates were placed in a 5% CO₂ incubator at 37°C for 6 hours and replaced with the medium containing 10% FBS to continue the culture.

The same procedure was performed in the negative control group. The RNA and protein were extracted after 48 hours of transfection for testing efficiency by using RT-PCR and Western blot. For the experiment, the cells were collected after 24 hours of transfection.

2.2.6 MTT

After 24 hours of transfection, 5000 cells were planted in each well of a 96-well plate, and cell viability was assessed at different time points. Before testing, made a 5mg/ml MTT stock solution with PBS. Mixed the MTT stock with cell culture medium depending on the 1:10 ratio. Then removed the old medium and washed the cells with PBS twice. Added the 100µl mixture MTT/medium into each well and placed the plate in an incubator (37°C, 5% CO₂) for four hours. After that, I discarded the supernatant, added 100ul of DMSO, and placed them on the shaker for 10 min. Using a VersaMax microplate reader, the absorbance of each well was measured at 570 nm relative to a background wavelength of 670 nm. Wells that were empty functioned as controls. The test was conducted three times with identical conditions each time.

2.2.7 Flow Cytometric Analysis of Cells

After 24 hours of transfection, each well of a 6-well plate was planted with 1X10⁵ cells and grown with the complete medium for 48 hours [136].

Harvested the cells to analyze the cell cycle changes using Flow cytometry and BrdU Flow kits. Briefly, removed the old medium and washed with PBS two times. Changed the new complete medium and added 20 μ l BrdU solution (1 mM BrdU in 1xPBS) directly into each well, then placed the plate in an incubator (37°C, 5% CO₂) for 1 hour. Collected the cells and put them in a new FACS tube for 5 minutes at 500g centrifugation. The supernatant was discarded, rinsed with 1 ml PBS, then centrifuged at 500g for five minutes. I discarded the supernatant and resuspended in 100 μ l of BD Cytotfix/Cytoperm buffer and cultured for 15 min. I washed with 1 ml of 1xBD Perm/Wash buffer, then centrifuged at 500g for 5 minutes. Removed the supernatant and suspended the cells for ten minutes in 100 μ l of BD Cytoperm Permeabilization Buffer Plus on ice. Washed with 1ml 1xBD Perm/Wash buffer and repeated centrifugation at 500g for 5 minutes. I removed the supernatant and resuspended in 100 μ l of BD Cytotfix/Cytoperm buffer and placed on ice for 5 minutes. Similarly, washed cells with 1ml 1xBD Perm/Wash buffer and spun for 5 minutes at 500g. Then, I removed the supernatant and resuspended cells in 100 μ l diluted DNase (300 μ g/ml) and incubated at 37°C for 1 hour. After washing with 1xBD Perm/Wash buffer, added 50 μ l diluted fluorescent anti-BrdU and set at room temperature for about 20 min. Then rinsed with 1ml 1xBD Perm/Wash buffer and centrifuged, poured the supernatant, resuspended cells in 20 μ l of 7-AAD solution. Finally, added 1ml of FACS buffer and measured by flow cytometry immediately.

2.2.8 Transwell assay

After 24 hours of transfection, trypsinized cells from the well and washed cells with PBS three times carefully. In the upper chamber of the 8.0 μ m pore size transwell plate, 100,000 cells were seeded in 200 μ l serum-free media,

and 600µl complete medium was appended to the lower compartment. Placed the transwell plate in the incubator (37°C, 5% CO₂) for 36 hours. After incubation, took out the upper chamber, discarded the medium, then I washed it by PBS two times. The top layer of unmigrated cells was removed. Next, I fixed the cells for 30 minutes by 4% paraformaldehyde and stained for additional 30 minutes at room temperature by 0.1% Crystal Violet (CV). The top chamber was then rinsed three times with PBS and gently dried. Under an inverted light microscope (400x magnification), the numbers of migrating cells in three randomly selected areas were counted. Three independent replicate experiments were conducted under the same conditions.

2.2.9 Bioinformatic analysis

KM-plotter (<https://kmplotter.com/analysis/>) is a survival analysis website available online, and this database provides a lot of data used in published publications for survival analysis [137]. In our study, the website provided the data from The Cancer Genome Atlas (TCGA) repository, which included 177 pancreatic cancer patients with the whole RNA-seq and survival information. The discrepancy in overall survival was estimated using a Kaplan–Meier curve and a log-rank test based on the median expression of our target gene mRNA. A P-value of 0.05 was considered statistically significant [138].

Meanwhile, TCGA also provided the methylation data based on the Illumina HumanMethylation450 (HM450) BeadChips.

The International Cancer Genome Consortium (ICGC) collected tumor information from 50 distinct cancer types, including aberrant gene expression and mutations, epigenetic modifications, clinical information,

and so on [139]. Our ICGC-PACA-CA cohort was downloaded from the ICGC database (<https://dcc.icgc.org/>). The expression data in the dataset was normalized to fragment per kilobase million (FPKM) values. Finally, 167 pancreatic cancer patients with complete clinical information were confirmed after removing duplicate and missing values. Kaplan-Meier analysis was conducted to examine the difference in patients' overall survival using SPSS.

2.2.10 Statistical analysis

All experiments were carried out separately at least three times. GraphPad Prism, SPSS, and R software were used to conduct the statistical analysis and draw pictures. Data were presented as mean \pm SEM. Using the student t-test and One-Way ANOVA, the disparity between the two and multiple groups was established, and a p-value of less than 0.05 was considered statistically significant. Correlations between two continuous data sets were evaluated using Pearson's test and provided as p and r values, with $r > 0.3$ and $p < 0.05$ indicating statistical significance. To evaluate survival, the Kaplan–Meier technique and log-rank test were utilized. Time-dependent ROC curves (1 year and 2 year) were drawn to predict overall survival.

3. Results

3.1 Expression of the SPOCK2 is lower in the pancreatic cancer cell lines and pancreatic stellate cells than in the normal pancreatic cell line

We compared the mRNA level of SPOCK2, SPOCK3, SMOC1, and SMOC2 between one normal pancreatic cell line, seven pancreatic cancer lines, and three pancreatic stellate cells using qRT-PCR. Our result found that only SPOCK2 consistently decreased in all pancreatic cancer cell lines and pancreatic stellate cells than in the normal human pancreatic ductal epithelial cell line (HPDE) (Figure 3A). The SPOCK3 only increased in two pancreatic cancer cell lines than HPDE (Figure 3B). The SMOC1 decreased in three pancreatic cancer cell lines and two pancreatic stellate cells than HPDE; however, it increased in one pancreatic cancer cell line (Figure 3C). The SMOC2 decreased in four pancreatic cancer cell lines and three pancreatic stellate cells than HPDE (Figure 3D).

Next, we combined the seven pancreatic cancer cell lines (PCCs) and three pancreatic stellate cells (PSCs) and continued to compare them with HPDE. We found that also SPOCK2 levels decreased in PCCs and PSCs than in HPDE, but there was no difference between PCCs and PSCs (Figure 4A). Interestingly, the SPOCK3 increased in PCCs more than HPDE and PSCs, but there was no difference between HPDE and PSCs (Figure 4B). The SMOC1 increased significantly in PCCs compared to PSCs but was no different compared to HPDE; meanwhile, there was no difference between HPDE and PSCs (Figure 4C). The SMOC2 decreased remarkably in PSCs than HPDE but was no different than PCCs, and there was no difference between PCCs and HPDE (Figure 4D).

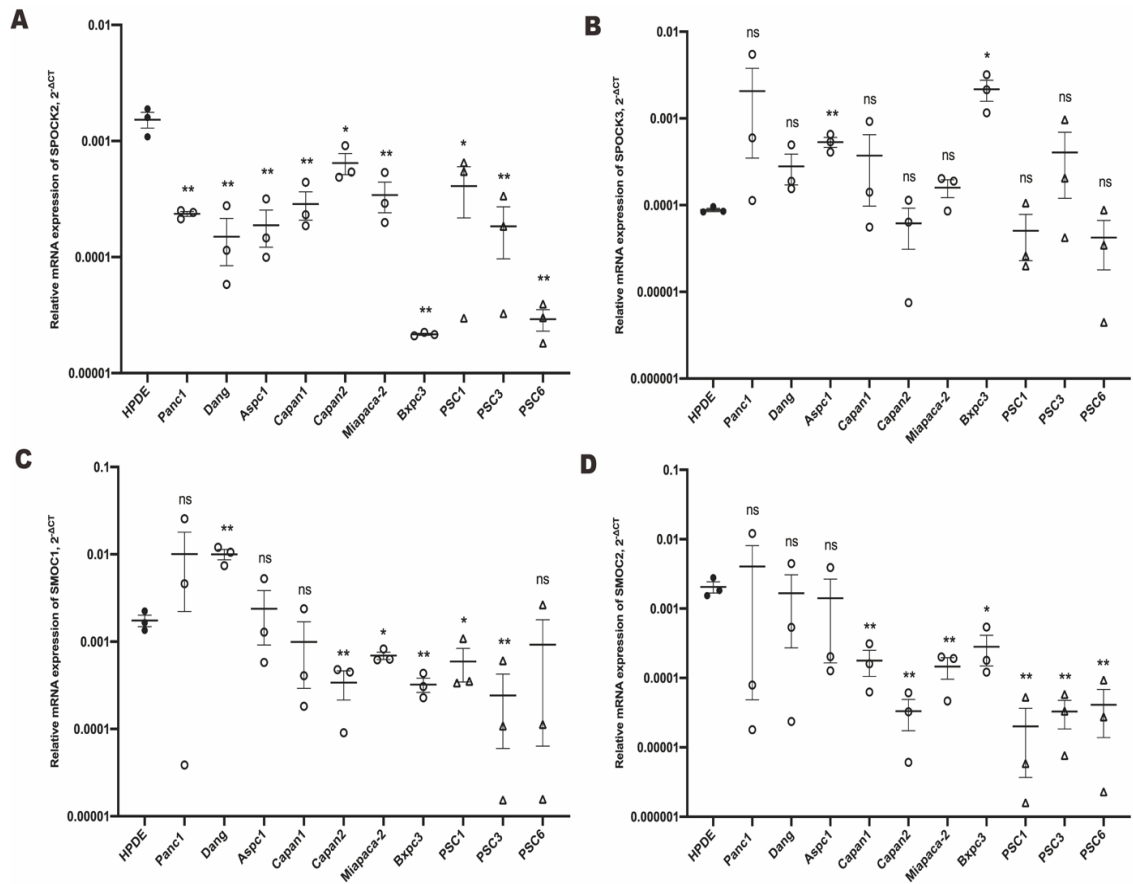


Figure 3. The expression of SPOCK2, SPOCK3, SMOC1, and SMOC2 in the normal pancreatic cell line, seven pancreatic cancer cell lines, and three pancreatic stellate cells in mRNA level.

The mRNA level of SPOCK2(A), SPOCK3(B), SMOC1(C), and SMOC2(D).

The mean of housekeeper genes RPS18 and B2M was utilized as a reference and quantified using the $2^{-\Delta Ct}$ method. Each pancreatic cancer cell line and the pancreatic stellate cell were compared to HPDE individually. Each sample was assayed in triplicate independently. * $P < 0.05$, ** $P < 0.01$, *** $P < 0.001$, **** $P < 0.0001$ and ns means no significance. The value was shown as mean \pm SEM

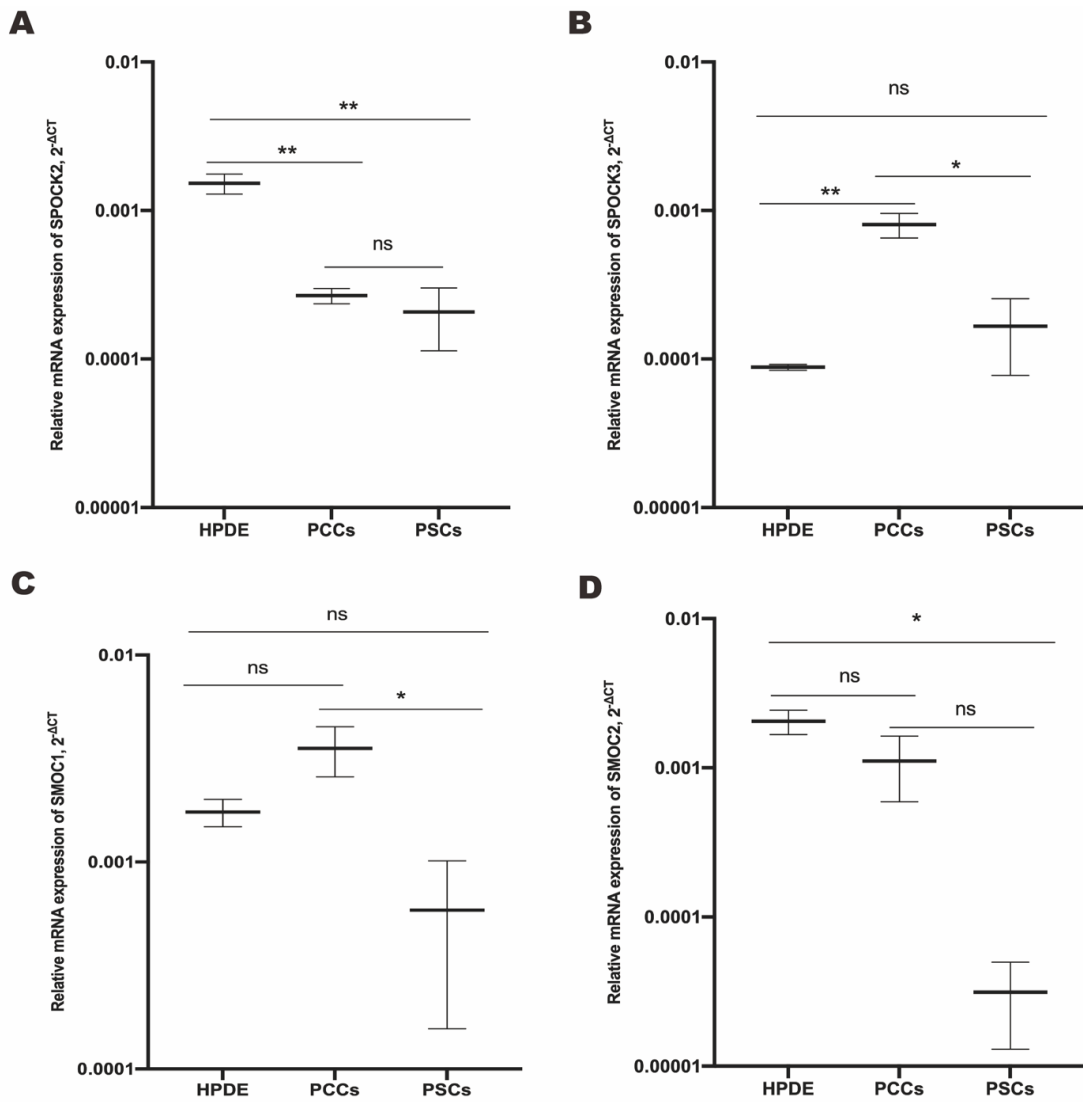


Figure 4. The mRNA level of SPOCK2, SPOCK3, SMOC1, and SMOC2 in HPDE, PCCs, and PSCs.

The mean of housekeeper genes RPS18 and B2M was utilized as a reference and quantified using the $2^{-\Delta Ct}$ method. * $P < 0.05$, ** $P < 0.01$, and ns mean no significance. The value was shown as mean \pm SEM.

PCCs, pancreatic cancer cell lines; PSCs, pancreatic stellate cells.

3.2 The low level of SPOCK2 is associated with poor prognosis of patients with pancreatic cancer in a bioinformatic analysis

We searched whether the expression of these four SPARC family genes was correlated with pancreatic cancer clinical prognosis using KM-plotter online tool. This website provided 177 pancreatic cancer patients from The Cancer Genome Atlas (TCGA) repository with the whole RNA-seq and survival information. Depending on the median expression of our genes were divided into high- and low- expression groups. After comparison, we found only SPOCK2 could affect overall survival, and high levels correlated with more prolonged survival (HR = 0.64, P= 0.031) (Figure 5).

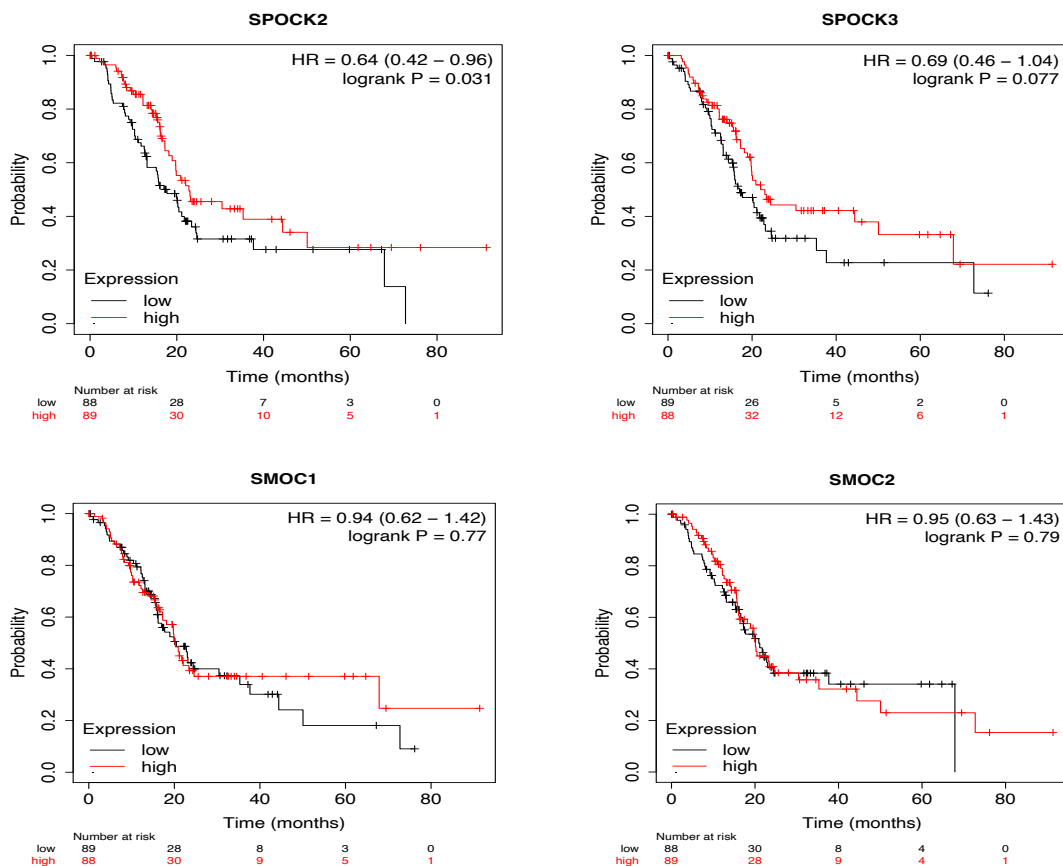


Figure 5. KM survival analysis of SPOCK2, SPOCK3, SMOC1, and SMOC2 in PDAC patients via KM Plotter. (<https://kmplot.com/analysis/>)

To further validate the correlation between these four genes and prognosis in pancreatic cancer, we use another cohort PACA-CA from International Cancer Genome Consortium (ICGC). After removing duplicate and missing values, this cohort included 167 pancreatic cancer patients with the whole RNA-seq and prognostic information (Supplementary Table 1). Similarly, our genes were divided into high- and low-expression groups based on the median expression. On univariate analysis, we found that only SPOCK2 was associated with overall survival. The median survival of patients with a lower level of its expression was less than that in patients with higher (Table 3). As evident from Kaplan–Meier survival curves in Fig. 6, patients with a greater SPOCK2 gene had a significantly longer survival rate than those with a lower gene.

Gene	Number of	Number of	Median survival in	<i>P</i> (log-rank	<i>HR</i>	<i>P</i>
Exp.	Case	Deaths	Months (95% CI)	test)		value
SPOCK2						
low	84	70	15.2 (8.6-21.8)	0.014	1.0	0.015
high	83	63	21.1 (18.1-24.1)		0.6 (0.4-0.9)	
SPOCK3						
low	84	66	19.7(15.0-24.5)	0.676	1.0	0.676
high	83	67	19.1(13.7-24.6)		1.1(0.8-1.5)	
SMOC1						
low	84	64	18.2(13.2-23.3)	0.299	1.0	0.300
high	83	69	20.3(15.6-24.9)		1.2(0.9-1.7)	
SMOC2						
low	84	63	19.7(13.2-26.3)	0.837	1.0	0.840
high	83	70	19.3(15.8-22.8)		1.0(0.7-1.5)	

Table 3. Correlation of SPOCK2, SPOCK3, SMOC1, and SMOC2 expression with survival in PDAC patients.

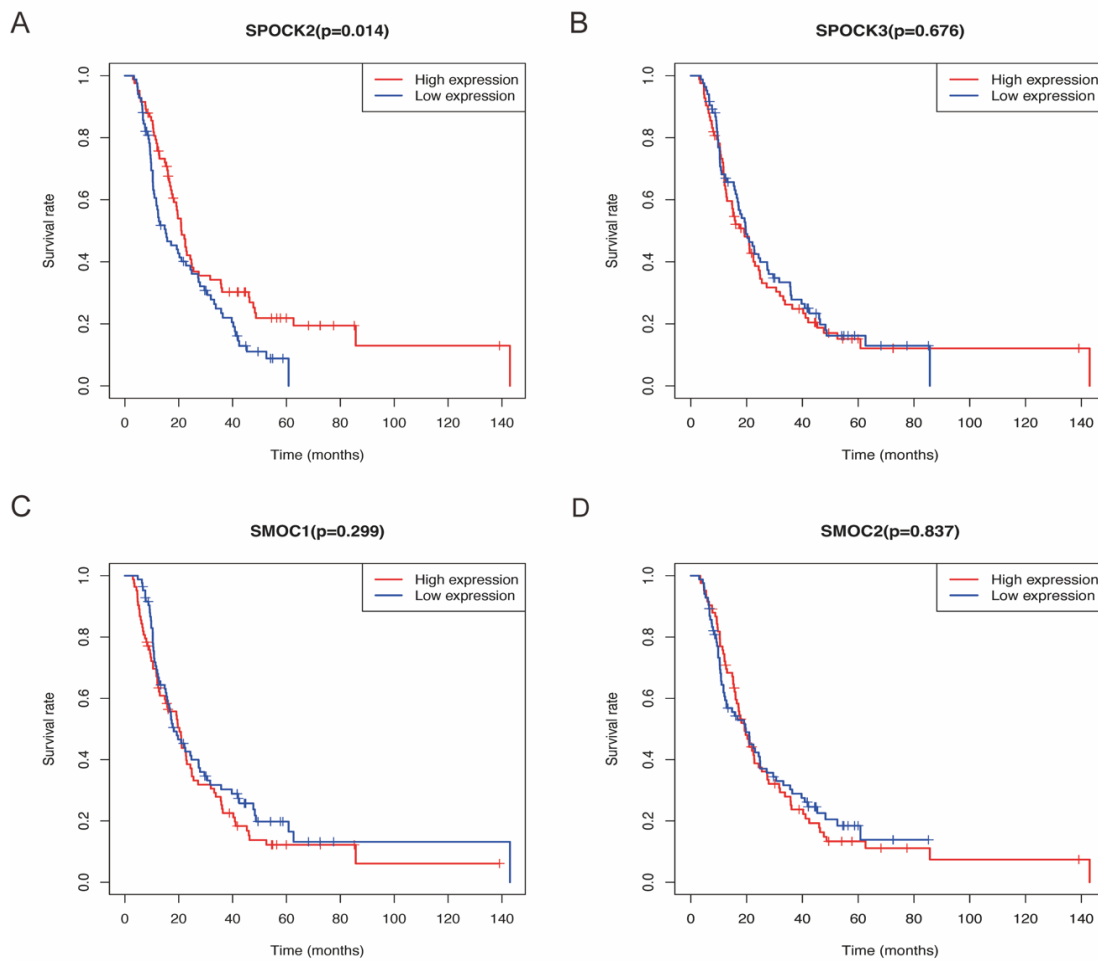


Figure 6. Kaplan–Meier curves show survival patterns for high and low expression (red and blue) in SPOCK2 gene (a), SPOCK3 gene (b), SMOC1 gene (c), and SMOC2 gene (d) in PDAC patients.

In summary, our result revealed that only SPOCK2 significantly differed among the normal pancreatic cell line, PDAC cell lines, and pancreatic stellate cells. It decreased in PDAC cell lines and pancreatic stellate cells stably. Meanwhile, increasing the level of SPOCK2 prolonged the survival time of PDAC patients by analyzing and confirming two different databases. Thus, it suggested that SPOCK2 was worth continuing to research profoundly and hypothesized that it acted the suppressing function in pancreatic cancer.

3.3 Decreased SPOCK2 expression in PDAC due to hypermethylation

DNA methylation is one of the common causes of silencing of human tumor suppressor gene expression. Chen et al. [140] found that the SPARC gene promoter was methylated and correlated with poor outcomes in gastric cancer. Hence, we hypothesized that the lower expression of SPOCK2 in PDAC might be due to hypermethylation.

First, we downloaded the raw data, including transcriptome profile (RNA-seq FPKM) and methylation (HM450) beta values from TCGA pancreatic cancer cohort for SPOCK2. Next, we combined each sample with the corresponding FPKM and beta values and performed a correlation analysis (Supplementary Table 2).

Our analysis revealed that as the methylation level in the promoter of SPOCK2 increased, its expression decreased accordingly, showing a negative linear correlation (Figure 7, $r = -0.586$, $P < 0.0001$).

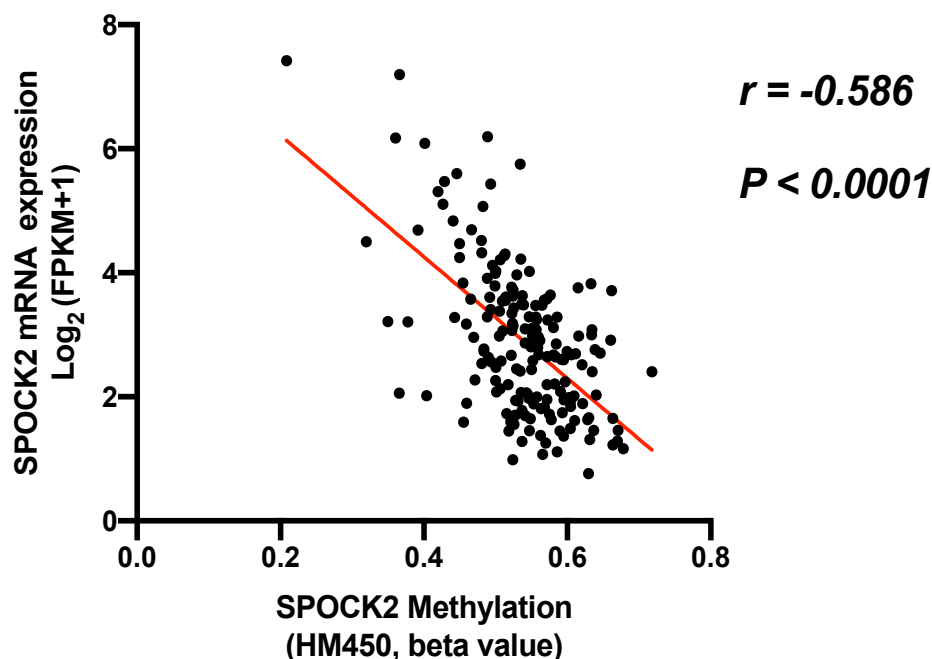


Figure 7. The correlation between expression and methylation of SPOCK2.

The y-axis represented the SPOCK2 gene's mRNA expression; the x-axis represented its promoter methylation (unit: beta value).

To further validate our bioinformatics analysis and explore DNA methylation's impact on SPOCK2 expression in PDAC cells. We treated three PDAC cell lines (Panc1, Dang, and Capan2) with 5-aza-2'-deoxycytidine (5-aza-DC), a DNA demethylating agent, for 48 hours at 1uM. Treatment with this dose of 5-aza-dC was sufficient to reactivate several methylation genes without causing cell death in prior experiments [141, 142]. After treatment, we extracted RNA from these three PDAC cell lines and examined them by qRT-PCR. Our result revealed that SPOCK2 expression increased after treatment of 5-aza-dC (Figure 8).

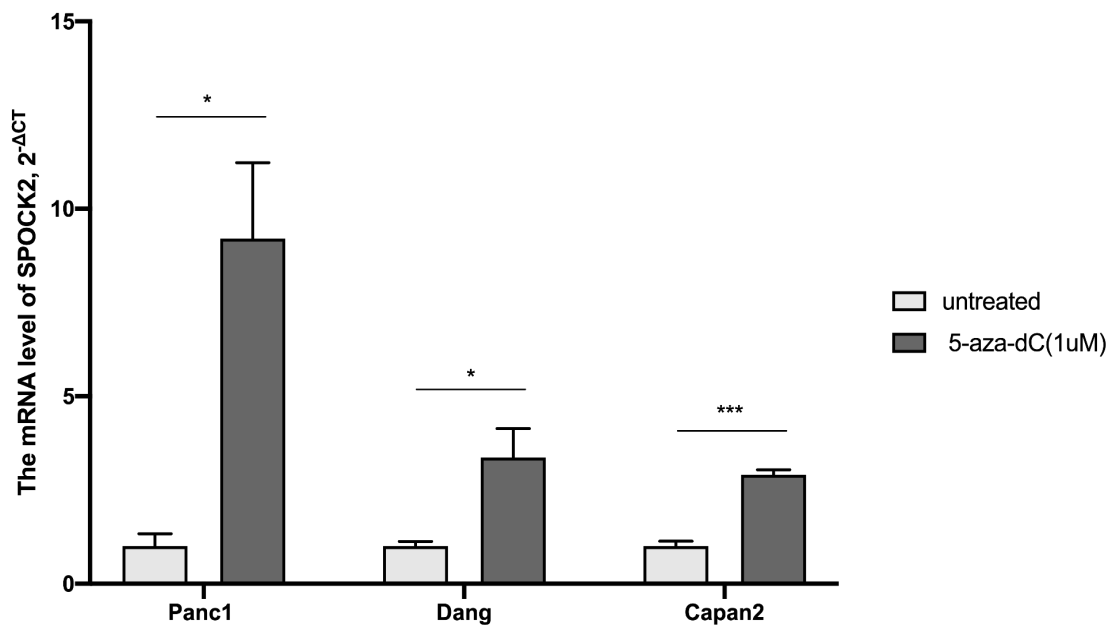


Figure 8. The mRNA expression of SPOCK2 in Panc1, Dang, and Capan2 cell lines after treatment with 5-aza-dC. The housekeeper gene GAPDH was utilized as a reference. The $2^{-\Delta C_t}$ method measured gene level and normalized relative expression detected in the corresponding untreated group, defined as 1.0. * $P < 0.05$, *** $P < 0.001$. The value was shown as mean \pm SEM.

After confirming that SPOCK2 could rise after demethylation at the mRNA level, we wanted to investigate whether it affects the expression of the protein. Hence, we detected the protein level of SPOCK2 through the same method of 5-aza-dC treatment, but we only chose the two PDAC cell lines (Panc1 and Capan2) this time. As our result, we found the SPOCK 2 protein level also could increase ($P < 0.05$) after demethylation, but not significantly than the mRNA level (Figure 9).

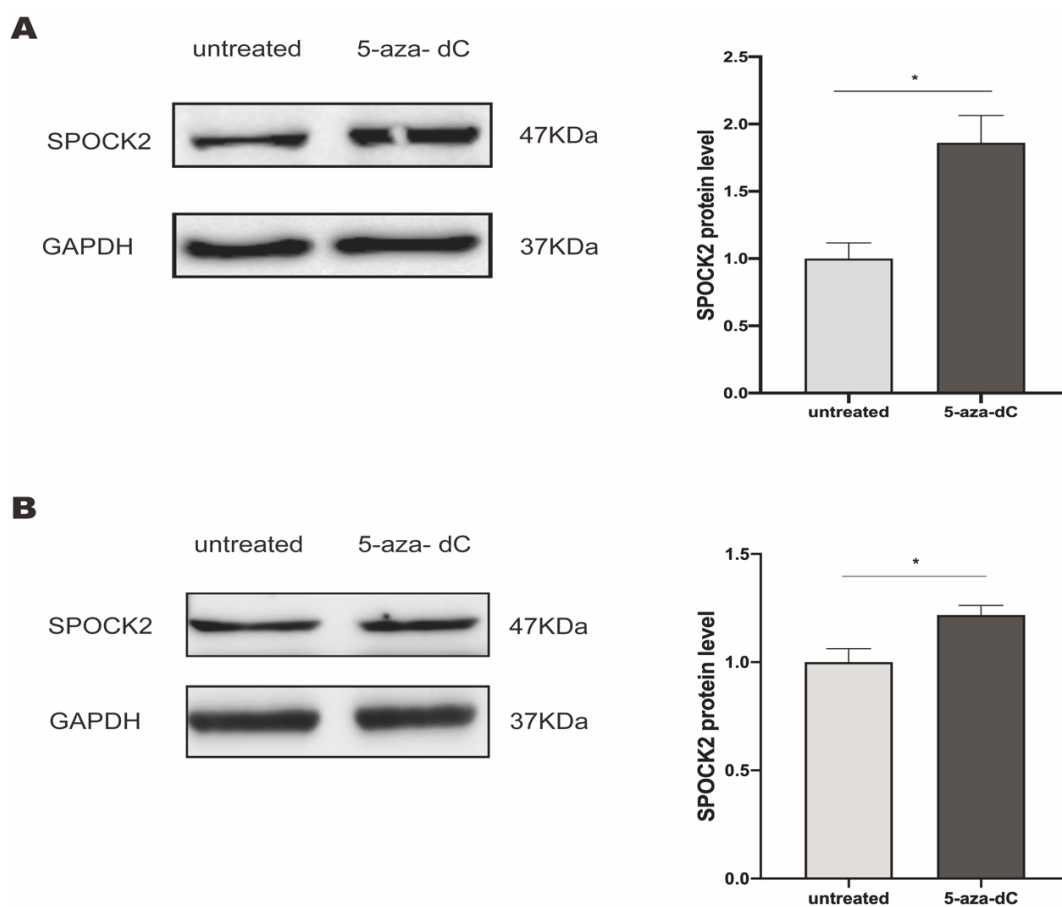


Figure 9. The protein expression of SPOCK2 in Panc1 and Capan2 cell lines after treatment with 5-aza-dC. Western blot analysis revealed that SPOCK2 protein increased in Panc1 (A) and Capan2 (B) cell lines after 5-aza-dC treatment. GAPDH was used as the loading control. ImageJ was used to determine the quantification and shown as a graph bar. * $P < 0.05$, the data were shown as mean \pm SEM.

3.4 Hypermethylation of SPOCK2 correlates with poor survival in PDAC

From the above results, we found that reducing the expression of SPOCK2 because of hypermethylation and thus might be unfavorable for the prognosis of PDAC patients. Whether the hypermethylation of SPOCK2 could influence survival directly or predict prognosis in PDAC. Therefore, we combined each sample's beta value with survival information also downloaded from TCGA (Supplementary Table 3). Generally, the beta value from 0.5-0.7 and 0.25-0.3 are considered hypermethylation and hypomethylation, respectively [143, 144]. So, we used a cut-off of 0.5 to divide into hypermethylation and non-hypermethylation two groups. Our univariate analysis showed that the median survival of patients with hypermethylation of SPOCK2 was less than the median survival in patients with non-hypermethylation (Table 4). As evident from Kaplan–Meier survival curves in Fig. 10, patients with hypermethylation of SPOCK2 had a significantly lower survival rate than those with non-hypermethylation. Hence, the hypermethylation of SPOCK2 might be regarded as a high risk for prognosis in PDAC.

	Number of Case	Number of Deaths	Median survival in Month (95%CI)	<i>P</i> (log-rank test)	<i>HR</i>	<i>P</i> value
SPOCK2						
Non-Hypermethylation	43	11	35.3(11.7-58.9)	0.028	1.0	
Hypermethylation	137	54	20.1(16.2-24.0)		2.1(1.1-3.9)	0.031

Table 4. Correlation of SPOCK2 methylation with survival in PDAC patients.

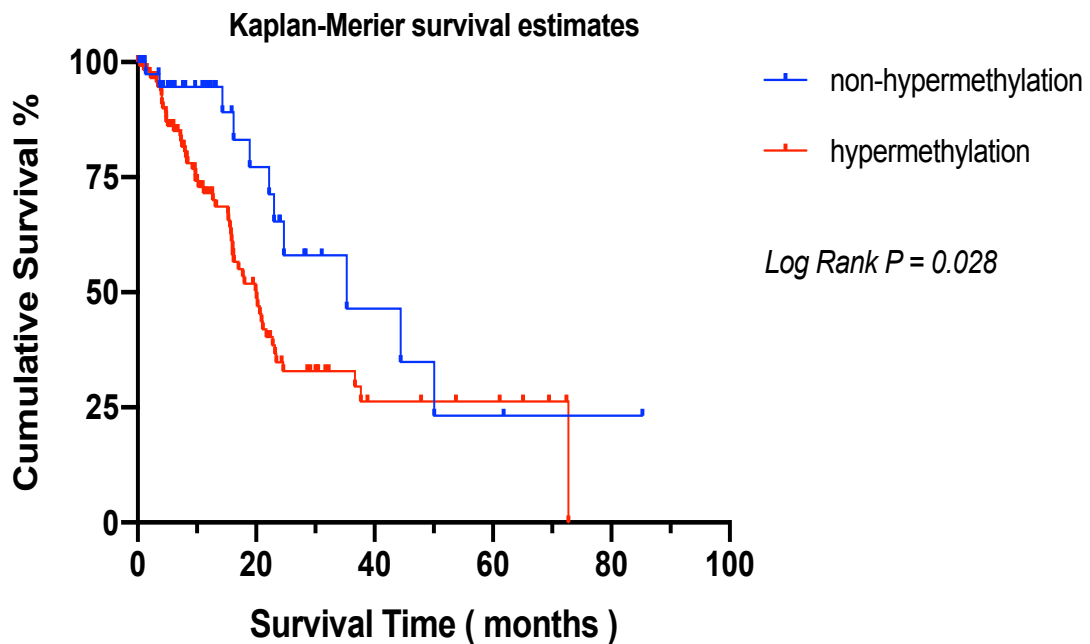


Figure 10. Kaplan–Meier curves show survival patterns for hypermethylation and non-hypermethylation (red and blue) of SPOCK2 in PDAC patients.

Meanwhile, an analysis of Time-dependent ROC curves (1 and 2 years) of SPOCK2 methylation in PDAC was performed. We found the methylation level of SPOCK2 show the ability to predict the survival of PDAC patients (1 year AUC = 0.700, 2 year AUC = 0.707) (Figure 11).

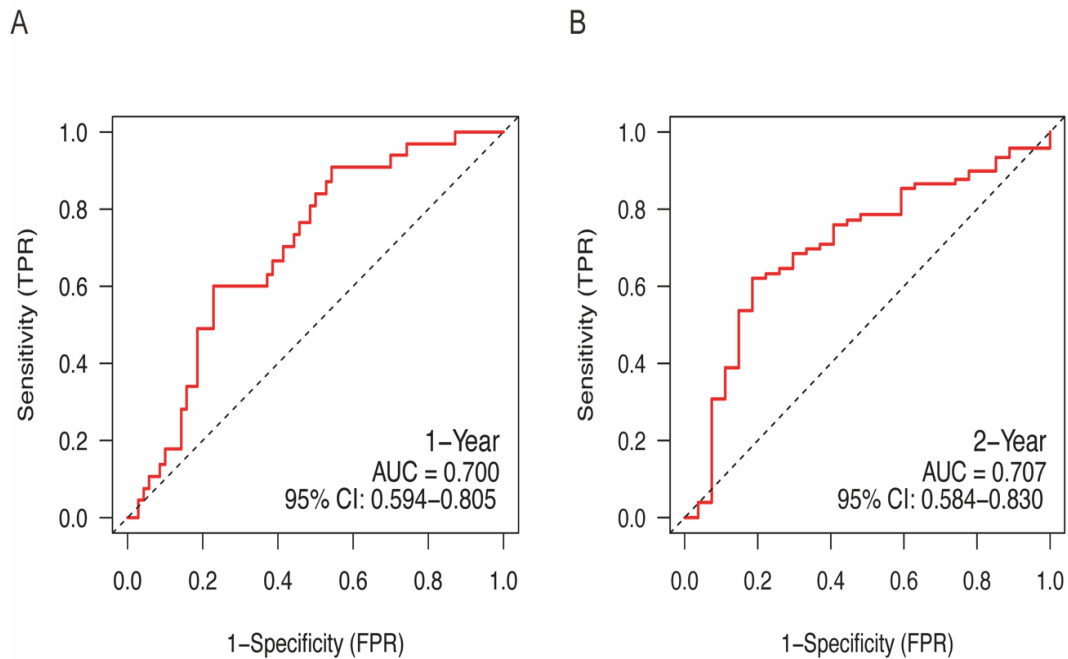


Figure 11. Time-dependent ROC curves were drawn to predict the survival for one year (A) and two year (B) in PDAC.

3.5 Knockdown of SPOCK2 induces certain phenotypic effects in PDAC

According to the above results, we suspected that SPOCK2 might perform as a suppressing gene in PDAC. So, we wanted to explore the biological role of SPOCK2 in PDAC initially and whether it could affect cancer cells.

From the mRNA expression of SPOCK2 (Figure 3 A), we found its expression level was higher in Capan2 than in other pancreatic cancer cell lines. Hence, we chose Capan2 for the following research.

First, we knocked down SPOCK2 by transfecting Capan2 with siRNA. The knockdown efficiency was evaluated through qRT-PCR and Western Blot, which showed about 70% and 40% decrease in mRNA and protein levels compared to the negative control (Figure 12).

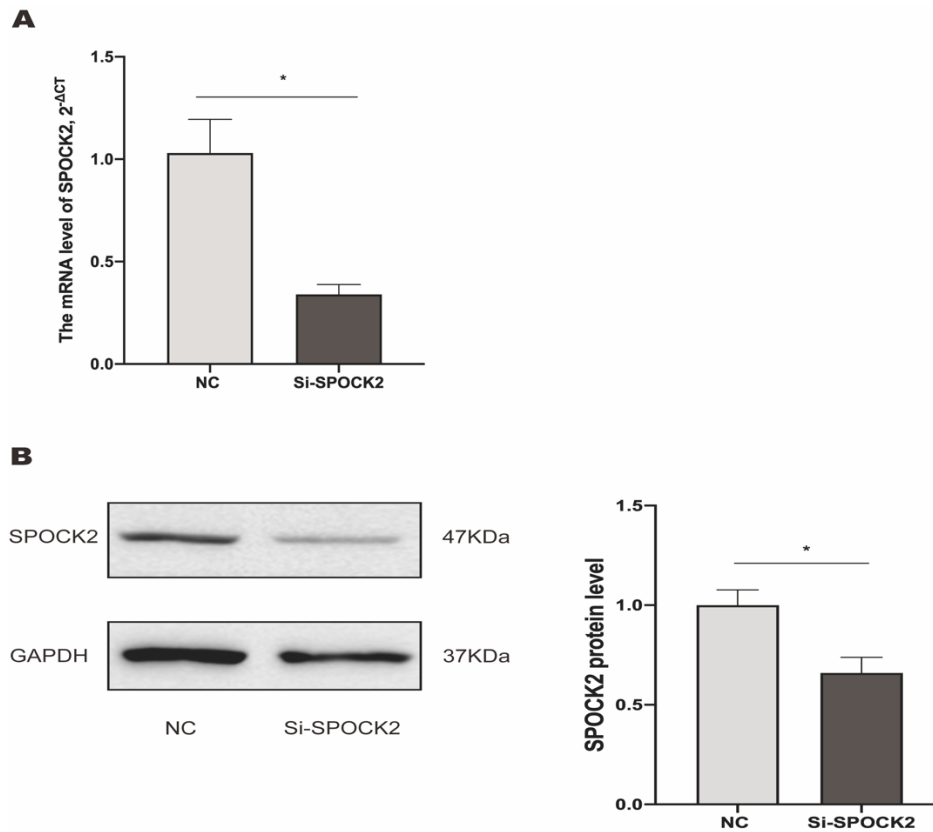


Figure 12. The expression of SPOCK2 after transfection of siRNA in Capan2.

(A) qRT-PCR showed the mRNA level. The housekeeper gene GAPDH was utilized as a reference. The $2^{-\Delta Ct}$ method measured gene level and normalized relative expression detected in the corresponding NC group, defined as 1.0. *P<0.05.

(B) Western blot analyzed the protein level. GAPDH was used as the loading control. ImageJ was used to determine the quantification and shown as a graph bar. *P<0.05.

Values were expressed as mean \pm SEM. NC, negative control. Si-SPOCK2, small interfering RNA for SPOCK2.

3.5.1 Knockdown of SPOCK2 increases the cell growth rate in PDAC cells

Next, we investigated whether SPOCK2 could impact PDAC cell growth. After 24 hours of transfection, we detected the cells' proliferation at different time points (12h, 24h, 48h, and 72h) by MTT in Capan2. Our results showed

that inhibiting the SPOCK2 expression could stimulate cell proliferation, especially during the 48 and 72 hours ($P < 0.05$, Figure 13), so we suggested that SPOCK2 could inhibit cell proliferation in pancreatic cancer.

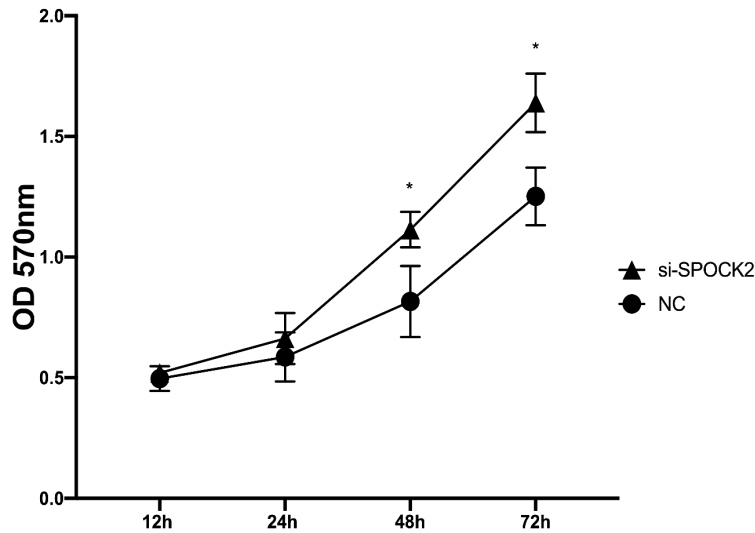


Figure 13. Effects of SPOCK2 knockdown on cell proliferation. The proliferation of cells was increased following SPOCK2 down-regulation by si-RNA in vitro. * $P < 0.05$, NC, negative control. si-SPOCK2, small interfering RNA for SPOCK2.

3.5.2 Knockdown of SPOCK2 causes the cell cycle change in PDAC cells

Although we discovered that SPOCK2 could influence PDAC cell growth, the mechanisms behind this phenomenon remain unknown. The cell cycle is thought to regulate cell proliferation generally [145, 146]; however, whether SPOCK2 participates in these mediation processes is unknown. Hence, flow cytometry was performed to detect the role of SPOCK2 interference in the cell cycle. Our results showed that compared to the negative control group, the S phase and G2/M phase hold an increasing tendency, but the G0/G1 phase significantly decreased in the SPOCK2 knockdown group ($P < 0.05$, Figure 14). Thus, combined with previous results, we speculated that

SPOCK2 could induce G0/G1 phase arrest to inhibit cell proliferation in pancreatic cancer further.

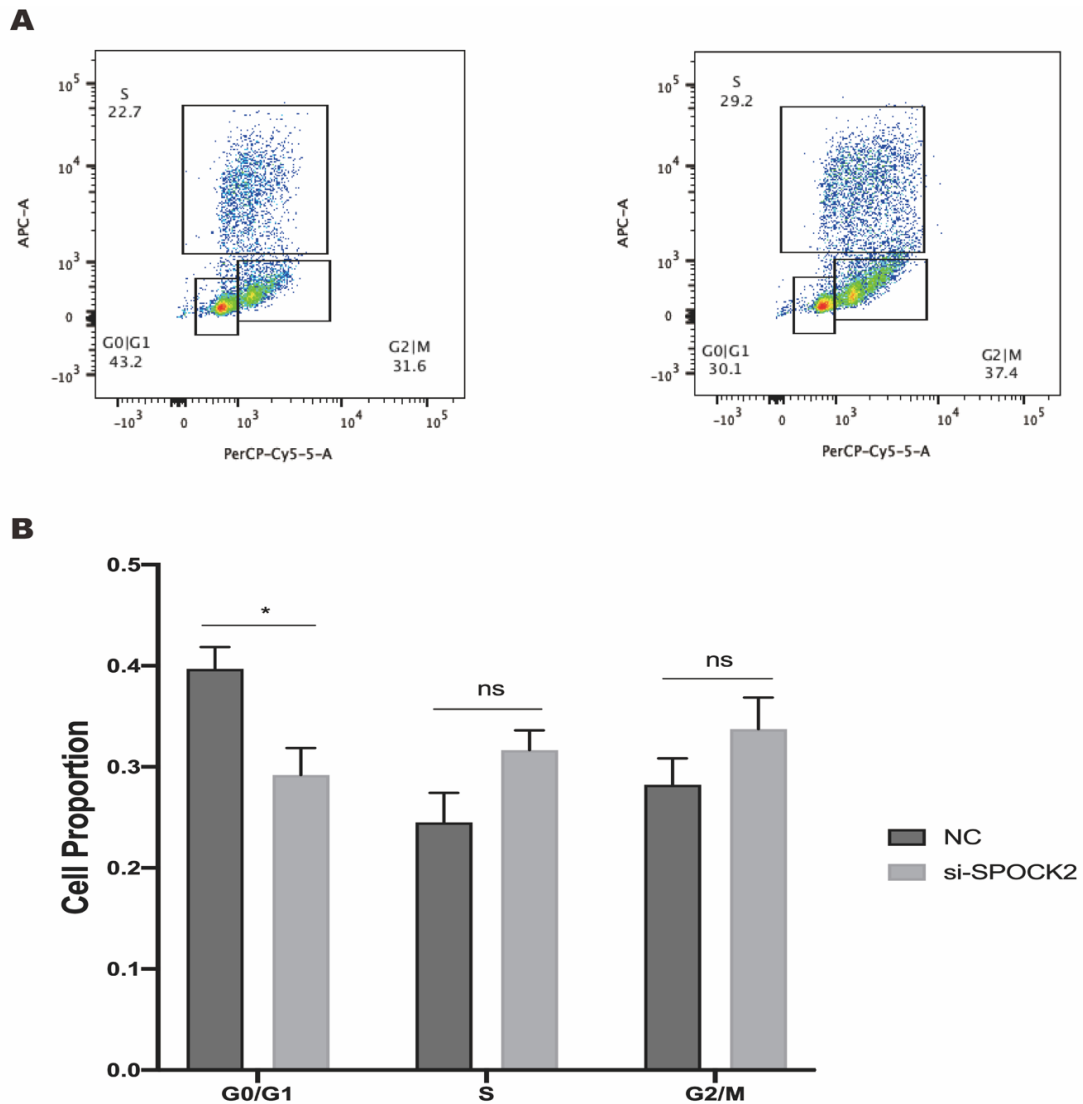


Figure 14. Cell cycle analysis of SPOCK2 knockdown in Capan2 cells.

(A) Flow cytometry dot plots showing the changes in the cell cycle.

(B) Statistical analysis was conducted on the percentage of different phases.

* $P < 0.05$, ns = of no significance. NC, negative control. si-SPOCK2, small interfering RNA for SPOCK2. Values were shown as mean \pm SEM.

3.5.3 Knockdown of SPOCK2 can stimulate migration in PDAC

After confirming the impact of SPOCK2 on the viability of PDAC cells, we want to continue to assess whether it affected the migration of PDAC cells. Therefore, we performed transwell assays to detect the migration ability in Capan2 cells after the knockdown of SPOCK2. One hundred thousand cells were seeded in the upper chamber with serum-free media after 24 hours of transfection by si-RNA and then measured migratory cells in the lower chamber side membrane after 36 hours. As seen in Figure 15, we found migratory cells were more in the SPOCK2 knockdown group than in the negative control group.

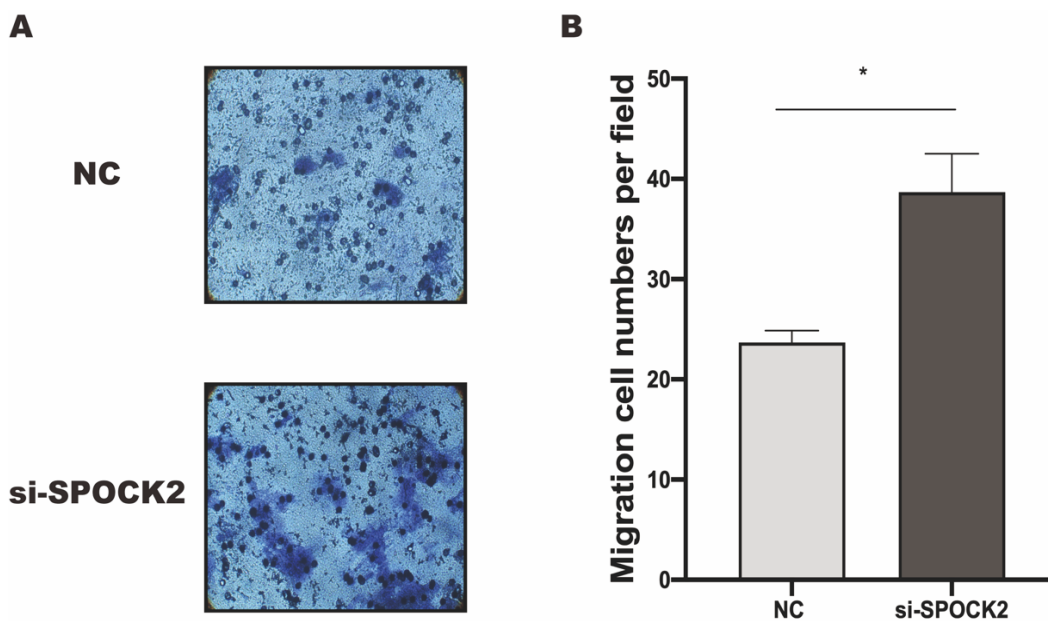


Figure 15. Effects of SPOCK2 knockdown on migration in PDAC cells. (A) Representative photos of transwell assay. (B) Quantification of transwell experiment. * $P < 0.05$, ns = of no significance. NC, negative control. si-SPOCK2, small interfering RNA for SPOCK2. Values were shown as mean \pm SEM.

3.5.4 Knockdown of SPOCK2 resulted in the downregulation of ZO-1

EMT is an efficient method for epithelial cells to acquire the capacity to migrate; hence, it has become a crucial mechanism for epithelial cell carcinoma infiltration and metastasis [147]. Therefore, we suspected whether there is a relationship between SPOCK2 and EMT or not. Hence, we chose EMT markers, including E-cadherin, N-cadherin, ZO-1, and Vimentin, tested by qRT-PCR after 48 hours of transfection by si-RNA in Capan2 cells. Our result showed no change with the epithelial marker E-cadherin and mesenchymal markers N-cadherin and Vimentin after SPOCK2 knockdown, but the epithelial marker ZO-1 decreased (Figure 16). Hence, we indicated might a positive relationship between ZO-1 and SPOCK2.

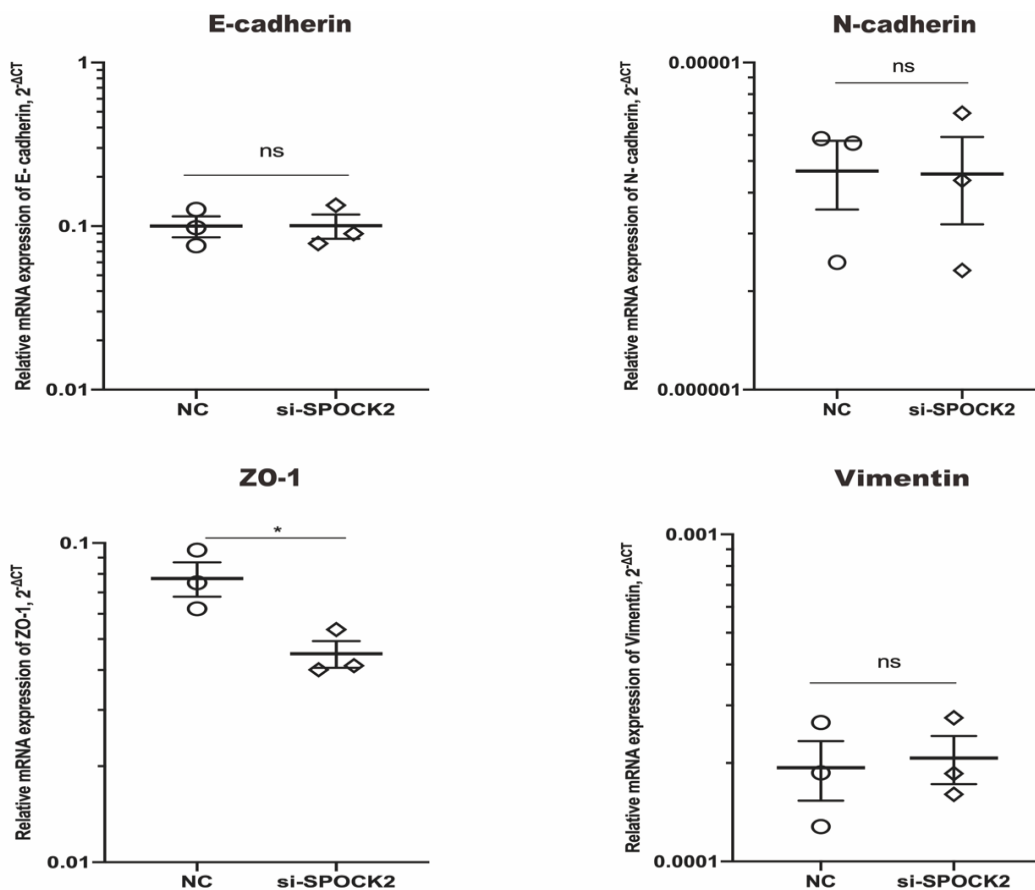


Figure 16. The changes of EMT markers (E-cadherin, N-cadherin, ZO-1, Vimentin) after SPOCK2 knockdown in Capan2 cells. The housekeeper gene GAPDH was utilized as a reference and quantified using the $2^{-\Delta Ct}$ method. *P<0.05. ns = of no significance. NC, negative control. si-SPOCK2, small interfering RNA for SPOCK2. Values were shown as mean \pm SEM.

After confirming the suppressing expression of ZO-1 after SPOCK2 knockdown at the mRNA level, we further tested whether SPOCK2 influenced the expression of ZO-1 at the protein level. Similarly, western blot analyzed the expression of ZO-1 protein after 48 hours of transfection. As seen in Figure 17, the expression of ZO-1 also decreased in protein level after SPOCK2 knockdown, though no more significant than the mRNA level.

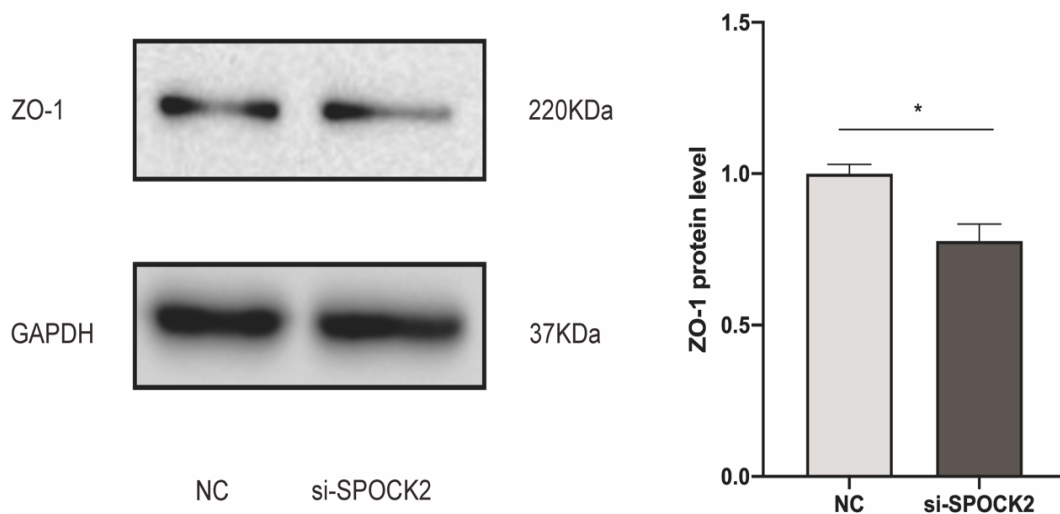


Figure 17. The ZO-1 protein decreased after SPOCK2 knockdown in Capan2 cells. GAPDH was used as the loading control. ImageJ was used to determine the quantification and shown as a graph bar. *P<0.05. NC, negative control. si-SPOCK2, small interfering RNA for SPOCK2. Values were shown as mean \pm SEM.

4. Discussion

Patients with pancreatic ductal adenocarcinoma (PDAC) are typically diagnosed at an advanced stage and are not eligible for resection, thereby making PDAC as a fatal disease [148]. Multiple treatments, including chemotherapy, radiotherapy and immunotherapy, have not brought enough success in improving the outcomes of patients with PDAC [149-151]. Therefore, identifying accurate tumor markers for the prevention, early detection and treatment of PDAC has gained more attention in last years. Table 5 lists some literature published about potential prognostic/therapeutic markers for PDAC this year.

Biomarker	Expression in PDAC tissue/cell lines	Biological role in PDAC cells (<i>in vitro</i>)	Prognosis of patients with PDAC (High expression)	Reference
SPON1	High	Promote cell growth	Unfavorable	Huo et al.2022[152]
YOD1	High	Facilitate proliferation and migration	Unfavorable	Zhang et al.2022[153]
SEMA3C	High	Promote cell growth	Unfavorable	Zhang et al.2022[154]
CAPN2	High	Facilitate proliferation, migration, and invasion	Unfavorable	Peng et al.2022[155]
ABCA12	High	Facilitate proliferation, migration, and invasion	Unfavorable	Zheng et al.2022[156]
ROBO4	Low	Inhibit migration and invasion	Favorable	Yamanaka et al.2022[157]
PRKCI	High	Facilitate proliferation, migration, and invasion	Unfavorable	Abdelatty et al.2022[158]
ASF1B	High	Facilitate proliferation, invasion, and migration	Unfavorable	Kim et al.2022[159]
CYP26A1	High	Facilitate proliferation, invasion, and migration	Unfavorable	Yu et al.2022[160]
ADAMTS12	High	Promote cells migration	Unfavorable	He et al.2022[161]

Table 5. Some potential prognostic/therapeutic markers for PDAC.

The SPARC protein family includes a wide range of proteins that regulate the interaction between cells and the external environment and have been associated with the aetiology of human diseases [69]. These proteins share three main domains [69, 70]. Some studies have shown that several SPARC protein members, such as SPARC [83], Hevin [92], SPOCK1 [94] and FSTL1 [70], performed biological functions in pancreatic cancer.

Therefore, we aimed to explore the effects of the rest members of the SPARC protein family, including SPOCK2, SPOCK3, SMOC1 and SMOC2, in pancreatic cancer.

4.1 SPOCK2 as a potential prognostic marker.

First, the mRNA levels of SPOCK2, SPOCK3, SMOC1 and SMOC2 were compared among the normal human pancreatic ductal epithelial cell line (HPDE), PDAC cell lines (PCCs) and pancreatic stellate cells (PSCs) using qRT-PCR. We found that among these genes, SPOCK2 was only significantly downregulated in all PCCs and PSCs compared to HPDE. In our research, the expression of SPOCK2 was the highest in Capan-2 cells with well differentiation [162]. However, in other PDAC cell lines with poor differentiation, the expression of Panc1 [163], Aspc1 [164], Bxpc3 [165] and Miapaca-2 [166] was significantly lower. Ren et al. [167] found that the absence of SPOCK2 expression indicated an early event in the malignant development of endometriosis. Similarly, another study reported that the SPOCK 2 mRNA level was higher in Stage I than in Stage (II +III +IV) in lung adenocarcinoma [168]. Therefore, SPOCK2 expects to be a link to differentiation in PDAC.

PSCs are now widely acknowledged as the primary source of stromal/desmoplasia reaction, characteristic of PDAC [169, 170]. This

response leads to hypoxia in the tumor, EMT, an increase in cancer's malignant behavior, and chemoresistance [171]. In addition, PSCs could release numerous molecules, such as TGF- β , which could induce EMT and contribute to enhancing metastasis in PDAC [172, 173]. Besides, PSCs were reported that could impede immune response, resulting in facilitating immune tolerance in pancreatic cancer [174, 175]. Hence, PSCs perform a crucial function in the progression of PDAC. The role of some biomarkers in PSCs has also been investigated in recent years. Masamune et al. [176] studied that PKM2 was highly expressed in PSCs, and knockdown of it could suppress the proliferation and migration of PSCs *in vitro*; meanwhile, the tumor-promoting effect was attenuated in the case of the PKM2-knockdown PSCs *in vivo*. Other studies reported that YAP1 was expressed at a higher level in PSCs of human PDAC, and knockdown of it could inhibit cell proliferation and promote apoptosis in PSCs, indicative of PSC phenotype turn to inactivation [177, 178]. Mizutani et al. [179] studied that Meflin expression was usually lost when PSCs were activated in PDAC, and increasing Meflin in PSCs could inhibit the growth of xenograft tumors; indicating that Meflin is a new marker of PSCs in the normal pancreas. Analysis of transcriptome revealed that Meflin expression was greater in quiescent PSCs than in activated PSCs [180]. Our results showed that the SPOCK2 mRNA level was significantly decreased in PSCs from PDAC patients. Interestingly, Vilorio et al. [70] found that the protein level of SPOCK2 was also very lower in activated PSCs by Western Blot. So, it is reasonable to speculate that SPOCK2 might impact the function of PSCs and thus further influence the progression of PDAC. But it is necessary to detect the SPOCK2 level in quiescent PSCs isolated from the healthy pancreas next step.

Subsequently, the relationship between the expression of these four SPARC genes and the overall survival of patients with PDAC was examined using

the KM-plotter online tool. Based on the data previously mentioned, only SPOCK2 was strongly related to survival, and patients with higher SPOCK2 expression had a better prognosis. Additionally, we used a cohort from ICGC with 167 patient samples with PDAC to validate these findings and got the same result that only SPOCK2 correlated with survival and contributed to prognosis. It is similar to Zhao et al. [168] study that the SPOCK2 protein level was higher in normal tissue than in lung cancer tissue, and its expression was favorably related to survival, suggesting it might serve as a potential prognostic marker in lung cancer. On the contrary, another research found SPOCK2 was much higher in the advanced stage of ovarian cancer than in the early stage; its overexpression predicted a poor prognosis [181]. Taking together, SPOCK2 might serve as a potential prognostic marker in PDAC.

4.2 SPOCK2 is methylated in PDAC and correlates with poor prognosis.

In cancer research, abnormal DNA methylation of tumor suppressor genes has emerged as a new area of interest [182]. Typically, hypermethylation of CpG islands in gene promoters leads to gene silencing [183]. A majority of tumor suppressor genes are found to have hypermethylation in their promoter regions in human malignancies, which is thought to contribute to cancer development [184]. Many tumor suppressor genes are methylated in pancreatic malignancy [185-189]. For example, RUNX3, a candidate tumor-suppressor gene, showed the methylation of the promoter CpG island of the gene in PDAC cell lines that did not express it; and activated RUNX3 mRNA level after treatment of methylation inhibitor 5-aza-dC [185]. Similarly, the tumor-suppressor gene TSLC1 was frequently methylated in primary pancreatic adenocarcinomas and high-grade PanIN lesions but not in low-

grade PanIN lesions and normal pancreas [187]. Previous studies have reported that SPOCK2 is frequently methylated in prostate, colon and breast cancers [190]. Ren et al. reported that epigenetic inactivation of SPOCK2 via promoter hypermethylation contributed to the malignant development of ovarian endometriosis [191].

This research sought to discover the underlying mechanisms of the downregulation of SPOCK2 expression in human PDAC cells. First, using bioinformatic analyses, a negative relationship was observed between the degree of methylation and mRNA expression of SPOCK2 in PDAC. Furthermore, to examine whether DNA methylation is a mechanism for silencing SPOCK2, the demethylating agent 5-aza-dC was used to treat pancreatic cancer cell lines, and the mRNA and protein expression of SPOCK2 were increased after treatment. These results suggest that SPOCK2 might be transcriptionally controlled by DNA methylation in PDAC.

Xu et al. [192] found that the hypermethylation of tumor suppressor gene SAMD14 was substantially related to a poor prognosis and might serve as an independent predictor for survival using multivariate Cox regression analysis in gastric cancer. Another study reported that TFPI-2 methylation could predict a poor outcome in non-small cell lung cancer based on multivariate analysis models [193]. Whether there is an association between the methylation status of SPOCK2 and prognosis has not yet been investigated in PDAC. So, we combined the survival data of each patient from the TCGA database with the methylation level of spock2. We found that hypermethylation of SPOCK2 correlated with the poor prognosis of patients with PDAC by the Kaplan–Meier method and univariate survival analysis. Because of the deficiency of clinical data in the TCGA database, we did not perform a multivariate analysis to detect whether methylation of SPOCK2 could predict prognosis or not in PDAC. Hence, we performed a

time-dependent ROC analysis to evaluate the ability of SPOCK2 methylation to predict the prognosis of PDAC by calculating the area under the ROC curve (AUC) [194, 195]. In our research, the methylation level of SPOCK2 showed a good prediction either for 1-year (AUC=0.700) or 2-year (AUC=0.707) prognosis of patients with PDAC. The same method has been used by Dietrich et al. [196] studied that CDO1 promoter methylation revealed a better accuracy in prediction for 48 months (AUC=0.70) of breast cancer patients by time-dependent ROC analysis, suggesting its methylation could act as a biomarker for survival prediction. Therefore, SPOCK2 methylation might serve as a future predictive or prognostic marker for PDAC.

Aberrant methylation of genes is an early event during tumorigenesis and can be detected in potential malignant tissues years before tumorigenesis [197-200]. Singh et al. [182] found the methylation indices of SPARC were significantly higher in PDAC than in chronic pancreatitis (CP), and the SPARC methylation level could differentiate early-stage PDAC from CP patients. Hence, it is interesting to investigate further whether the methylation status of SPOCK2 gene is an early event during the progression of PDAC. Aberrant methylation of SPOCK2 might serve as a potential biomarker for early diagnosis in PDAC.

4.3 SPOCK2 might inhibit the growth of PDAC cells.

Recently, it was reported that SPOCK2 was significantly overexpressed in the normal endometrium tissue compared to endometrial cancer [100]. Similarly, Liu et al. reported that the SPOCK2 level was markedly less in prostate cancer than in benign prostate hyperplasia [101]. However, to date, SPOCK2 has not been widely studied in PDAC. Our investigation

demonstrated that the expression of SPOCK2 was reduced in PCCs compared to normal pancreatic ductal cells.

Subsequently, the function of SPOCK2 was evaluated in the Capan-2 cell line, which had the highest SPOCK2 mRNA expression among PDAC cell lines. We observed that SPOCK2 knockdown promoted cell proliferation. Our data in the line of the research on endometrial cancer cells, where it was reported that upregulation of SPOCK2 could suppress proliferation of these cancer cells [100]. Another study has shown that the knockdown of SPOCK2 could promote the proliferation of the human endometrial epithelial cell [201]. Therefore, we speculate that SPOCK2 serves as a tumor suppressor gene in PDAC as the same role in endometrial cancer.

The cell cycle is intimately associated with tumor proliferation, and its modulation potentially could be an effective target for cancer treatment [202]. In addition, cell cycle analysis is a common technique to detect the proliferation status of cells. For this reason, we used a flow cytometry to observe the impact of SPOCK2 on the distribution of the cell cycle. According to our findings, the proportion of Capan-2 cells in the G0/G1 phase was remarkably shortened after SPOCK2 knockdown. Stagnation of cells in the G0/G1 phase usually indicates that their transformation to S and M phases is blocked, eventually resulting in slow growth and reduced cell proliferation [203]. In this study, decreased SPOCK2 expression relieved stagnation of cells in the G0/G1 phase, thereby promoting cell proliferation.

Mammalian cell proliferation requires passage through four distinct cell cycle stages (G0/G1, S, G2 and M) and is strongly regulated to ensure duplication of genetic material and cell division [204]. However, cancer can disrupt these regulatory mechanisms and lead to aberrant cell cycle activity [202]. Traditionally, the division of a cell consists of two sequential steps: mitosis (M), including nuclear division, and interphase comprising G1, S and

G2 phases [205]. DNA replication occurs in the S phase. The G1 phase precedes the S phase, during which the cell prepares for DNA synthesis, whereas the G2 phase follows the S phase, during which the cell prepares for mitosis. Before committing to DNA replication, G1 cells may enter a resting stage known as G0; a majority of non-growing and non-dividing cells are in the G0 phase in the human body [205]. It has been reported that tumor cell dormancy is characterised by persistent G0/G1 cell cycle arrest, during which inactive tumor cells are formed [206].

Ren et al. [100] studied that SPOCK2 upregulation could significantly enlarge the G0/G1 phase and shorten the S phase of the cell cycle in endometrial cancer cells, indicating that increased SPOCK2 could induce G0/G1 phase arrest and impact DNA synthesis to suppress cell proliferation further. However, our result showed that SPOCK2 only influenced the G0/G1 phase but not the S phase in the cell cycle of PDAC cells. All in all, given that SPOCK2 might potentially serve as a tumor suppressor in PDAC, we speculate that its antiproliferative effects are associated with G0/G1 arrest.

4.4 SPOCK2 might participate in cell migration and EMT in PDAC.

Previous studies have shown that upregulation of SPOCK2 can inhibit the invasive ability of human endometrial adenocarcinoma cells, whereas its downregulation can promote the invasion of endometrial epithelial cells [100, 201]. Liu et al. [101] also drew a similar conclusion that increasing SPOCK2 could potentially inhibit the ability of prostate cancer cells to invade and migrate. However, in another study, SPOCK2 was found to be overexpressed in patients with primary breast tumors who developed brain metastasis and it was suggested to be associated with the invasion of breast cancer into the brain [207]. So, SPOCK2 could have a function in tumor invasion and

metastasis. In our study, the transwell assay showed that SPOCK2 knockdown promoted the migration of PDAC cells.

Therefore, we speculated that SPOCK2 undergoes a genetic change associated with metastasis in PDAC cells. Metastasis is a multistep cellular process that is the main cause of mortality in patients with PDAC [208]. In metastasis, cancer cells migrate from a primary tumor to a secondary location in the body. Metastasis often entails several complex molecular and cellular components associated with cell proliferation and migration, basement membrane breakdown, invasion, adhesion and angiogenesis [209]. Studies have shown that changes in tight junctions perform a crucial function in cancer invasion and metastasis [210-216]. Tight junctions are the major intercellular junctions that close cellular gaps, maintain intercellular adhesion and impede cell migration [217, 218]. ZO-1 is an essential tight junction-related protein, and its structural damage and functional alterations are associated with the development of many epithelial malignancies and may also be a key component of tumor metastasis [219].

EMT is a pivotal phase in the development of tumors and performs an essential function in invasion and metastasis [132, 220-223]. During EMT, epithelial cells lose their characteristics and gain the phenotypic characteristics of mesenchymal cells [224]. EMT is also accompanied by the disintegration of tight junctions, which eventually leads to the redistribution of ZO-1 [225]. Ectopic expression of ZO-1 is involved in the regulation of cancer invasion, and EMT may mediate the underlying mechanisms [226]. Pual et al. [227] reported that ZO-1 participated in the invasion and metastasis of breast tumor cells. Similarly, a study reported the correlation between ZO-1 and tumor aggressiveness in gastric cancer [228]. In addition, ZO-1 expression was remarkably decreased in individuals with colorectal cancer liver metastases [229]. In lung cancer, ZO-1 expression was

commonly lost, and its high expression was closely associated with a good disease prognosis [230].

In our study, we found that knockdown of SPOCK2 could decrease both the mRNA and protein levels of the epithelial marker ZO-1. A study reported that the SPARC gene was downregulated in biliary tract cancer cells, and its expression was positively correlated with the expression of ZO-1 ($r = 0.9$, $p < 0.05$) [74]. Maybe, this is due to the fact that SPARC and SPOCK2 belong to the same gene family. However, increasing SPOCK2 could suppress MMP2 activation and inhibit cell invasion in endometrial cancer cells [100]. Interestingly, SPOCK2 upregulation inhibited the migration and invasion of prostate cancer cells by decreasing MMP2 activation [101]. MMP2 can degrade plasma fibronectin and laminin of the basement membrane and is involved in tumor development, invasion, and metastasis [231]. So, there might be a relationship between SPOCK2 and MMP2 in PDAC. It was reported that MMP2 could decompose tight junction proteins ZO-1 [232]. Hence, there is another possibility in PDAC that SPOCK2 influences MMP2 and further impacts ZO-1. The specific mechanism amongst SPOCK2, ZO-1, and MMP2 in PDAC needs further investigation.

Overall, SPOCK2 may act as a potential EMT suppressor to inhibit PDAC metastasis.

4.5 The limitations of this research.

In the current research, we found that SPOCK2 is downregulated in PDAC due to hypermethylation. However, it cannot be neglected that demethylation may change the expression of some other genes and influence SPOCK2 through a gene regulatory network. Therefore, methylation-specific PCR

(MS-PCR) should be used in future studies to elucidate the epigenetic mechanisms of SPOCK2 in PDAC.

In this study, a cell line with the highest SPOCK2 expression was used to examine the biological functions of SPOCK2 in pancreatic cancer cells after a knockdown by siRNA. So, there is another possibility that decreased SPOCK2 might change the other genes and impact the proliferation and migration of cells. Similarly, change in other genes might inhibit ZO-1 due to the knockdown of SPOCK2.

In future work, we will investigate the effects of SPOCK2 overexpression on a cell line with the lowest SPOCK2 expression. Meanwhile, the correlation between SPOCK2 and ZO-1 needs to be further clarified. In addition, we will explore the specific mechanism of action of SPOCK2.

5. Conclusion

Our analysis yielded the following major findings: a) SPOCK2 is downregulated in PDAC due to hypermethylation; b) SPOCK2 might act as a potential prognostic marker in PDAC, as SPOCK2 correlates positively with prognosis in PDAC; c) down-regulated SPOCK2 stimulated cancer cell proliferation by shortening the G0/G1 phase in the cell cycle; d) silencing of SPOCK2 can improve cancer cell migration by probably suppressing tight junction protein ZO-1. (Figure 18)

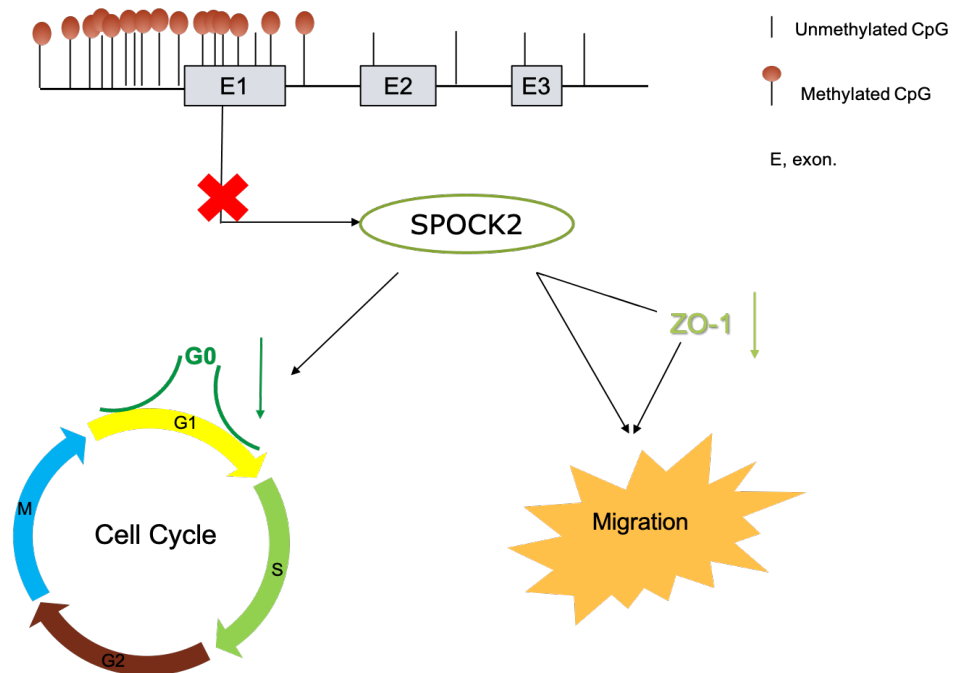


Figure 18. Graphic summary of SPOCK2.

References

1. Stevens, K.J. and C. Lisanti, Pancreas Imaging, in StatPearls. 2022: Treasure Island (FL).
2. Pandiri, A.R., Overview of exocrine pancreatic pathobiology. *Toxicol Pathol*, 2014. **42**(1): p. 207-16.
3. Jennings, R.E., et al., Human pancreas development. *Development*, 2015. **142**(18): p. 3126-37.
4. Feig, C., et al., The pancreas cancer microenvironment. *Clin Cancer Res*, 2012. **18**(16): p. 4266-76.
5. Ma, J. and A. Jemal, The rise and fall of cancer mortality in the USA: why does pancreatic cancer not follow the trend? *Future Oncol*, 2013. **9**(7): p. 917-9.
6. Han, D., et al., Analysis of radiotherapy impact on survival in resected stage I/II pancreatic cancer patients: a population-based study. *BMC Cancer*, 2021. **21**(1): p. 560.
7. Park, W., A. Chawla, and E.M. O'Reilly, Pancreatic Cancer: A Review. *JAMA*, 2021. **326**(9): p. 851-862.
8. Schawkat, K., et al., Pancreatic Ductal Adenocarcinoma and Its Variants: Pearls and Perils. *Radiographics*, 2020. **40**(5): p. 1219-1239.
9. McGuigan, A., et al., Pancreatic cancer: A review of clinical diagnosis, epidemiology, treatment and outcomes. *World J Gastroenterol*, 2018. **24**(43): p. 4846-4861.
10. Hruban, R.H., et al., An illustrated consensus on the classification of pancreatic intraepithelial neoplasia and intraductal papillary mucinous neoplasms. *Am J Surg Pathol*, 2004. **28**(8): p. 977-87.
11. Goh, B.K., et al., A review of mucinous cystic neoplasms of the pancreas defined by ovarian-type stroma: clinicopathological features of 344 patients. *World J Surg*, 2006. **30**(12): p. 2236-45.
12. Saad, A.M., et al., Trends in pancreatic adenocarcinoma incidence and mortality in the United States in the last four decades; a SEER-based study. *BMC Cancer*, 2018. **18**(1): p. 688.
13. Lin, L., et al., Global, regional, and national cancer incidence and death for 29 cancer groups in 2019 and trends analysis of the global cancer burden, 1990-2019. *J Hematol Oncol*, 2021. **14**(1): p. 197.
14. Sung, H., et al., Global Cancer Statistics 2020: GLOBOCAN Estimates of Incidence and Mortality Worldwide for 36 Cancers in 185 Countries. *CA Cancer J Clin*, 2021. **71**(3): p. 209-249.
15. Ferlay, J., C. Partensky, and F. Bray, More deaths from pancreatic cancer than breast cancer in the EU by 2017. *Acta Oncol*, 2016. **55**(9-10): p. 1158-1160.

16. Midha, S., S. Chawla, and P.K. Garg, Modifiable and non-modifiable risk factors for pancreatic cancer: A review. *Cancer Lett*, 2016. **381**(1): p. 269-77.
17. Rawla, P., T. Sunkara, and V. Gaduputi, Epidemiology of Pancreatic Cancer: Global Trends, Etiology and Risk Factors. *World J Oncol*, 2019. **10**(1): p. 10-27.
18. Surveillance, Epidemiology, and End Results Program. Cancer Stat Facts: Pancreatic Cancer. [cited 20 Jan 2021]. In: National Cancer Institute [Internet]. Available from: <https://seer.cancer.gov/statfacts/html/pancreas.html>
19. Hu, J.X., et al., Pancreatic cancer: A review of epidemiology, trend, and risk factors. *World J Gastroenterol*, 2021. **27**(27): p. 4298-4321.
20. Siegel, R.L., et al., Cancer statistics, 2022. *CA Cancer J Clin*, 2022. **72**(1): p. 7-33.
21. Ferlay, J., et al., Cancer incidence and mortality patterns in Europe: Estimates for 40 countries and 25 major cancers in 2018. *Eur J Cancer*, 2018. **103**: p. 356-387.
22. Silverman, D.T., et al., Why do Black Americans have a higher risk of pancreatic cancer than White Americans? *Epidemiology*, 2003. **14**(1): p. 45-54.
23. Yadav, D. and A.B. Lowenfels, The epidemiology of pancreatitis and pancreatic cancer. *Gastroenterology*, 2013. **144**(6): p. 1252-61.
24. Ilic, M. and I. Ilic, Epidemiology of pancreatic cancer. *World J Gastroenterol*, 2016. **22**(44): p. 9694-9705.
25. Batabyal, P., et al., Association of diabetes mellitus and pancreatic adenocarcinoma: a meta-analysis of 88 studies. *Ann Surg Oncol*, 2014. **21**(7): p. 2453-62.
26. Huang, B.Z., et al., New-Onset Diabetes, Longitudinal Trends in Metabolic Markers, and Risk of Pancreatic Cancer in a Heterogeneous Population. *Clin Gastroenterol Hepatol*, 2020. **18**(8): p. 1812-1821 e7.
27. Huxley, R., et al., Type-II diabetes and pancreatic cancer: a meta-analysis of 36 studies. *Br J Cancer*, 2005. **92**(11): p. 2076-83.
28. Jacobs, E.J., et al., Family history of cancer and risk of pancreatic cancer: a pooled analysis from the Pancreatic Cancer Cohort Consortium (PanScan). *Int J Cancer*, 2010. **127**(6): p. 1421-8.
29. Permuth-Wey, J. and K.M. Egan, Family history is a significant risk factor for pancreatic cancer: results from a systematic review and meta-analysis. *Fam Cancer*, 2009. **8**(2): p. 109-17.
30. Shi, C., R.H. Hruban, and A.P. Klein, Familial pancreatic cancer. *Arch Pathol Lab Med*, 2009. **133**(3): p. 365-74.
31. Klein, A.P., et al., Prospective risk of pancreatic cancer in familial pancreatic cancer kindreds. *Cancer Res*, 2004. **64**(7): p. 2634-8.

32. Ghiorzo, P., Genetic predisposition to pancreatic cancer. *World J Gastroenterol*, 2014. **20**(31): p. 10778-89.
33. Shi, C., J.A. Daniels, and R.H. Hruban, Molecular characterization of pancreatic neoplasms. *Adv Anat Pathol*, 2008. **15**(4): p. 185-95.
34. Jones, S., et al., Exomic sequencing identifies PALB2 as a pancreatic cancer susceptibility gene. *Science*, 2009. **324**(5924): p. 217.
35. Slater, E.P., et al., PALB2 mutations in European familial pancreatic cancer families. *Clin Genet*, 2010. **78**(5): p. 490-4.
36. Tischkowitz, M.D., et al., Analysis of the gene coding for the BRCA2-interacting protein PALB2 in familial and sporadic pancreatic cancer. *Gastroenterology*, 2009. **137**(3): p. 1183-6.
37. Ghadirian, P., H.T. Lynch, and D. Krewski, Epidemiology of pancreatic cancer: an overview. *Cancer Detect Prev*, 2003. **27**(2): p. 87-93.
38. Barreto, S.G., How does cigarette smoking cause acute pancreatitis? *Pancreatology*, 2016. **16**(2): p. 157-63.
39. Vrieling, A., et al., Cigarette smoking, environmental tobacco smoke exposure and pancreatic cancer risk in the European Prospective Investigation into Cancer and Nutrition. *Int J Cancer*, 2010. **126**(10): p. 2394-403.
40. Lynch, S.M., et al., Cigarette smoking and pancreatic cancer: a pooled analysis from the pancreatic cancer cohort consortium. *Am J Epidemiol*, 2009. **170**(4): p. 403-13.
41. Xu, S., et al., Characterization of Mouse Models of Early Pancreatic Lesions Induced by Alcohol and Chronic Pancreatitis. *Pancreas*, 2015. **44**(6): p. 882-7.
42. Setiawan, V.W., et al., Uniting Epidemiology and Experimental Disease Models for Alcohol-Related Pancreatic Disease. *Alcohol Res*, 2017. **38**(2): p. 173-182.
43. Xu, M., et al., Obesity and Pancreatic Cancer: Overview of Epidemiology and Potential Prevention by Weight Loss. *Pancreas*, 2018. **47**(2): p. 158-162.
44. Park, B.K., et al., Lifestyle, body mass index, diabetes, and the risk of pancreatic cancer in a nationwide population-based cohort study with 7.4 million Korean subjects. *Br J Cancer*, 2022.
45. El-Serag, H.B., et al., Risk of hepatobiliary and pancreatic cancers after hepatitis C virus infection: A population-based study of U.S. veterans. *Hepatology*, 2009. **49**(1): p. 116-23.
46. Hassan, M.M., et al., Association between hepatitis B virus and pancreatic cancer. *J Clin Oncol*, 2008. **26**(28): p. 4557-62.
47. Jin, Y., et al., Identification and impact of hepatitis B virus DNA and antigens in pancreatic cancer tissues and adjacent non-cancerous tissues. *Cancer Lett*, 2013. **335**(2): p. 447-54.

48. Song, C., et al., Associations Between Hepatitis B Virus Infection and Risk of All Cancer Types. *JAMA Netw Open*, 2019. **2**(6): p. e195718.
49. Darvishian, M., et al., Elevated risk of colorectal, liver, and pancreatic cancers among HCV, HBV and/or HIV (co)infected individuals in a population based cohort in Canada. *Ther Adv Med Oncol*, 2021. **13**: p. 1758835921992987.
50. Liu, T., et al., Hepatitis B virus infection and the risk of gastrointestinal cancers among Chinese population: A prospective cohort study. *Int J Cancer*, 2022. **150**(6): p. 1018-1028.
51. Wang, D.S., et al., ABO blood group, hepatitis B viral infection and risk of pancreatic cancer. *Int J Cancer*, 2012. **131**(2): p. 461-8.
52. Maisonneuve, P. and A.B. Lowenfels, Risk factors for pancreatic cancer: a summary review of meta-analytical studies. *Int J Epidemiol*, 2015. **44**(1): p. 186-98.
53. Risch, H.A., et al., ABO blood group, Helicobacter pylori seropositivity, and risk of pancreatic cancer: a case-control study. *J Natl Cancer Inst*, 2010. **102**(7): p. 502-5.
54. Etemad, B. and D.C. Whitcomb, Chronic pancreatitis: diagnosis, classification, and new genetic developments. *Gastroenterology*, 2001. **120**(3): p. 682-707.
55. Greten, F.R. and S.I. Grivennikov, Inflammation and Cancer: Triggers, Mechanisms, and Consequences. *Immunity*, 2019. **51**(1): p. 27-41.
56. Friess, H., et al., Growth factors and cytokines in pancreatic carcinogenesis. *Ann N Y Acad Sci*, 1999. **880**: p. 110-21.
57. Hammel, P., et al., Effect of Chemoradiotherapy vs Chemotherapy on Survival in Patients With Locally Advanced Pancreatic Cancer Controlled After 4 Months of Gemcitabine With or Without Erlotinib: The LAP07 Randomized Clinical Trial. *JAMA*, 2016. **315**(17): p. 1844-53.
58. Burris, H.A., 3rd, et al., Improvements in survival and clinical benefit with gemcitabine as first-line therapy for patients with advanced pancreas cancer: a randomized trial. *J Clin Oncol*, 1997. **15**(6): p. 2403-13.
59. Toschi, L., et al., Role of gemcitabine in cancer therapy. *Future Oncol*, 2005. **1**(1): p. 7-17.
60. Oettle, H., et al., Adjuvant chemotherapy with gemcitabine vs observation in patients undergoing curative-intent resection of pancreatic cancer: a randomized controlled trial. *JAMA*, 2007. **297**(3): p. 267-77.
61. Oettle, H., et al., Adjuvant chemotherapy with gemcitabine and long-term outcomes among patients with resected pancreatic cancer: the CONKO-001 randomized trial. *JAMA*, 2013. **310**(14): p. 1473-81.
62. Principe, D.R., et al., The Current Treatment Paradigm for Pancreatic Ductal Adenocarcinoma and Barriers to Therapeutic Efficacy. *Front Oncol*, 2021. **11**: p. 688377.

63. Von Hoff, D.D., et al., Increased survival in pancreatic cancer with nab-paclitaxel plus gemcitabine. *N Engl J Med*, 2013. **369**(18): p. 1691-703.
64. Conroy, T., et al., FOLFIRINOX or Gemcitabine as Adjuvant Therapy for Pancreatic Cancer. *N Engl J Med*, 2018. **379**(25): p. 2395-2406.
65. Galvano, A., et al., Moving the Target on the Optimal Adjuvant Strategy for Resected Pancreatic Cancers: A Systematic Review with Meta-Analysis. *Cancers (Basel)*, 2020. **12**(3).
66. Mizrahi, J.D., et al., Pancreatic cancer. *Lancet*, 2020. **395**(10242): p. 2008-2020.
67. Neoptolemos, J.P., et al., A randomized trial of chemoradiotherapy and chemotherapy after resection of pancreatic cancer. *N Engl J Med*, 2004. **350**(12): p. 1200-10.
68. Neoptolemos, J.P., et al., Adjuvant chemoradiotherapy and chemotherapy in resectable pancreatic cancer: a randomised controlled trial. *Lancet*, 2001. **358**(9293): p. 1576-85.
69. Bradshaw, A.D., Diverse biological functions of the SPARC family of proteins. *Int J Biochem Cell Biol*, 2012. **44**(3): p. 480-8.
70. Viloria, K., et al., A holistic approach to dissecting SPARC family protein complexity reveals FSTL-1 as an inhibitor of pancreatic cancer cell growth. *Sci Rep*, 2016. **6**: p. 37839.
71. Neuzillet, C., et al., Stromal expression of SPARC in pancreatic adenocarcinoma. *Cancer Metastasis Rev*, 2013. **32**(3-4): p. 585-602.
72. Bradshaw, A.D. and E.H. Sage, SPARC, a matricellular protein that functions in cellular differentiation and tissue response to injury. *J Clin Invest*, 2001. **107**(9): p. 1049-54.
73. Podhajcer, O.L., et al., The role of the matricellular protein SPARC in the dynamic interaction between the tumor and the host. *Cancer Metastasis Rev*, 2008. **27**(4): p. 691-705.
74. Aghamaliyev, U., et al., Downregulation of SPARC Is Associated with Epithelial-Mesenchymal Transition and Low Differentiation State of Biliary Tract Cancer Cells. *Eur Surg Res*, 2019. **60**(1-2): p. 1-12.
75. Watkins, G., et al., Increased levels of SPARC (osteonectin) in human breast cancer tissues and its association with clinical outcomes. *Prostaglandins Leukot Essent Fatty Acids*, 2005. **72**(4): p. 267-72.
76. Wang, C.S., et al., Overexpression of SPARC gene in human gastric carcinoma and its clinic-pathologic significance. *Br J Cancer*, 2004. **91**(11): p. 1924-30.
77. Sansom, O.J., et al., Deficiency of SPARC suppresses intestinal tumorigenesis in APCMin/+ mice. *Gut*, 2007. **56**(10): p. 1410-4.
78. Yiu, G.K., et al., SPARC (secreted protein acidic and rich in cysteine) induces apoptosis in ovarian cancer cells. *Am J Pathol*, 2001. **159**(2): p. 609-22.

79. Miyoshi, K., et al., SPARC mRNA expression as a prognostic marker for pancreatic adenocarcinoma patients. *Anticancer Res*, 2010. **30**(3): p. 867-71.
80. Sato, N., et al., SPARC/osteonectin is a frequent target for aberrant methylation in pancreatic adenocarcinoma and a mediator of tumor-stromal interactions. *Oncogene*, 2003. **22**(32): p. 5021-30.
81. Gao, J., et al., Methylation of the SPARC gene promoter and its clinical implication in pancreatic cancer. *J Exp Clin Cancer Res*, 2010. **29**: p. 28.
82. Guweidhi, A., et al., Osteonectin influences growth and invasion of pancreatic cancer cells. *Ann Surg*, 2005. **242**(2): p. 224-34.
83. Chen, G., et al., Inhibition of endogenous SPARC enhances pancreatic cancer cell growth: modulation by FGFR1-III isoform expression. *Br J Cancer*, 2010. **102**(1): p. 188-95.
84. Infante, J.R., et al., Peritumoral fibroblast SPARC expression and patient outcome with resectable pancreatic adenocarcinoma. *J Clin Oncol*, 2007. **25**(3): p. 319-25.
85. Mantoni, T.S., et al., Stromal SPARC expression and patient survival after chemoradiation for non-resectable pancreatic adenocarcinoma. *Cancer Biol Ther*, 2008. **7**(11): p. 1806-15.
86. Framson, P.E. and E.H. Sage, SPARC and tumor growth: where the seed meets the soil? *J Cell Biochem*, 2004. **92**(4): p. 679-90.
87. Nelson, P.S., et al., Hevin, an antiadhesive extracellular matrix protein, is down-regulated in metastatic prostate adenocarcinoma. *Cancer Res*, 1998. **58**(2): p. 232-6.
88. Xiang, Y., et al., SPARCL1 suppresses metastasis in prostate cancer. *Mol Oncol*, 2013. **7**(6): p. 1019-30.
89. Li, P., et al., Down-regulated SPARCL1 is associated with clinical significance in human gastric cancer. *J Surg Oncol*, 2012. **105**(1): p. 31-7.
90. Jakharia, A., B. Borkakoty, and S. Singh, Expression of SPARC like protein 1 (SPARCL1), extracellular matrix-associated protein is down regulated in gastric adenocarcinoma. *J Gastrointest Oncol*, 2016. **7**(2): p. 278-83.
91. Zhang, H., et al., SPARCL1: a potential molecule associated with tumor diagnosis, progression and prognosis of colorectal cancer. *Tumour Biol*, 2011. **32**(6): p. 1225-31.
92. Esposito, I., et al., Tumor-suppressor function of SPARC-like protein 1/Hevin in pancreatic cancer. *Neoplasia*, 2007. **9**(1): p. 8-17.
93. Alliel, P.M., et al., Testican, a multidomain testicular proteoglycan resembling modulators of cell social behaviour. *Eur J Biochem*, 1993. **214**(1): p. 347-50.
94. Li, J., et al., A potential prognostic marker and therapeutic target: SPOCK1 promotes the proliferation, metastasis, and apoptosis of pancreatic ductal adenocarcinoma cells. *J Cell Biochem*, 2020. **121**(1): p. 743-754.

95. Li, Y., et al., SPOCK1 is regulated by CHD1L and blocks apoptosis and promotes HCC cell invasiveness and metastasis in mice. *Gastroenterology*, 2013. **144**(1): p. 179-191 e4.
96. Chen, Q., et al., SPOCK1 promotes tumor growth and metastasis in human prostate cancer. *Drug Des Devel Ther*, 2016. **10**: p. 2311-21.
97. Chen, M.L., et al., High SPOCK1 Expression is Associated with Advanced Stage, T Value, and Gleason Grade in Prostate Cancer. *Medicina (Kaunas)*, 2019. **55**(7).
98. Miao, L., et al., SPOCK1 is a novel transforming growth factor-beta target gene that regulates lung cancer cell epithelial-mesenchymal transition. *Biochem Biophys Res Commun*, 2013. **440**(4): p. 792-7.
99. Veenstra, V.L., et al., Stromal SPOCK1 supports invasive pancreatic cancer growth. *Mol Oncol*, 2017. **11**(8): p. 1050-1064.
100. Ren, F., et al., SPOCK2 Affects the Biological Behavior of Endometrial Cancer Cells by Regulation of MT1-MMP and MMP2. *Reprod Sci*, 2020. **27**(7): p. 1391-1399.
101. Liu, G., F. Ren, and Y. Song, Upregulation of SPOCK2 inhibits the invasion and migration of prostate cancer cells by regulating the MT1-MMP/MMP2 pathway. *PeerJ*, 2019. **7**: p. e7163.
102. Weber, H., et al., SPOCK3, a risk gene for adult ADHD and personality disorders. *Eur Arch Psychiatry Clin Neurosci*, 2014. **264**(5): p. 409-21.
103. Buga, A.M., et al., Identification of new therapeutic targets by genome-wide analysis of gene expression in the ipsilateral cortex of aged rats after stroke. *PLoS One*, 2012. **7**(12): p. e50985.
104. Kamioka, M., et al., Testican 3 expression in adult T-cell leukemia. *Leuk Res*, 2009. **33**(7): p. 913-8.
105. Nakada, M., et al., Suppression of membrane-type 1 matrix metalloproteinase (MMP)-mediated MMP-2 activation and tumor invasion by testican 3 and its splicing variant gene product, N-Tes. *Cancer Res*, 2001. **61**(24): p. 8896-902.
106. Gao, Q., H.P. Mok, and J. Zhuang, Secreted modular calcium-binding proteins in pathophysiological processes and embryonic development. *Chin Med J (Engl)*, 2019. **132**(20): p. 2476-2484.
107. Vannahme, C., et al., Characterization of SMOC-1, a novel modular calcium-binding protein in basement membranes. *J Biol Chem*, 2002. **277**(41): p. 37977-86.
108. Zhang, G.H., et al., Seven genes for the prognostic prediction in patients with glioma. *Clin Transl Oncol*, 2019. **21**(10): p. 1327-1335.
109. Aoki, H., et al., Epigenetic silencing of SMOC1 in traditional serrated adenoma and colorectal cancer. *Oncotarget*, 2018. **9**(4): p. 4707-4721.

110. Alabiad, M.A., et al., Prognostic and clinicopathological significance of TMEFF2, SMOC-2, and SOX17 expression in endometrial carcinoma. *Exp Mol Pathol*, 2021. **122**: p. 104670.
111. Huang, X.Q., et al., Overexpression of SMOC2 Attenuates the Tumorigenicity of Hepatocellular Carcinoma Cells and Is Associated With a Positive Postoperative Prognosis in Human Hepatocellular Carcinoma. *J Cancer*, 2017. **8**(18): p. 3812-3827.
112. Jang, B.G., et al., SMOC2, an intestinal stem cell marker, is an independent prognostic marker associated with better survival in colorectal cancers. *Sci Rep*, 2020. **10**(1): p. 14591.
113. Gu, C., et al., FSTL1 interacts with VIM and promotes colorectal cancer metastasis via activating the focal adhesion signalling pathway. *Cell Death Dis*, 2018. **9**(6): p. 654.
114. Wu, M., et al., FSTL1 promotes growth and metastasis in gastric cancer by activating AKT related pathway and predicts poor survival. *Am J Cancer Res*, 2021. **11**(3): p. 712-728.
115. Ni, X., et al., FSTL1 suppresses tumor cell proliferation, invasion and survival in non-small cell lung cancer. *Oncol Rep*, 2018. **39**(1): p. 13-20.
116. Vogelstein, B., et al., Cancer genome landscapes. *Science*, 2013. **339**(6127): p. 1546-58.
117. Das, P.M. and R. Singal, DNA methylation and cancer. *J Clin Oncol*, 2004. **22**(22): p. 4632-42.
118. Akhavan-Niaki, H. and A.A. Samadani, DNA methylation and cancer development: molecular mechanism. *Cell Biochem Biophys*, 2013. **67**(2): p. 501-13.
119. Agathangelou, A., et al., Methylation associated inactivation of RASSF1A from region 3p21.3 in lung, breast and ovarian tumours. *Oncogene*, 2001. **20**(12): p. 1509-18.
120. Dammann, R., et al., Frequent RASSF1A promoter hypermethylation and K-ras mutations in pancreatic carcinoma. *Oncogene*, 2003. **22**(24): p. 3806-12.
121. Melkonyan, H.S., et al., SARPs: a family of secreted apoptosis-related proteins. *Proc Natl Acad Sci U S A*, 1997. **94**(25): p. 13636-41.
122. Watanabe, H., et al., Aberrant methylation of secreted apoptosis-related protein 2 (SARP2) in pure pancreatic juice in diagnosis of pancreatic neoplasms. *Pancreas*, 2006. **32**(4): p. 382-9.
123. Hollingsworth, M.A. and B.J. Swanson, Mucins in cancer: protection and control of the cell surface. *Nat Rev Cancer*, 2004. **4**(1): p. 45-60.
124. Hollingsworth, M.A., et al., Expression of MUC1, MUC2, MUC3 and MUC4 mucin mRNAs in human pancreatic and intestinal tumor cell lines. *Int J Cancer*, 1994. **57**(2): p. 198-203.

125. Balague, C., et al., Altered expression of MUC2, MUC4, and MUC5 mucin genes in pancreas tissues and cancer cell lines. *Gastroenterology*, 1994. **106**(4): p. 1054-61.
126. Balague, C., et al., In situ hybridization shows distinct patterns of mucin gene expression in normal, benign, and malignant pancreas tissues. *Gastroenterology*, 1995. **109**(3): p. 953-64.
127. Andrianifahanana, M., et al., Mucin (MUC) gene expression in human pancreatic adenocarcinoma and chronic pancreatitis: a potential role of MUC4 as a tumor marker of diagnostic significance. *Clin Cancer Res*, 2001. **7**(12): p. 4033-40.
128. Swartz, M.J., et al., MUC4 expression increases progressively in pancreatic intraepithelial neoplasia. *Am J Clin Pathol*, 2002. **117**(5): p. 791-6.
129. Zhu, Y., et al., The increase in the expression and hypomethylation of MUC4 gene with the progression of pancreatic ductal adenocarcinoma. *Med Oncol*, 2011. **28 Suppl 1**: p. S175-84.
130. Thiery, J.P., et al., Epithelial-mesenchymal transitions in development and disease. *Cell*, 2009. **139**(5): p. 871-90.
131. Micalizzi, D.S., S.M. Farabaugh, and H.L. Ford, Epithelial-mesenchymal transition in cancer: parallels between normal development and tumor progression. *J Mammary Gland Biol Neoplasia*, 2010. **15**(2): p. 117-34.
132. Elaskalani, O., et al., Epithelial-mesenchymal transition as a therapeutic target for overcoming chemoresistance in pancreatic cancer. *World J Gastrointest Oncol*, 2017. **9**(1): p. 37-41.
133. Wang, S., S. Huang, and Y.L. Sun, Epithelial-Mesenchymal Transition in Pancreatic Cancer: A Review. *Biomed Res Int*, 2017. **2017**: p. 2646148.
134. Natsume, A., et al., The DNA demethylating agent 5-aza-2'-deoxycytidine activates NY-ESO-1 antigenicity in orthotopic human glioma. *Int J Cancer*, 2008. **122**(11): p. 2542-53.
135. Kohi, S., et al., A novel epigenetic mechanism regulating hyaluronan production in pancreatic cancer cells. *Clin Exp Metastasis*, 2016. **33**(3): p. 225-30.
136. Peng, Y.P., et al., PEG10 overexpression induced by E2F-1 promotes cell proliferation, migration, and invasion in pancreatic cancer. *J Exp Clin Cancer Res*, 2017. **36**(1): p. 30.
137. Lanczky, A. and B. Györfy, Web-Based Survival Analysis Tool Tailored for Medical Research (KMplot): Development and Implementation. *J Med Internet Res*, 2021. **23**(7): p. e27633.
138. Nagy, A., G. Munkacsy, and B. Györfy, Pancancer survival analysis of cancer hallmark genes. *Sci Rep*, 2021. **11**(1): p. 6047.
139. International Cancer Genome, C., et al., International network of cancer genome projects. *Nature*, 2010. **464**(7291): p. 993-8.

140. Chen, Z.Y., et al., Aberrant methylation of the SPARC gene promoter and its clinical implication in gastric cancer. *Sci Rep*, 2014. **4**: p. 7035.
141. Sato, N., et al., Effects of 5-aza-2'-deoxycytidine on matrix metalloproteinase expression and pancreatic cancer cell invasiveness. *J Natl Cancer Inst*, 2003. **95**(4): p. 327-30.
142. Sato, N., et al., Discovery of novel targets for aberrant methylation in pancreatic carcinoma using high-throughput microarrays. *Cancer Res*, 2003. **63**(13): p. 3735-42.
143. Men, C., et al., Identification of DNA methylation associated gene signatures in endometrial cancer via integrated analysis of DNA methylation and gene expression systematically. *J Gynecol Oncol*, 2017. **28**(6): p. e83.
144. Shinawi, T., et al., DNA methylation profiles of long- and short-term glioblastoma survivors. *Epigenetics*, 2013. **8**(2): p. 149-56.
145. Jia, W., et al., Autophagy regulates T lymphocyte proliferation through selective degradation of the cell-cycle inhibitor CDKN1B/p27Kip1. *Autophagy*, 2015. **11**(12): p. 2335-45.
146. Bi, H., et al., DEC1 regulates breast cancer cell proliferation by stabilizing cyclin E protein and delays the progression of cell cycle S phase. *Cell Death Dis*, 2015. **6**: p. e1891.
147. Debnath, P., et al., Epithelial-mesenchymal transition and its transcription factors. *Biosci Rep*, 2022. **42**(1).
148. Werner, J., et al., Advanced-stage pancreatic cancer: therapy options. *Nat Rev Clin Oncol*, 2013. **10**(6): p. 323-33.
149. Elsayed, M. and M. Abdelrahim, The Latest Advancement in Pancreatic Ductal Adenocarcinoma Therapy: A Review Article for the Latest Guidelines and Novel Therapies. *Biomedicines*, 2021. **9**(4).
150. Yan, Y., et al., Combining Immune Checkpoint Inhibitors With Conventional Cancer Therapy. *Front Immunol*, 2018. **9**: p. 1739.
151. Leroux, C. and G. Konstantinidou, Targeted Therapies for Pancreatic Cancer: Overview of Current Treatments and New Opportunities for Personalized Oncology. *Cancers (Basel)*, 2021. **13**(4).
152. Huo, Y., et al., Increased SPON1 promotes pancreatic ductal adenocarcinoma progression by enhancing IL-6 trans-signalling. *Cell Prolif*, 2022. **55**(5): p. e13237.
153. Zhang, Z., et al., YOD1 serves as a potential prognostic biomarker for pancreatic cancer. *Cancer Cell Int*, 2022. **22**(1): p. 203.
154. Zhang, D., et al., SEMA3C Supports Pancreatic Cancer Progression by Regulating the Autophagy Process and Tumor Immune Microenvironment. *Front Oncol*, 2022. **12**: p. 890154.

155. Peng, X., et al., Calpain2 Upregulation Regulates EMT-Mediated Pancreatic Cancer Metastasis via the Wnt/beta-Catenin Signaling Pathway. *Front Med (Lausanne)*, 2022. **9**: p. 783592.
156. Zheng, S., et al., ABCA12 Promotes Proliferation and Migration and Inhibits Apoptosis of Pancreatic Cancer Cells Through the AKT Signaling Pathway. *Front Genet*, 2022. **13**: p. 906326.
157. Yamanaka, M., et al., Downregulation of ROBO4 in Pancreatic Cancer Serves as a Biomarker of Poor Prognosis and Indicates Increased Cell Motility and Proliferation Through Activation of MMP-9. *Ann Surg Oncol*, 2022.
158. Abdelatty, A., et al., PKC α Is a Promising Prognosis Biomarker and Therapeutic Target for Pancreatic Cancer. *Pathobiology*, 2022: p. 1-12.
159. Kim, J.H., et al., Downregulation of ASF1B inhibits tumor progression and enhances efficacy of cisplatin in pancreatic cancer. *Cancer Biomark*, 2022.
160. Yu, Y., et al., CYP26A1 Is a Novel Cancer Biomarker of Pancreatic Carcinoma: Evidence from Integration Analysis and In Vitro Experiments. *Dis Markers*, 2022. **2022**: p. 5286820.
161. He, R.Z., et al., ADAMTS12 promotes migration and epithelial-mesenchymal transition and predicts poor prognosis for pancreatic cancer. *Hepatobiliary Pancreat Dis Int*, 2022.
162. Kyriazis, A.A., et al., Morphological, biological, biochemical, and karyotypic characteristics of human pancreatic ductal adenocarcinoma Capan-2 in tissue culture and the nude mouse. *Cancer Res*, 1986. **46**(11): p. 5810-5.
163. Lieber, M., et al., Establishment of a continuous tumor-cell line (panc-1) from a human carcinoma of the exocrine pancreas. *Int J Cancer*, 1975. **15**(5): p. 741-7.
164. Chen, W.H., et al., Human pancreatic adenocarcinoma: in vitro and in vivo morphology of a new tumor line established from ascites. *In Vitro*, 1982. **18**(1): p. 24-34.
165. Tan, M.H., et al., Characterization of a new primary human pancreatic tumor line. *Cancer Invest*, 1986. **4**(1): p. 15-23.
166. Yunis, A.A., G.K. Arimura, and D.J. Russin, Human pancreatic carcinoma (MIA PaCa-2) in continuous culture: sensitivity to asparaginase. *Int J Cancer*, 1977. **19**(1): p. 128-35.
167. Ren, F., D.B. Wang, and T. Li, [Epigenetic inactivation of SPOCK2 in the malignant transformation of ovarian endometriosis]. *Zhonghua Fu Chan Ke Za Zhi*, 2011. **46**(11): p. 822-5.
168. Zhao, J., et al., SPOCK2 Serves as a Potential Prognostic Marker and Correlates With Immune Infiltration in Lung Adenocarcinoma. *Front Genet*, 2020. **11**: p. 588499.
169. Apte, M.V., et al., Desmoplastic reaction in pancreatic cancer: role of pancreatic stellate cells. *Pancreas*, 2004. **29**(3): p. 179-87.

170. Apte, M.V. and J.S. Wilson, Mechanisms of pancreatic fibrosis. *Dig Dis*, 2004. **22**(3): p. 273-9.
171. McCarroll, J.A., et al., Role of pancreatic stellate cells in chemoresistance in pancreatic cancer. *Front Physiol*, 2014. **5**: p. 141.
172. Tang, D., et al., Persistent activation of pancreatic stellate cells creates a microenvironment favorable for the malignant behavior of pancreatic ductal adenocarcinoma. *Int J Cancer*, 2013. **132**(5): p. 993-1003.
173. Kikuta, K., et al., Pancreatic stellate cells promote epithelial-mesenchymal transition in pancreatic cancer cells. *Biochem Biophys Res Commun*, 2010. **403**(3-4): p. 380-4.
174. Tang, D., et al., High expression of Galectin-1 in pancreatic stellate cells plays a role in the development and maintenance of an immunosuppressive microenvironment in pancreatic cancer. *Int J Cancer*, 2012. **130**(10): p. 2337-48.
175. Wu, Q., et al., Functions of pancreatic stellate cell-derived soluble factors in the microenvironment of pancreatic ductal carcinoma. *Oncotarget*, 2017. **8**(60): p. 102721-102738.
176. Masamune, A., et al., Pyruvate Kinase Isozyme M2 Plays a Critical Role in the Interactions Between Pancreatic Stellate Cells and Cancer Cells. *Dig Dis Sci*, 2018. **63**(7): p. 1868-1877.
177. Morvaridi, S., et al., Role of YAP and TAZ in pancreatic ductal adenocarcinoma and in stellate cells associated with cancer and chronic pancreatitis. *Sci Rep*, 2015. **5**: p. 16759.
178. Xiao, Y., et al., YAP1-mediated pancreatic stellate cell activation inhibits pancreatic cancer cell proliferation. *Cancer Lett*, 2019. **462**: p. 51-60.
179. Mizutani, Y., et al., Meflin-Positive Cancer-Associated Fibroblasts Inhibit Pancreatic Carcinogenesis. *Cancer Res*, 2019. **79**(20): p. 5367-5381.
180. Ohlund, D., et al., Distinct populations of inflammatory fibroblasts and myofibroblasts in pancreatic cancer. *J Exp Med*, 2017. **214**(3): p. 579-596.
181. Lou, W., et al., Dysregulation of pseudogene/lncRNA-hsa-miR-363-3p-SPOCK2 pathway fuels stage progression of ovarian cancer. *Aging (Albany NY)*, 2019. **11**(23): p. 11416-11439.
182. Singh, N., et al., Clinical significance of promoter methylation status of tumor suppressor genes in circulating DNA of pancreatic cancer patients. *J Cancer Res Clin Oncol*, 2020. **146**(4): p. 897-907.
183. Shu, J., et al., Silencing of bidirectional promoters by DNA methylation in tumorigenesis. *Cancer Res*, 2006. **66**(10): p. 5077-84.
184. Herman, J.G. and S.B. Baylin, Gene silencing in cancer in association with promoter hypermethylation. *N Engl J Med*, 2003. **349**(21): p. 2042-54.

185. Wada, M., et al., Frequent loss of RUNX3 gene expression in human bile duct and pancreatic cancer cell lines. *Oncogene*, 2004. **23**(13): p. 2401-7.
186. Bellacosa, A., Role of MED1 (MBD4) Gene in DNA repair and human cancer. *J Cell Physiol*, 2001. **187**(2): p. 137-44.
187. Jansen, M., et al., Aberrant methylation of the 5' CpG island of TSLC1 is common in pancreatic ductal adenocarcinoma and is first manifest in high-grade PanINs. *Cancer Biol Ther*, 2002. **1**(3): p. 293-6.
188. Guo, M., et al., Epigenetic changes associated with neoplasms of the exocrine and endocrine pancreas. *Discov Med*, 2014. **17**(92): p. 67-73.
189. Lyn-Cook, B.D., et al., Gender differences in gemcitabine (Gemzar) efficacy in cancer cells: effect of indole-3-carbinol. *Anticancer Res*, 2010. **30**(12): p. 4907-13.
190. Chung, W., et al., Identification of novel tumor markers in prostate, colon and breast cancer by unbiased methylation profiling. *PLoS One*, 2008. **3**(4): p. e2079.
191. Ren, F., et al., Identification of differentially methylated genes in the malignant transformation of ovarian endometriosis. *J Ovarian Res*, 2014. **7**: p. 73.
192. Xu, X., et al., SAMD14 promoter methylation is strongly associated with gene expression and poor prognosis in gastric cancer. *Int J Clin Oncol*, 2020. **25**(6): p. 1105-1114.
193. Wu, D., et al., TFPI-2 methylation predicts poor prognosis in non-small cell lung cancer. *Lung Cancer*, 2012. **76**(1): p. 106-11.
194. Heagerty, P.J., T. Lumley, and M.S. Pepe, Time-dependent ROC curves for censored survival data and a diagnostic marker. *Biometrics*, 2000. **56**(2): p. 337-44.
195. Kamarudin, A.N., T. Cox, and R. Kolamunnage-Dona, Time-dependent ROC curve analysis in medical research: current methods and applications. *BMC Med Res Methodol*, 2017. **17**(1): p. 53.
196. Dietrich, D., et al., CDO1 promoter methylation is a biomarker for outcome prediction of anthracycline treated, estrogen receptor-positive, lymph node-positive breast cancer patients. *BMC Cancer*, 2010. **10**: p. 247.
197. Paska, A.V. and P. Hudler, Aberrant methylation patterns in cancer: a clinical view. *Biochem Med (Zagreb)*, 2015. **25**(2): p. 161-76.
198. Marino, N., et al., Aberrant epigenetic and transcriptional events associated with breast cancer risk. *Clin Epigenetics*, 2022. **14**(1): p. 21.
199. Singh, A., S. Gupta, and M. Sachan, Epigenetic Biomarkers in the Management of Ovarian Cancer: Current Prospectives. *Front Cell Dev Biol*, 2019. **7**: p. 182.
200. Pouliot, M.C., et al., The Role of Methylation in Breast Cancer Susceptibility and Treatment. *Anticancer Res*, 2015. **35**(9): p. 4569-74.

201. Ren, F., et al., Downregulation of SPOCK2 promotes the proliferation, adhesion, and invasion of endometrial epithelial cells. *Gynecol Endocrinol*, 2021. **37**(3): p. 273-277.
202. Otto, T. and P. Sicinski, Cell cycle proteins as promising targets in cancer therapy. *Nat Rev Cancer*, 2017. **17**(2): p. 93-115.
203. Mao, Z., et al., Secreted protein acidic and rich in cysteine inhibits the growth of human pancreatic cancer cells with G1 arrest induction. *Tumour Biol*, 2014. **35**(10): p. 10185-93.
204. Harper, J.V. and G. Brooks, The mammalian cell cycle: an overview. *Methods Mol Biol*, 2005. **296**: p. 113-53.
205. Vermeulen, K., D.R. Van Bockstaele, and Z.N. Berneman, The cell cycle: a review of regulation, deregulation and therapeutic targets in cancer. *Cell Prolif*, 2003. **36**(3): p. 131-49.
206. Davis, J.E., Jr., et al., Tumor Dormancy and Slow-Cycling Cancer Cells. *Adv Exp Med Biol*, 2019. **1164**: p. 199-206.
207. Pedrosa, R., et al., Differential Expression of BOC, SPOCK2, and GJD3 Is Associated with Brain Metastasis of ER-Negative Breast Cancers. *Cancers (Basel)*, 2021. **13**(12).
208. Das, S. and S.K. Batra, Pancreatic cancer metastasis: are we being pre-EMT'ed? *Curr Pharm Des*, 2015. **21**(10): p. 1249-55.
209. Chaffer, C.L. and R.A. Weinberg, A perspective on cancer cell metastasis. *Science*, 2011. **331**(6024): p. 1559-64.
210. Bhat, A.A., et al., Tight Junction Proteins and Signaling Pathways in Cancer and Inflammation: A Functional Crosstalk. *Front Physiol*, 2018. **9**: p. 1942.
211. Knights, A.J., et al., Holding Tight: Cell Junctions and Cancer Spread. *Trends Cancer Res*, 2012. **8**: p. 61-69.
212. Martin, T.A. and W.G. Jiang, Tight junctions and their role in cancer metastasis. *Histol Histopathol*, 2001. **16**(4): p. 1183-95.
213. Martin, T.A. and W.G. Jiang, Loss of tight junction barrier function and its role in cancer metastasis. *Biochim Biophys Acta*, 2009. **1788**(4): p. 872-91.
214. Kyuno, D., et al., Role of tight junctions in the epithelial-to-mesenchymal transition of cancer cells. *Biochim Biophys Acta Biomembr*, 2021. **1863**(3): p. 183503.
215. Martin, T.A., M.D. Mason, and W.G. Jiang, Tight junctions in cancer metastasis. *Front Biosci (Landmark Ed)*, 2011. **16**(3): p. 898-936.
216. Salvador, E., M. Burek, and C.Y. Forster, Tight Junctions and the Tumor Microenvironment. *Curr Pathobiol Rep*, 2016. **4**: p. 135-145.
217. Van Itallie, C.M. and J.M. Anderson, Architecture of tight junctions and principles of molecular composition. *Semin Cell Dev Biol*, 2014. **36**: p. 157-65.

218. Shen, L., et al., Tight junction pore and leak pathways: a dynamic duo. *Annu Rev Physiol*, 2011. **73**: p. 283-309.
219. Martin, T.A., The role of tight junctions in cancer metastasis. *Semin Cell Dev Biol*, 2014. **36**: p. 224-31.
220. Francou, A. and K.V. Anderson, The Epithelial-to-Mesenchymal Transition (EMT) in Development and Cancer. *Annu Rev Cancer Biol*, 2020. **4**: p. 197-220.
221. Heerboth, S., et al., EMT and tumor metastasis. *Clin Transl Med*, 2015. **4**: p. 6.
222. Cho, E.S., et al., Therapeutic implications of cancer epithelial-mesenchymal transition (EMT). *Arch Pharm Res*, 2019. **42**(1): p. 14-24.
223. Mittal, V., Epithelial Mesenchymal Transition in Tumor Metastasis. *Annu Rev Pathol*, 2018. **13**: p. 395-412.
224. Shu, Y.J., et al., SPOCK1 as a potential cancer prognostic marker promotes the proliferation and metastasis of gallbladder cancer cells by activating the PI3K/AKT pathway. *Mol Cancer*, 2015. **14**: p. 12.
225. Fanning, A.S., C.M. Van Itallie, and J.M. Anderson, Zonula occludens-1 and -2 regulate apical cell structure and the zonula adherens cytoskeleton in polarized epithelia. *Mol Biol Cell*, 2012. **23**(4): p. 577-90.
226. Zhao, J.L., et al., The LIM domain protein FHL1C interacts with tight junction protein ZO-1 contributing to the epithelial-mesenchymal transition (EMT) of a breast adenocarcinoma cell line. *Gene*, 2014. **542**(2): p. 182-9.
227. Paul, A., et al., PKCzeta Promotes Breast Cancer Invasion by Regulating Expression of E-cadherin and Zonula Occludens-1 (ZO-1) via NFkappaB-p65. *Sci Rep*, 2015. **5**: p. 12520.
228. Ohtani, S., et al., Expression of tight-junction-associated proteins in human gastric cancer: downregulation of claudin-4 correlates with tumor aggressiveness and survival. *Gastric Cancer*, 2009. **12**(1): p. 43-51.
229. Kaihara, T., et al., Dedifferentiation and decreased expression of adhesion molecules, E-cadherin and ZO-1, in colorectal cancer are closely related to liver metastasis. *J Exp Clin Cancer Res*, 2003. **22**(1): p. 117-23.
230. Ni S, Xu L, Huang J, et al. Increased ZO-1 expression predicts valuable prognosis in non-small cell lung cancer. *Int J Cliu Exp Pathol*, 2013. **6**(12): 2887-2895.
231. Quintero-Fabian, S., et al., Role of Matrix Metalloproteinases in Angiogenesis and Cancer. *Front Oncol*, 2019. **9**: p. 1370.
232. Feng, S., et al., Matrix metalloproteinase-2 and -9 secreted by leukemic cells increase the permeability of blood-brain barrier by disrupting tight junction proteins. *PLoS One*, 2011. **6**(8): p. e20599.

Supplemental materials

Supplementary Table 1. ICGC original data.

Donor	Survival time (Days)	Survival event	SPOCK2 Exp	SPOCK3 Exp	SMOC1 Exp	SMOC2 Exp	Donor	Survival time (Days)	Survival event	SPOCK2 Exp	SPOCK3 Exp	SMOC1 Exp	SMOC2 Exp
DO221539	1733	live	3.56625377	0.47516776	2.76225929	50.0029219	DO224648	958	dead	1.41558311	2.76631429	6.85816736	23.319165
DO221540	290	dead	1.23482007	0.18098021	3.15623853	31.7862653	DO224656	1208	dead	0.76301739	1.11830907	8.81935419	13.2081537
DO221541	195	dead	0.9079088	0	71.6669206	28.0304569	DO224688	633	dead	6.15197054	0.54830531	7.74981676	6.83994554
DO221542	375	live	3.75080494	0.18324437	290.81095	154.605072	DO224698	472	dead	4.95185185	1.14594218	27.0383602	5.09535006
DO221543	2045	live	2.30393615	0	0.86601949	35.9720983	DO224705	455	dead	1.65378386	0.5102847	0.65435341	10.3520592
DO221544	467	live	4.17581285	1.02003996	58.3206038	24.0383346	DO224712	239	dead	3.27719658	2.22586924	4.44669741	4.81835838
DO221545	260	live	1.05441694	0	1.58536618	0.68714929	DO224719	522	dead	2.81527477	0.63479697	3.58168459	16.5826538
DO221546	480	dead	52.4195671	0.78663719	1.74846275	11.5133483	DO224734	271	dead	1.17733662	0	4.55189606	6.57646623
DO224633	742	dead	2.18362602	1.20015389	3.69358417	4.89169868	DO224740	684	dead	2.47768959	0	9.10634887	12.5585979
DO224642	547	dead	4.36739349	0.23707511	0.97282734	43.4831743	DO224750	165	dead	6.6436736	0	3.94305802	413.020332
DO224752	257	live	17.3082863	6.82977147	39.7030295	4.69982361	DO227684	745	dead	1.4089763	1.4750375	13.7700102	2.62345955
DO224764	244	live	2.09956594	1.13370841	4.98441723	0.54010216	DO227687	823	dead	19.3228294	0.1000718	1.12926063	16.0186354
DO224767	324	dead	1.71088236	0.20896152	0	2.09054803	DO227695	531	dead	2.61919529	0.16935875	0.98452128	31.3139788
DO224770	200	live	0	0.1968548	0	4.3765041	DO227736	158	dead	1.38724279	1.28016233	4.63507943	2.51124281
DO224779	228	dead	1.54146289	0.56480755	1.35197009	11.5104752	DO227742	482	dead	3.51845101	0	39.0310512	20.6223622
DO224782	389	dead	0.5263666	0.77146412	17.0154721	50.7392644	DO35082	371	dead	1.75618306	0.65998275	11.9161253	9.39061172
DO224784	816	dead	1.39307922	1.22505186	5.86477105	1.81570187	DO35083	1264	live	2.28376652	0.18595446	0.190764	2.48049972
DO227581	177	dead	8.88071255	0.30990311	6.67628756	83.7111937	DO35085	224	dead	0.86993008	4.00715737	12.332396	9.31371359
DO227596	142	dead	2.94214016	0.41067803	8.63664637	9.35850892	DO35104	1091	dead	0.11328233	2.58534227	14.6601498	1.26226827
DO227604	164	dead	7.86235958	10.6369767	23.2531481	39.554561	DO35116	1646	live	0.81008406	0.13192132	36.1340012	4.69262978
DO227633	1074	dead	3.2933451	0	17.2071628	39.8393678	DO35126	280	dead	0.30821338	0.45172997	31.2224865	59.5043314
DO227648	311	dead	1.99359254	0.48698161	0.66610256	2.52621709	DO35128	361	dead	5.62561331	12.2695324	21.1459452	43.0989237

Donor	Survival time (Days)	Survival event	SPOCK2 Exp	SPOCK3 Exp	SMOC1 Exp	SMOC2 Exp	Donor	Survival time (Days)	Survival event	SPOCK2 Exp	SPOCK3 Exp	SMOC1 Exp	SMOC2 Exp
DO227671	673	dead	3.46989646	1.52568607	3.47810328	2.63816549	DO35132	90	dead	113.853048	1.89751996	467.964433	2.36304673
DO35136	1347	live	0.63711412	0.08488911	2.52545572	2.73653671	DO35230	263	dead	0.73990224	0	1.6687175	10.7486919
DO35138	247	dead	0.00499465	2.10338139	55.2262366	0.25768296	DO35236	1343	live	6.03231536	1.47353412	3.48841308	7.05596147
DO35140	1262	dead	0.61619957	0.45156348	2.96475348	5.12000408	DO35242	201	dead	1.49444927	0	579.058879	8.16367767
DO35144	311	dead	1.74518084	0	2.09917014	10.8044527	DO35258	362	dead	4.34050782	1.06027056	10.4107801	17.6790649
DO35148	1013	dead	1.85984949	0.71733433	15.0121049	24.0015583	DO35290	673	dead	4.69667277	19.2017133	23.0433496	33.8294336
DO35152	330	dead	0.53737978	0	0	8.05467256	DO35305	746	dead	8.20218678	0.14841304	3.95854149	9.23871141
DO35160	209	dead	0.16061492	2.17094526	24.5785388	1.69605098	DO35330	1359	dead	1.7409312	3.08315795	49.2976274	5.43634408
DO35184	102	dead	2.03581646	0.5425045	5.28709062	40.7060014	DO35350	146	dead	1.48364693	5.36374888	5.6511927	3.54519985
DO35198	463	dead	0.74757497	0.12174178	0.24978103	15.2921809	DO35360	2174	live	2.13223751	1.70459635	2.62302616	6.00033135
DO35210	886	dead	0.20670153	0	0.31078561	2.35733044	DO35365	889	live	1.40834425	0	2.42001462	7.53906277
DO35222	1234	dead	1.49750213	0.43895991	4.05281864	14.3132283	DO35442	1331	live	9.90782614	0.83455803	3.08211506	4.45296319
DO35226	627	dead	5.75790385	0	3.77772359	12.9626576	DO35454	315	dead	1.46791913	0	1.54496052	32.1265921
DO35228	1623	live	0.29960242	0	1.35139959	10.7385769	DO35496	1072	dead	1.25902745	0	1.08171878	12.6004006
DO49418	1448	dead	2.53803184	0	0.21200289	1.26347307	DO49454	294	dead	0.77952575	0.16321491	20.4272297	2.3586012
DO49419	681	dead	0.66954248	0	38.3548536	18.9804333	DO49457	904	live	1.34800904	0	0	13.5150662
DO49420	1164	live	4.63575359	0.59599539	3.91302555	11.6602241	DO49463	730	dead	0.5098561	0.74726566	23.7643822	7.47599265
DO49421	385	dead	15.7726714	0	0.99503346	5.39099849	DO49469	573	dead	2.27178942	1.33185049	4.78204134	5.49897963
DO49424	341	dead	41.3616646	0.47054068	1.04587332	10.3739515	DO49472	578	dead	0.23103877	0	0.63685934	11.6060406
DO49427	1483	live	1.45443922	0.444101	2.00458388	11.9467134	DO49475	628	dead	8.66647636	0.58029155	70.1792838	2.3652062
DO49430	821	dead	0.94056317	0.34463183	0.7070908	16.0899986	DO49478	653	live	0.26151413	0.76657131	2.35919383	14.4861444
DO49433	456	dead	41.9398878	1.07839985	36.2863654	18.221106	DO49481	383	dead	8.46943648	7.05066792	9.47424624	7.72718448
DO49436	663	dead	2.24597267	0	0	13.638744	DO51464	144	dead	1.24231563	0	0.6792294	2.76000114
DO49439	608	dead	0.64889659	0.1902098	4.29284674	35.5216807	DO51465	1226	dead	1.74449243	0	5.24585524	2.36846288
DO49442	995	dead	0.48243757	0.90910281	5.44025929	1.68427529	DO51466	351	dead	2.18059216	0.56399362	22.5646501	5.85143378
DO49448	951	dead	2.28502817	0.23921639	0.24540349	11.7002445	DO51467	471	dead	1.47247776	0.23979142	1.96794719	13.8608006
DO49451	918	dead	0.57234148	1.08556641	0.75930241	3.23621267	DO51468	1083	dead	13.6925066	0.0891924	475.430238	22.2089076

Donor	Survival time (Days)	Survival event	SPOCK2 Exp	SPOCK3 Exp	SMOC1 Exp	SMOC2 Exp	Donor	Survival time (Days)	Survival event	SPOCK2 Exp	SPOCK3 Exp	SMOC1 Exp	SMOC2 Exp
DO51469	314	dead	8.12775358	0.6311186	22.5795354	10.9618116	DO51484	1460	dead	7.70068834	0.18203935	2.8012143	9.61192129
DO51470	444	dead	1.89692066	0.67108359	0.88513781	7.45981309	DO51485	1879	dead	5.20406933	0.16824913	2.99174605	10.8475623
DO51472	590	dead	2.58040741	0.07415587	43.1338656	11.2932102	DO51487	2555	live	3.58754472	0	6.06830029	7.5983521
DO51473	4289	dead	2.38645057	0.34976782	1.07644269	12.4417411	DO51489	1253	live	15.352412	0	35.0629126	6.96547832
DO51474	1633	live	3.23301009	1.32235256	72.3495436	0.85746299	DO51490	232	dead	13.4427253	0	2.60797149	38.5035587
DO51475	1824	dead	0.94922531	0.34780573	2.31920903	5.02610331	DO51491	539	live	3.78113634	2.04171061	3.88981822	22.695801
DO51476	1576	dead	0.49043585	1.00632359	25.9562583	0.31961042	DO51492	282	dead	1.55691627	0	2.00648393	1.44945904
DO51478	311	dead	0.76917629	0.25051907	1.28499252	14.0631786	DO51493	512	dead	3.8404062	0.26803115	1.51229938	15.940076
DO51479	1691	live	6.92813586	0	23.8428586	5.51829992	DO51494	631	dead	2.10148354	0.44000272	4.06244673	7.33665252
DO51480	228	dead	2.18331106	0.13912821	3.71089225	8.35141907	DO51495	729	dead	2.40981001	0	0.40258493	24.5163238
DO51481	587	dead	5.43041856	0.19412294	6.37259977	8.63153782	DO51496	197	dead	1.14426472	0.13975671	1.14697108	4.58295946
DO51482	379	dead	1.20542276	0.72747139	0	36.9674234	DO51497	313	dead	0.59778987	0	15.7290981	2.92178697
DO51483	107	dead	6.40444289	0	7.79521685	12.1732597	DO51498	294	dead	1.55711368	0.20746988	1.91552296	7.37999985
DO51500	482	live	25.2609435	0.53271162	6.01138668	0.74020756	DO51514	1191	dead	1.9171283	0	1.6088338	4.43089334
DO51501	294	dead	14.8956865	0.80858218	2.98618339	7.37037099	DO51515	1799	live	53.1828232	1.93416603	149.211192	0.21500328
DO51502	310	dead	7.46980239	0	0.81681486	7.96576816	DO51517	1389	dead	5.03080868	0.33515255	174.661043	14.5297609
DO51503	837	dead	1.42781133	0	2.68347809	14.2480574	DO51518	129	dead	0.46830238	0.34318143	11.7059114	2.86112194
DO51504	494	dead	3.53597006	0.1480703	1.36709993	13.4968719	DO51519	579	dead	88.1142183	0.69153281	9.75450639	39.9730663
DO51505	351	dead	1.61214152	7.84456124	3.1026326	2.52146611	DO51520	139	dead	1.16292766	1.18569301	4.18123688	14.7454026
DO51506	1068	dead	6.07742134	0.08907314	7.21877748	8.02016132	DO51522	201	dead	0.40198776	0.68736439	3.82791596	4.9119375
DO51507	2571	dead	3.39822493	0.27669864	8.65758318	13.3797381	DO51523	318	dead	2.22632166	1.08766228	0.37193121	3.42565061
DO51509	515	dead	0.57191009	0.27940483	2.00641958	16.4611855	DO51524	1251	live	0.72385954	0	1.39931661	4.38034532
DO51510	287	dead	1.8079451	0	8.15499521	16.7895414	DO51525	690	dead	6.81513159	2.93780346	13.7880752	4.16374623
DO51511	592	dead	1.23945607	0	2.79537202	4.54351948	DO51526	1380	dead	6.23125244	0	20.6697204	25.0138333
DO51512	184	dead	1.02299508	3.49846666	47.6817796	0.55556008	DO51527	349	dead	0.78864734	2.23468849	54.8615752	12.163503
DO51513	400	live	1.25814628	0	2.83752446	3.07468858	DO51528	2325	live	71.650564	0.07267402	0.29821465	140.888967

Donor	Survival time (Days)	Survival event	SPOCK2 Exp	SPOCK3 Exp	SMOC1 Exp	SMOC2 Exp	Donor	Survival time (Days)	Survival event	SPOCK2 Exp	SPOCK3 Exp	SMOC1 Exp	SMOC2 Exp
DO51529	276	dead	3.96217481	0	1.02712395	6.01005072	DO51543	1431	dead	2.4221873	0.51771642	1.28983045	11.2633036
DO51530	625	dead	4.04587964	1.80472308	24.9939069	49.8669848	DO51545	190	dead	0.34501579	0.75850358	1.5562431	2.24842133
DO51531	1273	dead	1.31473283	0	1.97676355	42.4112855	DO51548	2177	live	2.16715421	1.3475079	316.066718	4.17271979
DO51532	1761	live	1.17783143	0	1.47577148	2.45198162	DO51549	229	live	1.84786124	0	1.04188034	50.0506531
DO51533	4173	live	4.79640475	2.30829395	13.885066	68.2300401							
DO51534	278	dead	0.67862058	0	0	15.4786757							
DO51535	764	dead	9.19576012	3.20261631	12.046646	32.9304733							
DO51536	446	dead	2.26928894	1.82927878	11.2595479	31.2410228							
DO51537	503	dead	3.81547486	0.07876217	0.56559493	2.71413022							
DO51538	361	dead	0.33918824	1.65709321	1.35996187	1.84203665							
DO51540	141	dead	2.47537748	1.44190264	30.2519455	6.77324629							
DO51541	325	dead	3.35204794	2.48754263	0.82936117	6.01424508							
DO51542	369	dead	1.52209858	0.34320755	0.17604214	2.09831581							

Supplementary Table 2. mRNA expression and methylation level of SPOCK2 from TCGA.

Samples ID	mRNA log ₂ (FPKM +1)	Methylation (beta value)	Samples ID	mRNA log ₂ (FPKM +1)	Methylation (beta value)	Samples ID	mRNA log ₂ (FPKM +1)	Methylation (beta value)
TCGA-FB-AAQ1-01A	2.035761996	0.54457779	TCGA-IB-AAUU-01A	5.105124847	0.426264272	TCGA-HZ-8519-01A	3.077478505	0.63406371
TCGA-IB-7888-01A	3.908840536	0.48803515	TCGA-PZ-A5RE-01A	2.583018357	0.551813069	TCGA-3A-A9IR-01A	2.402944467	0.717791481
TCGA-2J-AABO-01A	2.961007042	0.559248378	TCGA-HV-A7OL-01A	3.179466468	0.523419958	TCGA-HV-AA8V-01A	1.97647534	0.545955878
TCGA-FB-A5VM-01A	2.984571157	0.551326981	TCGA-IB-7897-01A	4.219985838	0.534940788	TCGA-Q3-A5QY-01A	6.170370581	0.360296435
TCGA-HZ-8315-01A	5.751012004	0.534017201	TCGA-H6-A45N-01A	3.099522334	0.550226021	TCGA-HZ-A9TJ-06A	4.322043547	0.480625883
TCGA-IB-7893-01A	1.615088688	0.610160137	TCGA-3A-A9IX-01A	4.024345034	0.500188718	TCGA-3A-A9IL-01A	3.17304928	0.459096648
TCGA-2L-AAQE-01A	2.757133927	0.638554028	TCGA-XD-AAUH-01A	4.520519612	0.480183128	TCGA-H6-8124-01A	2.028447628	0.639914194
TCGA-HZ-8003-01A	3.095401598	0.540983041	TCGA-HZ-A77O-01A	1.447419442	0.518441216	TCGA-3E-AAAY-01A	3.345025406	0.522694681
TCGA-YH-A8SY-01A	1.59144462	0.455201416	TCGA-IB-A5SO-01A	3.630612154	0.53720805	TCGA-HZ-A9TJ-01A	1.725941247	0.515345281
TCGA-M8-A5N4-01A	1.593301057	0.520798751	TCGA-F2-6879-01A	1.650519271	0.66322167	TCGA-LB-A8F3-01A	1.778075819	0.536794406
TCGA-2J-AABT-01A	3.469063987	0.555418497	TCGA-3A-A9IV-01A	1.805749408	0.563094056	TCGA-US-A77E-01A	3.207897067	0.377666488
TCGA-YY-A8LH-01A	2.238025811	0.596579647	TCGA-IB-7886-01A	2.474625396	0.500207034	TCGA-HV-AA8X-01A	1.225527635	0.663254439
TCGA-IB-7654-01A	1.954588605	0.571331853	TCGA-IB-8127-01A	2.704940779	0.645510431	TCGA-HZ-A77Q-01A	3.594946899	0.513429702
TCGA-FB-A78T-01A	2.205240753	0.582059535	TCGA-XN-A8T3-01A	2.414345243	0.534190156	TCGA-HZ-7924-01A	5.469253278	0.428498949
TCGA-2J-AAB8-01A	2.126896354	0.506181778	TCGA-FB-AAQ0-01A	1.072730061	0.565576914	TCGA-HZ-7289-01A	4.499667977	0.319345981
TCGA-FB-A4P6-01A	3.4803968	0.53905112	TCGA-S4-A8RM-01A	2.975248451	0.615473484	TCGA-HZ-7926-01A	5.431196725	0.492778196
TCGA-3A-A9I5-01A	2.063794336	0.542837519	TCGA-IB-AAUP-01A	5.305898427	0.419658747	TCGA-RB-AA9M-01A	2.594960668	0.594714343
TCGA-HZ-8005-01A	1.45142599	0.546859962	TCGA-HZ-8317-01A	1.886359466	0.553216518	TCGA-3A-A9IO-01A	2.912845005	0.660361389
TCGA-2J-AAB9-01A	3.609134589	0.514564458	TCGA-3A-A9I9-01A	2.194526745	0.517485882	TCGA-2J-AABH-01A	2.076306251	0.501119742
TCGA-XN-A8T5-01A	4.693512646	0.466205036	TCGA-F2-6880-01A	0.760484998	0.629574114	TCGA-IB-7645-01A	4.119421719	0.495554526
TCGA-HZ-8638-01A	2.448407828	0.528757128	TCGA-2L-AAQJ-01A	2.192680632	0.571287073	TCGA-2J-AABA-01A	2.645728281	0.571979
TCGA-L1-A7W4-01A	3.710232487	0.661622824	TCGA-3A-A9IH-01A	3.575941338	0.571267196	TCGA-HZ-A4BH-01A	3.552461442	0.51345976
TCGA-US-A779-01A	1.251771703	0.569911838	TCGA-IB-A5ST-01A	4.684240731	0.391459677	TCGA-Q3-AA2A-01A	1.717647752	0.575023904
TCGA-HZ-7925-01A	2.630025158	0.489868196	TCGA-3A-A9IU-01A	2.513745347	0.620304641	TCGA-FB-AAQ2-01A	2.066571159	0.535271344

Samples ID	mRNA log ₂ (FPKM +1)	Methylation (beta value)	Samples ID	mRNA log ₂ (FPKM +1)	Methylation (beta value)	Samples ID	mRNA log ₂ (FPKM +1)	Methylation (beta value)
TCGA-2L-AAQM-01A	4.297765318	0.513280733	TCGA-IB-A5SS-01A	3.821261523	0.632656048	TCGA-IB-7651-01A	2.665548995	0.521817609
TCGA-IB-7649-01A	3.63666815	0.576022262	TCGA-FB-AAPZ-01A	2.995945477	0.63354033	TCGA-HZ-7923-01A	4.20797452	0.506012231
TCGA-LB-A9Q5-01A	1.828851212	0.567964515	TCGA-2J-AABI-01A	7.192305171	0.365849021	TCGA-HZ-8637-01A	4.243119015	0.449759198
TCGA-HZ-A8P0-01A	3.210821917	0.349382258	TCGA-IB-AAUO-01A	1.739764264	0.592717294	TCGA-HZ-A77P-01A	2.679467885	0.559883051
TCGA-S4-A8RO-01A	1.889114218	0.621355434	TCGA-2J-AAB6-01A	1.366024852	0.594518299	TCGA-IB-7646-01A	1.929036253	0.530996759
TCGA-3A-A9IC-01A	1.925455789	0.5520628	TCGA-2J-AABF-01A	3.830353341	0.45446598	TCGA-HV-A5A3-01A	1.457788424	0.636840434
TCGA-IB-AAUN-01A	2.012995621	0.609087531	TCGA-HZ-8002-01A	3.476387247	0.56473782	TCGA-HZ-7920-01A	3.76454802	0.522294942
TCGA-HZ-A49G-01A	2.693498927	0.611557969	TCGA-FB-AAQ6-01A	1.628504101	0.628185733	TCGA-FB-AAPU-01A	1.66083762	0.629918731
TCGA-S4-A8RP-01A	2.401144399	0.634575084	TCGA-2J-AAB1-01A	2.906940126	0.561503341	TCGA-HZ-7922-01A	3.381584098	0.505189831
TCGA-HZ-A49H-01A	3.279292761	0.442513357	TCGA-HV-A5A6-01A	1.699328666	0.527390456	TCGA-IB-A6UF-01A	1.161898668	0.677883427
TCGA-IB-AAUM-01A	2.726454371	0.599344547	TCGA-HZ-8001-01A	3.287116058	0.54653865	TCGA-OE-A75W-01A	2.677426764	0.605369807
TCGA-HZ-A8P1-01A	1.45667143	0.670446256	TCGA-3E-AAAZ-01A	1.998523486	0.55743663	TCGA-3A-A9IZ-01A	1.281192315	0.536883256
TCGA-2J-AABV-01A	1.109326846	0.58568018	TCGA-IB-7885-01A	2.955673578	0.469251224	TCGA-3A-A9IN-01A	3.069021657	0.522628732
TCGA-F2-7276-01A	3.720031179	0.524070399	TCGA-2J-AABR-01A	3.784312545	0.498759221	TCGA-XD-AAUG-01A	2.975427408	0.505110241
TCGA-HV-A5A5-01A	3.430189167	0.525307703	TCGA-IB-A5SP-01A	2.084105903	0.590358676	TCGA-3A-A9IS-01A	4.831870067	0.440453678
TCGA-2J-AABU-01A	2.601298175	0.59163004	TCGA-3A-A9I7-01A	3.285605292	0.488350466	TCGA-IB-AAUT-01A	3.962099218	0.5294689
TCGA-US-A77J-01A	5.066310065	0.48202048	TCGA-FB-AAPP-01A	7.416443216	0.208554724	TCGA-Z5-AAPL-01A	6.086332659	0.401077197
TCGA-2J-AABE-01A	2.43832448	0.550028738	TCGA-F2-A7TX-01A	2.852892673	0.584201216	TCGA-HZ-A4BK-01A	3.28323301	0.585424205
TCGA-RB-A7B8-01A	2.559844551	0.493839209	TCGA-XD-AAUL-01A	3.990877036	0.499532212	TCGA-US-A776-01A	2.01618374	0.403676479
TCGA-IB-A6UG-01A	6.191609374	0.488773254	TCGA-F2-A44H-01A	1.94071797	0.527571494	TCGA-IB-7889-01A	3.560004488	0.567526167
TCGA-3A-A9J0-01A	1.696125188	0.54104784	TCGA-IB-7644-01A	2.258999981	0.499798464	TCGA-IB-AAUR-01A	5.596062759	0.445593449
TCGA-IB-AAUQ-01A	3.244018158	0.557075338	TCGA-3A-A9IB-01A	1.628063707	0.577388425	TCGA-IB-A7M4-01A	3.115916043	0.580434522
TCGA-FB-A7DR-01A	2.536925592	0.480441986	TCGA-IB-AAUW-01A	3.080982337	0.556500019	TCGA-FB-AAPS-01A	3.540770724	0.509129772
TCGA-2L-AAQL-01A	2.644268442	0.583392414	TCGA-HZ-7919-01A	3.060770564	0.509614782	TCGA-LB-A7SX-01A	2.056455932	0.365339397
TCGA-HZ-7918-01A	4.020008219	0.547128006	TCGA-F2-7273-01A	3.28435034	0.556170393	TCGA-IB-AAUS-01A	3.571879705	0.464935014
TCGA-IB-7887-01A	1.89243078	0.45936842	TCGA-2L-AAQI-01A	1.9854838	0.601792807	TCGA-HV-A7OP-01A	0.983454373	0.523729196

Samples ID	mRNA log ₂ (FPKM +1)	Methylation (beta value)	Samples ID	mRNA log ₂ (FPKM +1)	Methylation (beta value)	Samples ID	mRNA log ₂ (FPKM +1)	Methylation (beta value)
TCGA-IB-7652-01A	2.268971285	0.471132874	TCGA-F2-A8YN-01A	1.377671129	0.562438198	TCGA-IB-A5SQ-01A	2.869734213	0.549867377
TCGA-2J-AAB4-01A	2.576198335	0.507487602	TCGA-HZ-A49I-01A	2.674582294	0.580382347	TCGA-FB-AAPQ-01A	1.6432982	0.548429952
TCGA-US-A774-01A	2.802597166	0.549010219	TCGA-HV-A5A4-01A	1.916286081	0.603945583			
TCGA-IB-8126-01A	3.237565891	0.572485363	TCGA-HZ-8636-01A	2.865916538	0.541010579			
TCGA-F2-A44G-01A	1.554008128	0.525508045	TCGA-FB-AAPY-01A	3.602982692	0.491472654			
TCGA-IB-AAUV-01A	3.40242218	0.492779624	TCGA-FB-A4P5-01A	4.274169274	0.511905463			
TCGA-FB-AAQ3-01A	1.485163278	0.604047773	TCGA-2L-AAQA-01A	1.311593918	0.631103248			
TCGA-RL-AAAS-01A	3.622035791	0.523616853	TCGA-H8-A6C1-01A	2.732145692	0.483413995			
TCGA-IB-7890-01A	1.84244189	0.604508279	TCGA-2J-AABP-01A	2.76819038	0.483397766			
TCGA-XD-AAUI-01A	3.144094923	0.524163207	TCGA-US-A77G-01A	1.446795102	0.589360101			
TCGA-2J-AABK-01A	1.94883884	0.595256375	TCGA-IB-A7LX-01A	3.753862139	0.614786748			
TCGA-FB-A545-01A	1.284577295	0.669904449	TCGA-IB-7891-01A	3.491308228	0.535790689			
TCGA-3A-A9IJ-01A	4.46912738	0.449631278	TCGA-YB-A89D-01A	2.796018397	0.55870389			

Supplementary Table 3. The prognosis of patients and methylation of SPOCK2 from TCGA.

Patients ID	Survival time (Days)	Survival event	Methylation (beta value)	Patients ID	Survival time (Days)	Survival event	Methylation (beta value)	Patients ID	Survival time (Days)	Survival event	Methylation (beta value)
TCGA-HZ-8638	91	live	0.528757128	TCGA-XD-AAUI	202	live	0.524163207	TCGA-3A-A9IN	2084	live	0.522628732
TCGA-M8-A5N4	584	live	0.520798751	TCGA-IB-AAUN	144	dead	0.609087531	TCGA-IB-A5SS	460	dead	0.632656048
TCGA-IB-AAUP	290	live	0.419658747	TCGA-IB-7647	666	dead	0.461483446	TCGA-2L-AAQA	143	dead	0.631103248
TCGA-3A-A9IO	1436	live	0.660361389	TCGA-IB-AAUV	229	live	0.492779624	TCGA-FZ-5919	741	dead	0.46328258
TCGA-IB-7888	1332	dead	0.48803515	TCGA-FB-AAPY	1059	dead	0.491472654	TCGA-FB-AAQ6	244	dead	0.628185733
TCGA-FB-A78T	1	live	0.582059535	TCGA-Q3-AA2A	94	live	0.575023904	TCGA-HZ-8519	3	live	0.63406371
TCGA-HV-A7OL	252	live	0.523419958	TCGA-RB-A7B8	36	live	0.493839209	TCGA-IB-7885	851	live	0.469251224
TCGA-2J-AABO	345	live	0.559248378	TCGA-FB-A545	1	live	0.669904449	TCGA-S4-A8RO	197	live	0.621355434
TCGA-FB-AAPS	228	live	0.509129772	TCGA-2J-AABR	327	live	0.498759221	TCGA-IB-A5ST	8	live	0.391459677
TCGA-2J-AABI	330	live	0.365849021	TCGA-IB-AAUO	239	dead	0.592717294	TCGA-IB-A7LX	250	dead	0.614786748
TCGA-HZ-A8P1	7	live	0.670446256	TCGA-3A-A9I7	718	live	0.488350466	TCGA-US-A779	511	dead	0.569911838
TCGA-2L-AAQE	684	dead	0.638554028	TCGA-HV-A5A3	128	dead	0.636840434	TCGA-US-A77G	12	dead	0.589360101
TCGA-2J-AABK	484	live	0.595256375	TCGA-IB-7886	123	dead	0.500207034	TCGA-3A-A9IZ	308	dead	0.536883256
TCGA-FZ-5926	541	dead	0.584340825	TCGA-HV-A5A4	232	live	0.603945583	TCGA-XD-AAUL	188	live	0.499532212
TCGA-PZ-A5RE	247	live	0.551813069	TCGA-IB-AAUQ	183	dead	0.557075338	TCGA-2L-AAQJ	394	dead	0.571287073
TCGA-IB-AAUM	8	live	0.599344547	TCGA-HZ-7919	20	live	0.509614782	TCGA-IB-7897	486	dead	0.534940788
TCGA-IB-A7M4	181	live	0.580434522	TCGA-S4-A8RM	397	live	0.615473484	TCGA-HZ-8315	28	live	0.534017201
TCGA-RL-AAAS	9	live	0.523616853	TCGA-IB-7651	603	dead	0.521817609	TCGA-HZ-8636	5	live	0.541010579
TCGA-IB-A6UG	41	dead	0.488773254	TCGA-IB-AAUU	153	live	0.426264272	TCGA-IB-7893	117	dead	0.610160137
TCGA-3A-A9IU	458	dead	0.620304641	TCGA-2L-AAQM	914	live	0.513280733	TCGA-US-A774	695	dead	0.549010219
TCGA-HV-AA8X	532	dead	0.663254439	TCGA-2J-AABE	663	live	0.550028738	TCGA-IB-8127	194	live	0.645510431
TCGA-3E-AAAY	2172	live	0.522694681	TCGA-3A-A9IB	224	dead	0.577388425	TCGA-2J-AABU	277	dead	0.59163004
TCGA-2J-AABA	607	dead	0.571979	TCGA-F2-6880	295	live	0.629574114	TCGA-HV-AA8V	910	live	0.545955878
TCGA-2J-AABV	652	dead	0.58568018	TCGA-XN-A8T5	720	live	0.466205036	TCGA-3A-A9IH	874	live	0.571267196
TCGA-FB-AAPP	485	dead	0.208554724	TCGA-3A-A9IL	2558	live	0.459096648	TCGA-IB-8126	17	live	0.572485363

Patients ID	Survival time (Days)	Survival event	Methylation (beta value)	Patients ID	Survival time (Days)	Survival event	Methylation (beta value)	Patients ID	Survival time (Days)	Survival event	Methylation (beta value)
TCGA-HZ-7289	240	live	0.319345981	TCGA-HZ-7926	8	live	0.492778196	TCGA-HZ-A49G	23	live	0.611557969
TCGA-HZ-A49H	29	live	0.442513357	TCGA-HZ-A4BH	194	live	0.51345976	TCGA-OE-A75W	110	live	0.605369807
TCGA-Q3-A5QY	105	live	0.360296435	TCGA-2J-AAB8	80	live	0.506181778	TCGA-HZ-8002	24	live	0.56473782
TCGA-IB-7644	347	live	0.499798464	TCGA-LB-A9Q5	155	live	0.567964515	TCGA-F2-7273	360	live	0.556170393
TCGA-IB-7652	476	live	0.471132874	TCGA-IB-7889	481	dead	0.567526167	TCGA-IB-A5SQ	219	dead	0.549867377
TCGA-IB-AAUW	179	live	0.556500019	TCGA-2J-AAB4	729	live	0.507487602	TCGA-FZ-5924	480	dead	0.56917923
TCGA-HV-A5A5	289	live	0.525307703	TCGA-3A-A9I9	634	dead	0.517485882	TCGA-YH-A8SY	388	live	0.455201416
TCGA-3A-A9IV	976	live	0.563094056	TCGA-US-A77J	568	dead	0.48202048	TCGA-HZ-A4BK	46	live	0.585424205
TCGA-2L-AAQL	292	dead	0.583392414	TCGA-H8-A6C1	396	live	0.483413995	TCGA-IB-7890	598	dead	0.604508279
TCGA-F2-A7TX	95	dead	0.584201216	TCGA-2J-AABT	319	live	0.555418497	TCGA-HZ-8001	19	live	0.54653865
TCGA-F2-A44G	153	live	0.525508045	TCGA-FB-A5VM	75	live	0.551326981	TCGA-HZ-7923	8	live	0.506012231
TCGA-HZ-8005	120	dead	0.546859962	TCGA-HV-A5A6	1953	live	0.527390456	TCGA-IB-A6UF	248	live	0.677883427
TCGA-F2-A44H	158	live	0.527571494	TCGA-HZ-8003	21	live	0.540983041	TCGA-IB-AAUT	188	live	0.5294689
TCGA-LB-A7SX	127	live	0.365339397	TCGA-IB-AAUS	179	live	0.464935014	TCGA-F2-6879	334	dead	0.66322167
TCGA-3A-A9IR	1164	live	0.717791481	TCGA-Z5-AAPL	21	live	0.401077197	TCGA-FB-A4P6	7	live	0.53905112
TCGA-FB-AAQ3	31	dead	0.604047773	TCGA-HZ-7922	4	live	0.505189831	TCGA-HZ-A9TJ	603	live	0.515345281
TCGA-HZ-A77P	13	live	0.559883051	TCGA-2J-AAB6	293	dead	0.594518299	TCGA-3A-A9IX	901	live	0.500188718
TCGA-US-A77E	430	dead	0.377666488	TCGA-FB-AAPU	381	dead	0.629918731	TCGA-3A-A9I5	1612	live	0.542837519
TCGA-HV-A7OP	859	live	0.523729196	TCGA-2J-AAB1	66	dead	0.561503341	TCGA-3E-AAAZ	2182	dead	0.55743663
TCGA-F2-A8YN	167	live	0.562438198	TCGA-H6-A45N	233	live	0.550226021	TCGA-RB-AA9M	42	live	0.594714343
TCGA-3A-A9IJ	1854	live	0.449631278	TCGA-IB-7645	1502	dead	0.495554526	TCGA-FZ-5920	61	dead	0.641049416
TCGA-HZ-7918	28	live	0.547128006	TCGA-H6-8124	181	live	0.639914194	TCGA-2L-AAQI	103	dead	0.601792807
TCGA-IB-7654	476	dead	0.571331853	TCGA-FZ-5923	619	dead	0.619627819	TCGA-HZ-8317	16	live	0.553216518
TCGA-IB-AAUR	128	live	0.445593449	TCGA-FB-AAQ0	473	dead	0.565576914	TCGA-3A-A9J0	377	live	0.54104784
TCGA-3A-A9IC	738	dead	0.5520628	TCGA-2J-AABF	691	dead	0.45446598	TCGA-2J-AABP	355	live	0.483397766

Patients ID	Survival time (Days)	Survival event	Methylation (beta value)	Patients ID	Survival time (Days)	Survival event	Methylation (beta value)	Patients ID	Survival time (Days)	Survival event	Methylation (beta value)
TCGA-FZ-5922	1101	dead	0.585304757	TCGA-3A-A9IS	932	live	0.440453678	TCGA-HZ-7925	361	live	0.489868196
TCGA-2J-AAB9	627	dead	0.514564458	TCGA-IB-7646	145	dead	0.530996759	TCGA-HZ-A77O	11	live	0.518441216
TCGA-L1-A7W4	164	live	0.661622824	TCGA-US-A776	844	live	0.403676479	TCGA-IB-7887	110	dead	0.45936842
TCGA-HZ-7924	369	live	0.428498949	TCGA-FB-A7DR	166	live	0.480441986	TCGA-FB-AAQ1	123	dead	0.54457779
TCGA-FB-A4P5	4	live	0.511905463	TCGA-XN-A8T3	951	live	0.534190156				
TCGA-XD-AAUH	164	live	0.480183128	TCGA-F2-7276	216	dead	0.524070399				
TCGA-YB-A89D	160	live	0.55870389	TCGA-IB-7649	476	dead	0.576022262				
TCGA-IB-A5SP	300	live	0.590358676	TCGA-FB-AAPQ	1130	dead	0.548429952				
TCGA-2J-AABH	671	live	0.501119742	TCGA-YY-A8LH	1834	live	0.596579647				
TCGA-IB-A5SO	329	live	0.53720805	TCGA-FB-AAPZ	226	live	0.63354033				
TCGA-IB-7891	488	live	0.535790689	TCGA-FB-AAQ2	153	dead	0.535271344				
TCGA-S4-A8RP	702	dead	0.634575084	TCGA-LB-A8F3	35	live	0.536794406				
TCGA-HZ-A77Q	33	live	0.513429702	TCGA-XD-AAUG	161	live	0.505110241				

Acknowledgements

First and foremost, I would like to express sincere gratitude to my supervisor Prof. Dr. Alexandr Bazhin, who allowed me to conduct research in the lab at the Ludwig-Maximilians-University. He is amiable and approachable and has always helped and encouraged me whenever I meet difficulties in study and life. Every progress I made was inseparable from his careful guidance of him. My thesis was completed under his insightful advice every step, from topic selection, design, and implementation to the final draft and revision. His profound professional knowledge, keen scientific thinking, and rigorous academic attitude inspire me.

My sincere thanks go to my doctoral father, Prof. Dr. med. Jan G. D’Haese, no matter how busy the clinical work is, also helps me as much as he can when I need it. I also would like to thank continuous support from my co-supervisor, PD Dr. med. Clemens Gießen-Jung.

In addition, I want to thank Ms. Natalja, Shristee, and Sevdije, who provided me with technical support. At the same time, I would like to thank each one of my coworkers in the lab for making my life so colorful in Germany.

Thanks to the China Scholarship Council for supporting my life during my three years in Germany.

Finally, I would like to thank my family for their unfailing care and support, which made it possible for me to finish my studies in Germany.

Affidavit



Affidavit

Su, Kaifeng

Surname, first name

Street

Zip code, town, country

I hereby declare, that the submitted thesis entitled:

The SPOCK2 expression is downregulated in pancreatic ductal adenocarcinoma due to hypermethylation of its gene

.....

is my own work. I have only used the sources indicated and have not made unauthorised use of services of a third party. Where the work of others has been quoted or reproduced, the source is always given.

I further declare that the submitted thesis or parts thereof have not been presented as part of an examination degree to any other university.

München, 12.01.2023

place, date

Kaifeng Su

Signature doctoral candidate